MEMBRANE AND SORPTION MATERIALS AND TECHNOLOGIES: PRESENT AND FUTURE

KYIV 2018

V.I. Vernadskii Institute
of General and Inorganic Chemistry
of the National Academy of Science of Ukraine

Institute of Physical Organic Chemistry
of the National Academy of Science of Belarus

MEMBRANE AND SORPTION MATERIALS AND TECHNOLOGIES: PRESENT AND FUTURE

EDITORS: Yu.S. Dzyazko

T.V. Plisko

M.O. Chaban

REVIEWERS: D.D. Kucheruk

V.G. Myronchuk

ArtOK publisher

KYIV 2018

УДК 544.018.2: 544.472.3 + 555.11+666.22

Колективна монографія «Membrane and Sorption Materials and Technologies: Present and Future» - під ред. докт. хім. наук Ю. С. Дзязько, канд. хім. наук Т.В. Пліско, М.О. Чабан – 88 с.

Колективна монографія включає статті за матеріалами українсько-білоруського семінару, який було проведено 10 жовтня 2018 р. на базі Інституту загальної та неорганічної хімії ім. В. І. Вернадського НАН України за участю фахівців Інституту фізико-органічної хімії НАН Білорусі за підтримки Відділення хімії НАН України, Відділення хімії та наук про Землю НАН Білорусі, Відділу міжнародних зв'язків НАН України. У монографії наведено результати досліджень мембранних та сорбційних процесів, які направлені на вилучення токсичних і цінних компонентів із розчинів техногенного та природного походження, зокрема з біологічних рідин. Розглядаються різні аспекти модифікування мембран для надання їм необхідних функціональних властивостей, у фокусі уваги також знаходяться перспективні матеріали, які можуть бути використані в якості модифікаторів. Результати робіт можуть бути застосовані у водопідготовці, хімічній, фармацевтичній, харчовій промисловості.

Монографія є корисною для фахівців в області мембранних та сорбційних технологій, а також для студентів вищих навчальних закладів.

Рецензенти: докт. хім. наук, старш. наук. співр. Д.Д. Кучерук (Інститут колоїдної хімії та хімії води ім. А.В. Думанського НАН України), докт. техн. наук, проф. В.Г. Мирончук (Національний університет харчових технологій МОН України).

Рекомендовано до друку Вченою радою ІЗНХ ім. В. І. Вернадського НАН України (протокол № 12 від 22 листопада 2018 р.).

CONTENT

CHAPTER 2

INTERACTION OF CARBON QUANTUM DOTS WITH SOLUTIONS OF PALLADIUM AND RUTENIUM

V.M. Ogenko, L.B. Kharkova, O.G. Yanko, S.I. Orysyk, M.I. Buriak

V.I. Vernadskii Institute of General and Inorganic Chemistry of the NAS of Ukraine

e-mail kharkova.ljudmila@gmail.com

Abstract. *The processes of interaction in the surface layer of carbon quantum dots (CQD) with solutions of ruthenium and palladium were investigated by methods of electronic and IR spectroscopy. It has been established that in both aqueous and alcoholic solutions of CQD, the characteristic absorption bands of $\pi \rightarrow \pi^*$, $n \rightarrow \pi^*$ electron transitions in the UV region undergo corresponding changes, which indicate both sorption of metals on the CQD surface, and possible coordination of them with CQD. This is confirmed by the changes of stripes, which are related to ligand to metal charge transfer transition (LMCTT) and d-d electron transitions in the visible region. The analysis of IR spectra of the CQD also showed the presence of a number of characteristic absorption bands for functionalized CQDs, which proves the local fixation of metals on the CQD surface.*

Keywords: *quantum dots, metal-carbon, catalytic systems, ruthenium, palladium.*

Introduction. Among the modern methods for separation of solids, liquids and salts by ultrafiltration, the method of changing the sizes of filtering labyrinths of porous systems by embedding hydrophobic-hydrophilic impurities into them becomes of increasing importance [1]. In this respect, the most interesting are layered structures of oxidized carbon, where adsorption centers of the predetermined ratio can be formed. In this way, it is possible to divide the reacting molecules by the energies of the adsorption interaction on the frontal hydrophobic surface and the hydrophilic perimeter of the adsorbent, which provides better conditions for chemical interactions in the surface layer.

Also of interest is the possibility of directed catalytic transformations in the surface layer of the composite filter. In works by G.B. Sergeyeva and V.I. Bukhtiyarova it is shown that the systems based on nanosized metals exhibit quantum-dimensional effects [2, 3]. However, obtaining catalysts of the predetermined sizes is a difficult task.

In this paper, the interaction of solutions of palladium and ruthenium with carbon quantum dots (CQD, 1-10 nm) is investigated.

Experimental. The work is devoted to the study of processes for the synthesis of nanocatalysts that are based on carbon quantum dots and metals of the platinum group, namely ruthenium and palladium.

CQD solutions were synthesized by autoclave hydrothermal method in fluoroplastic reactor [4]. Two solutions of CQD in alcohol with a concentration of 36.0 and 39.0 mg/ml were prepared by centrifugation at 4000 rpm. Solutions of

palladium chloride (C_{Pd} = 5.6 mg/ml) were obtained by dissolving the metal powder in a 0.1 M hydrochloric acid solution in the presence of hydrogen peroxide. The ruthenium solution was prepared by dissolving metal chloride in the HCl solution of the same concentration (C_{Ru} = 5.3 ml/ml). The concentrations of CQD in alcoholic solutions were determined by the weight method, drying 1 ml of the solution on the watch glass, and palladium with ruthenium by the atomic adsorption method.

Electronic absorption spectra are registered on the Specord UV-VIS device, with the thickness of the quartz cuvette of 1 cm. The alcohol solutions for absorbance measurement were prepared directly in the cuvette in the following sequence: the calculated volume of the initial solution of CQD was diluted with 96% alcohol, and the required volume of the metal solution was added to this mixture by means of addition of calculated concentrations of the components. Aqueous solutions were prepared in the same sequence. The IR spectra were recorded with the Specord M-80 spectrometer, applying 3 drops of the solution to the thallium glass, followed by drying of the solution.

Result and discussion. Figure 2.1 shows the electronic absorption spectra of alcoholic solutions of palladium with different metal concentrations (curves 1-3), CQD with palladium (curve 4), 96% alcohol (curve 5) and CQD solution (curve 6).
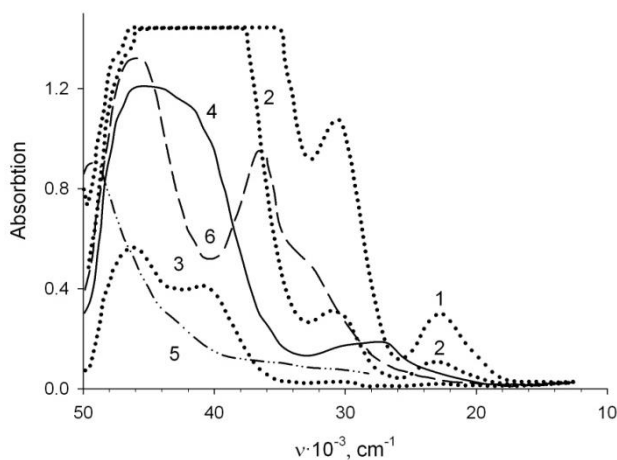
Fig. 2.1. *Absorption spectra of alcoholic solutions of CQD and palladium, mg/ml:*
1 – C_{CQD}= 0; C_{Pd}= 0.147; 2 – C_{CQD}= 0; C_{Pd}= 0.0368; 3 – C_{CQDf}= 0; C_{Pd}= 0.0037;
4 – C_{CQD}= 0.036; C_{Pd}= 0.0087; 5 – C_{C2H5OH}=96%; 6 – C_{CQD}= 0,030, C_{Pd}= 0.

As seen from the Figure, a 96% alcohol solution shows only one absorption band (AB) at 49300 cm^{-1} (Table 2.1), which corresponds to the n→σ* transition. For the solution of CQD, three ABs at 46000, 36700 cm^{-1} and also at 32500 cm^{-1} (as a shoulder) are seen, they correspond to the so-called β-, p- and α-AB, the intensity of which is different. The most intensive is β-AB at 46000 cm^{-1} (ε = 44), and the least intensive is α-AB at 32500 cm^{-1} (ε = 17.8). The AB data that relate to the classical unsaturated hydrocarbons are in the bathochromic shift. This shift is caused by the large number of the condensed rings of CQD and the corresponding polarity of a

Membrane and Sorption Materials and Technologies: Present and Future

solvent. At the same time, the stronger bathchromic shift of the *p*-band leads to the appearance of the α-AB in the form of a shoulder.

In the alcoholic solution of palladium chloride (curves 1-3), there are three ABs in the UV region. Two of them are located at 46000 and 41000 cm^{-1}: they correspond to ligand to metal charge transfer transitions (LMCTT) of Cl→Pd ($2e_u$→$3b_{1g}$ and $3e_u,b_{2u}$→$3b_{1g}$). Other AB is at 30700 cm^{-1} (LMCTT). One absorption band is in the visible region at 22700 cm^{-1}, it corresponds to d-d electron transitions in the metal ion ($2e_g$→$3b_{1g}$) and indicates the hydrolyzed form of the metal. The most likely form corresponds to the $[PdCl_3(H_2O)]^-$ composition. At the same time, no change of the AB position is observed, when the concentration of metal decreases.

Table 2.1. Bands of absorption of investigated solutions

Solution component	Positions of absorption bands in UV-VIS region, cm^{-1}					
Alcohol solutions						
Alcohol	49.3					
Graphene	46.0	36.7	32.5 shoulder			
Palladium	46.0	41.0	30.7	22.7		
Graphene and palladium	46-43.8	40.3	29.8	22.0; 26.5		
Aqueous solutions						
Graphene	46.0	36.7	32.5 shoulder			
Ruthenium	46.0	34.8	30.0 shoulder	27.7	25,7	21,7
Graphene and rithenium	46.0	36.0	30.0 shoulder	27.0 shoulder		

In contrast, the position of the AB in the spectra of the solution of CQD with palladium is somewhat different: the AB of d-d electronic transitions demonstrate a bathochromic shift to 700 cm^{-1}. Moreover, a new low-intensity AB appears at 26500 cm^{-1} indicating not only sorption of palladium on the CQD surface, but also the possible complex formation of palladium with carbon quantum dots. After all, the change of d-d electronic transitions (AB at 28000 cm^{-1}) shows the change in the coordinating environment of the metal. In addition, the position of the AB in the UV region is also changed as compared with the solution of the CQD themselves [5-7].

Figure 2.2 shows the absorption spectra of aqueous solutions of CQD and ruthenium. Since water (as well as alcohol) is also a polar solvent, the position of β-, p- and α-AB in the spectrum of the aqueous solution (curve 1) is not different from their position in the spectrum of alcohol solution of CQD (see Figure 1, curve 6). When the CQD are absent, three ABs are observed in the aqueous solution of ruthenium in the UV region (curve 2). Two intensive at bands at 46000 and 34800 cm^{-1} are visible, much less intensive shoulder-like AB at 40500·cm^{-1} is also seen. The bands are responsible for electronic transitions with charge transfer from metal to

ligand. Additionally, there are less intensive ABs at 30000, 27700, 25700 and 21700 cm^{-1} in the spectrum of ruthenium solution. These bands are responsible for LMCTT and d-d-electronic transitions ($^2T_2 \rightarrow ^4T_2$, $^1T_2 \rightarrow ^4T_1$, $^3T_1 \rightarrow ^1T_2$). It should be noted that the spectroscopy data characterize the location of the metal ion both in the three- (27700, 25700 cm^{-1}) and tetravalent (21700 cm^{-1}) state. Regarding the aqueous solution of CQD with ruthenium, only LMCTT (30000 cm^{-1}) and d-d electron transitions (26000 cm^{-1}) remain. These transitions characterize the trivalent state of the metal ion. In addition, one of the AB that is related to LMCTT shows a hypsochromic shift to 700 cm^{-1} in the UV region. Together it all indicates the changes of the nature of coordination environment of the ruthenium ions. They probably form coordination links with the CQD similarly to the palladium ions, [5-8].
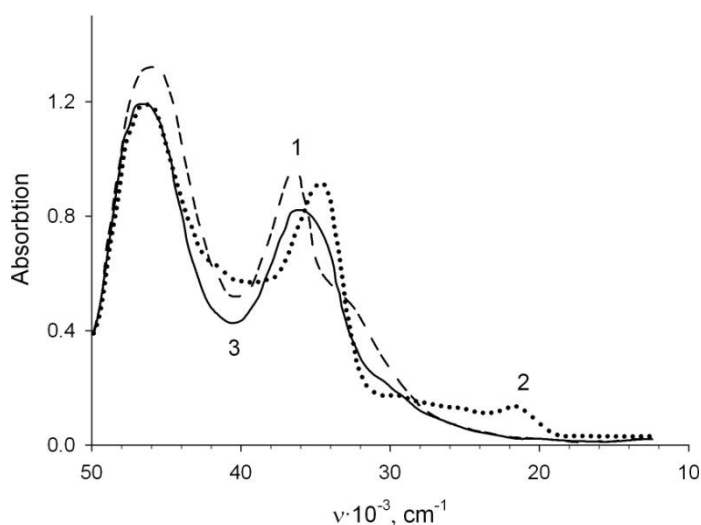
Fig. 2.2. *Absorption spectra of aqueous solutions of graphene and ruthenium (the concentration is expressed in mg/ml):*
$1 - C_{CQD} = 0,325$, $C_{Ru} = 0$; $2 - C_{CQD} = 0$, $C_{Ru} = 0,147$; $3 - C_{CQD}$ $0,0135$, $C_{Ru} = 0,0025$.

The IR spectra of CQD with palladium have been also obtained. The spectra include a number of characteristic absorption bands for functionalized CQDs. There are wide ABs at 3500, 3260 and 2930-3000 cm^{-1} in the high-frequency region, these bands are characteristic for stretching vibrations of H_2O as well as NH and aromatic CH fragments. Several absorption bands of the valence vibrations of carbonyl group (C=O) at 1830, 1840 and 1850 cm^{-1} indicate the presence of an anhydride group in the test sample with six-membered conjugate saturated and unsaturated rings. The AB of a doublet character at 1770 cm^{-1} indicates a C=O(NH) bond in the sample, and the AB at 1680 cm^{-1} as well as the doublet at 1640 cm^{-1} characterize the vibrations of ν(C=N) and δ(NH). Stretching vibrations for C=C bonds of aromatic rings are expressed as several ABs in the region of 1610-1540 cm^{-1}. At 1420 and 1280 cm^{-1}, there are in-plane deformation vibrations of C-H and -C-N- bonds respectively. The out of plane vibration of C-H corresponds to the band at 980 cm^{-1}. The AB of δ(C-H) in the spectra is also characteristic for 1,3- and 1,2,3-substituted aromatic derivatives. There is an AB that is related to ν(Pd-Cl) vibration in the low-frequency region at 330-340 cm^{-1}.

Conclusions. Thus, the investigation of the spectral characteristics of aqueous and alcohol solutions of carbon quantum dots with ruthenium and palladium showed a possible adsorption of metals on the surface of carbon quantum-sized carriers with the formation of coordination bonds with them on their accessible surface, which confirms the local fixation of metals on this surface. These systems are promising for the development of quantum-sized catalytic systems, which could be used as membrane modifiers. This approach allows us to create new types of the membranes, which combine predetermined hydrophilic-hydrophobic properties and catalytic ability.

References

1. *Goncharuk V.V., Ogenko V.M., Dubrovina I.V., Kucheruk D.D., Naboka O.V.* Carbon-silica composites with cllulose acetate, polyisocyanete and copper chloride // Physics and Chemistry of Solid State. 2016, V. 17. N 3. P. 407-412.
2. *Sergeev G.B.* Nanochemistry, Moscow University Publisher, Moscow, 2003. P. 201-217.
3. *Bukhtiyarov V.I., Moroz В.Л., Bekk I.E., Prosvirin I.P.* Size effects in catalysis by supported metal nanoparticles // Catalysis in Industry. 2009. V.1. N 1. P. 17-28.
4. *Eletskii A.V., Iskandarova I.M., Knizhnik A.A., Krasikov D.N.* Graphene: fabrication methods and thermophysical properties. // Physics-Uspekhi. 2011. V. 54. N 3. P. 227-258.
5. *Obraztsova E.D., Rybin M.G., ObraztsovP.A.* Graphene optical properties. In: *Carbon Photonics* (Konov V.I., ed.), Nauka, Moscow, 2017. P. 261-293.
6. *Bel'skaya O.B., Gulyaeva O.B., Gulyaeva T.I., Arbuzov A.B., Duplyakin V.K., Likholobov V.A.* Interaction between Pt(IV) and Pd(II) Chloro Complexes in Solution and on the ɣ-Al_2O_3 Surface // Kinetics and Catalysis. 2010. V. 51. N 1. P. 105–119.
7. *Hola K., Sudovska M., Kalitchuk S., Nachtigallova D.,Rogach A., Otyapka M., Zoril R..* Grafitic nitrogen triggers red fluorescence in carbon dots. // ACS NANO. 2017. V.11. N 12. P. 12402-12410.
8. *Buslaeva T.M., Simanova S.A.* State of platinum metals in aqueous solutions of hydrochloride acid and chlorides. Ruthenium, osmium // Russ. J. Coord. Chem. 2000. V. 26. N 6. P. 379-387.

ВЗАЄМОДІЯ ВУГЛЕЦЕВИХ КВАНТОВИХ ТОЧОК З РОЗЧИНАМИ ПАЛАДІЮ ТА РУТЕНІЮ

В.М. Огенко, Л.Б. Харькова, О.Г. Янко, С.І. Орисик, М.І. Буряк
Інститут загальної та неорганічної хімії ім.. В.І. Вернадського НАН України
email kharkova.ljudmila@gmail.com

Резюме. Методами електронної та ІЧ-спектроскопії досліджено процеси взаємодії в поверхновому шарі вуглецевих квантових точок (ВКТ) з розчинами рутенію та паладію. Встановлено, що, як у водному, так і в спиртовому розчинах ВКТ характеристичні смуги поглинання π→π*, n→π* електронних переходів в УФ-області та ППЗЛМ і d-d електронних переходів у видимій області зазнають відповідні зміни, які свідчить як про сорбцію металів на поверхні ВКТ, так і про можливе координування їх з ВКТ. Аналіз ІЧ-спектрів ВКТ також показав наявність ряду характеристичних смуг поглинання для функціоналізованих ВКТ, що доказує локальну фіксацію металів на поверхні ВКТ.

Ключові слова: квантові точки, метал-вуглець, каталітичні системи, рутеній, паладій.

UDC 544.47:544.72

CHAPTER 3

ADSORPTION MECHANISMS OF SELF-ORGANIZATION OF INORGANIC CARRIER – PREPARATION OF HETEROSTRUCTURES OF NATIVE ENZYMES

K.O. Kazdobin[1], K.D. Pershina[2], M.O. Khodykina[1], O.K. Trunova[1]

V.I. Vernadsky Institute of General and Inorganic Chemistry of the Ukrainian National Academy of Sciences, Kyiv, Ukraine.

E-mail: kazdobin@ionc.kiev.ua

[2]*Inter-Agensy Department of Electrochemical Energy Systems of the Ukrainian National Academy of Sciences, Kyiv, Ukraine*

Abstract: The influence of heterostructures (core-shell) formed by the native enzyme preparation extracted from black radish and white cabbage, immobilized on inorganic carriers with different surface nature on electrochemical properties of obtained materials is shown. Depending on the nature of support the mechanism for the binding of enzymes and their activity vary by the rate of activation. Based on the voltammetry of immobilized enzyme drugs on inorganic supports, the possibility of using these heterostructures as a basis for the devices for energy storage is shown.

Keywords: Native enzyme, immobilization, inorganic carrier, graphene, capacitor.

Introduction. Currently, the priority of electrochemical technology is the generation of energy from biomass [1-4]. Most studies are devoted to the creation of nanocomposite systems for the conversion of energy, components of which are electrically conductive "hierarchical" carbon materials, obtained by pyrolysis of natural raw materials [3-5]. Thus, currents of the order of 1 A/cm^2 of supercapacitor electrode based on products of white cabbage leaves pyrolysis [4], electrodes for lithium batteries based on rice husks [5] were obtained. The biofuel element [6], in which the cathode is zinc, and the anode is a laccase enzyme based on mushroom mildew is developed.

Enzymes, mainly peroxidase, are widely used in the biosensorics [7]. To enhance the biosensor signal, the adsorption of the enzyme to the quantum dot of metals, graphene, carbon nanotubes is used. In the biosensorics, the preparation of pure enzymes is needed. Inorganic materials, predominantly silicates, are investigated as carriers in a much smaller volume. Native enzyme preparations (extracts from plants) have not yet been investigated.

Experimental. We have studied a new class of materials – native enzyme drugs (NEDs), adsorbed on inorganic carriers with various acid-basic characteristics of the surface. As carriers, inorganic materials with a layered or gel structure were

used, namely, aluminosilicates: bentonite and its acidic (phosphate) form, kaolin, and pyrogenic silica aerosol 300. NEDs were adsorbed from root extract of radish black and white cabbage leaves.

According to the basic idea of the work, adsorption and subsequent crosslinking of the inorganic component with the enzyme drug creates heterostructures capable of spatial distribution of charges, changes the mechanism of chemical and electrochemical reactions, and opens new areas of application of the obtained materials.

For the study of heterostructures in the system of inorganic carrier-NED the following physico-chemical and electrochemical methods were used: atomic absorption spectrophotometry (AAS), spectrophotometry, scanning electron microscopy (SEM), cyclic voltammetry (CVA), electrochemical impedance spectroscopy (EIS) [8-12].

On the basis of heterostructures such as inorganic carrier - NED - graphene, electrodes are synthesized, their electrochemical properties and possible applications are investigated.

Results and discussion. According to the data of atomic absorption analysis, in native and immobilized enzyme drugs the metal ions of variable valence (Fe^{3+}, Cu^{2+}, Ni^{2+}, Mn^{2+}, Zn^{2+}) that are capable of redox transitions and the formation of surface complexes with charge transfer on the surface of inorganic carriers has been established (Table 3.1).

Obviously, the content of metal ions in the samples is significantly different. This indicates the differences in the composition and structure of the catalytic and adsorption centers of the protein molecule, which affects the electrochemical properties of the heterostructures being formed.

Table 3.1. The content of metal ions in the native / immobilized on inorganic carriers enzyme drug based on extract from radish black/white cabbage

System	Metal ions content, %				
	$Fe^{3+} \times 10^{-3}$	$Cu^{2+} \times 10^{-4}$	$Ni^{2+} \times 10^{-5}$	$Zn^{2+} \times 10^{-4}$	$Mn^{2+} \times 10^{-4}$
NED	1.85/0.63	1.20/0.10	6.72/7.40	5.38/3.46	– /0.64
Bentonite + NED	2.55/3.15	0.32/0.06	6.50/7.40	4.62/3.40	–/0.64
Mod. bent. + NED	1.40/1.35	0.17/0.03	6.70/4.70	4.30/23.00	–/0.64
Aerosil 300+ NED	0.30/1.74	0.012/ 0.016	2.40/1.20	1.50/0.99	–/0.06
Kaolin + NED	0.77/1.25	0.12/0.06	5.01/7.40	2.90/3.47	–/0.48

The analysis of irreversible binding of metal ions has established that natural bentonite selectively binds Cu^{2+} /Cu^{2+}, Ni^{2+}, Mn^{2+}, Zn^{2+} ions, modified with phosphate-ions bentonite – Fe^{3+}, Cu^{2+}, Zn^{2+}/ Cu^{2+}, Ni^{2+} ions, kaolin – ions Fe^{3+}, Cu^{2+}, Ni^{2+}, Zn^{2+}/ Fe^{3+}, Cu^{2+}, Ni^{2+}, Zn^{2+}, and aerosol 300 – all metal ions (Fe^{3+},

Cu^{2+}, Ni^{2+}, Zn^{2+}/ Fe^{3+}, Cu^{2+}, Ni^{2+}, Mn^{2+}, Zn^{2+}). This dependence (Table 3.2) is in accordance with the structure of the carrier and the structure formed by the ion in the original enzyme. The presence of all metal ions indicates the presence of three classes of enzymes: peroxidase, superoxide dismutase, and catalase.

Table 3.2. Equivalent ratios of immobilized metal ions on the surface of inorganic supports

Support	Equivalent ratios	
	Black radish extract	White cabbage extract
Bentonite + NED	Cu_1	Cu_1: $Ni_{1.6}$: $Zn_{6.8}$: $Mn_{1.8}$
Mod.bent. + NED	$Fe_{11.7}$: $Cu_{5.5}$: Zn_1	Cu_1 : $Ni_{1.67}$
Kaolin + NED	$Fe_{89.8}$: $Cu_{9.8}$: Ni_1 : Zn_{19}	$Cu_{1.2}$: $Ni_{1.8}$: Zn_7 : Mn_1
Aerosil 300+ NED	$Fe_{40.1}$: $Cu_{3.1}$: Ni_1 : $Zn_{9.6}$	$Fe_{33.5}$: $Cu_{2.5}$: Ni_2 : Zn_{16} : Mn_1

Scanning electron microscopy of the obtained materials [11] showed that the adsorption of the native enzyme preparation on the surface of the carriers is accompanied by denaturation of the polysaccharide portion of the enzymes and the formation of a surface heterostructure. Namely in this heterostructure the spatial divide of charges of metal-containing fragments of enzymes occurs. This phenomenon is determined by the acidic - basic properties of the support surface.
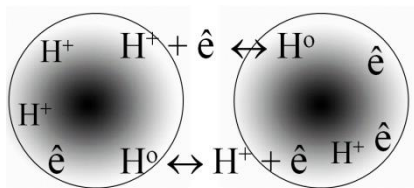
Fig. 3.1. Scheme of charge exchange in the particles of heterostructures.

The impedance measurements of suspensions established proton conductivity, as well as the divide into two groups [10]. In one group, the charge transfer was similar to that of imperfect electrolytes [13]. It includes all the systems of inorganic carrier − NED of white cabbage and NED of black radish adsorbed on bentonite and its acidic form. The second group (the systems of carrier and NED of black radish adsorbed on kaolin and aerosol) included systems with charge transfer according to two mechanisms: along a matrix and a shell (Figures 3.1, 3.2).

a)   b)

Fig. 3.2. Equivalent schemes of suspensions based on aerosol 300-NED of black radish (a) and white cabbage (b).

To find out the nature of the results obtained, the electronic spectra of 20% NED solutions obtained from different extracts were studied. They confirmed

the formation of structures with charge transfer on the carrier surface. This indicates the mechanism of "crosslinking" the enzyme with the carrier.

Two peaks are revealed on the electronic spectra obtained from the NED of black radish (Figure 3.3a). The peak of 29920 cm^{-1} corresponds to Fe^{3+} ions with the d^5 configuration and the coordination number of 6 (octahedral symmetry group). This corresponds to a low spin octahedron with a of $T_{2g} \rightarrow {}^2A_{2g}$, ${}^2T_{1g}$. The triplet in the region of 30960 cm^{-1} confirms this assumption. A Gauss spectral deconvolution revealed a Cu^{2+} band with a maximum of 13459 cm^{-1}, which corresponds to a distorted hexagonal bipyramid with a coordination number of 5 ($A_{1g} \rightarrow T_{1g}$ transfer).

a

b
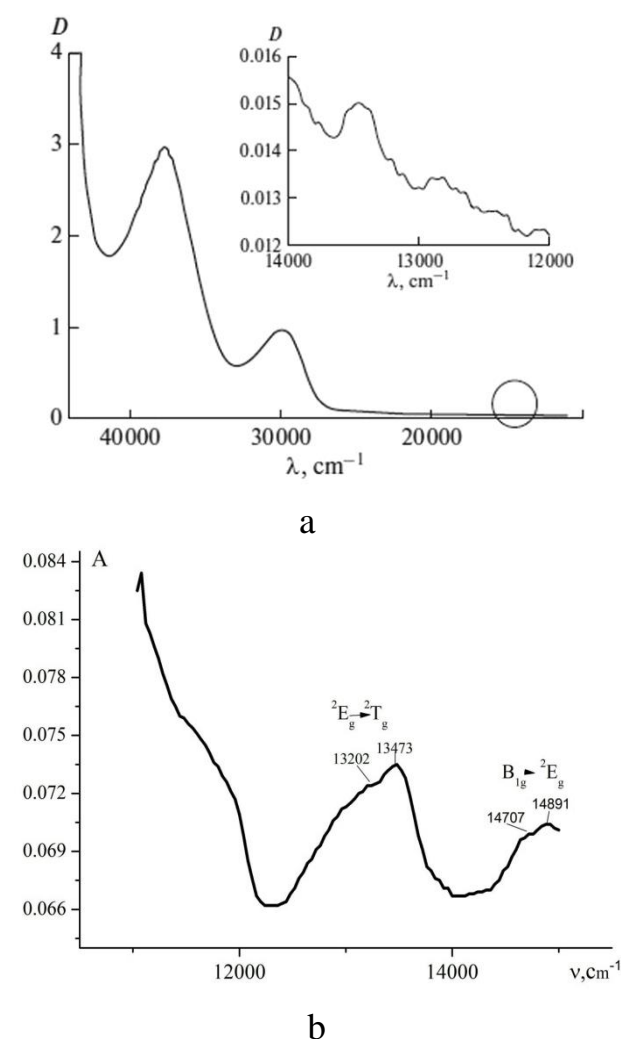
Fig. 3.3. *Electron absorption spectra of the NED ($C_{e.p.} = 20\%$, $\lambda = 5000 - 11000$ cm^{-1}, l=1 cm): extracted from radish black (a), white cabbage (b).*

In electron spectra obtained from NED of white cabbage (Figure 3.3b), the peaks correspond to Cu^{2+} ion (distorted octahedron) with transfers of ${}^2E_g \rightarrow {}^2T_g$ (13202 and 13473 cm^{-1}) and $B_{1g} \rightarrow {}^2E_g$ (14707 and 14891 cm^{-1}). No other interactions were detected.

An enzyme drug, which was prepared from radish black, contains two interacting enzymes: peroxidase and superoxide dismutase in approximately equal ratios [14]. The spectrum of NED of white cabbage extract indicates only the presence of Cu^{2+} ion.

It has been established by CVA [12] that the heterostructures based on aerosol 300-NED of the radish black root behave as a supercapacitor (Figure 3.4a) [1]. Somewhat lower values of the current and voltage data have been obtained for the white cabbage extract (Figure 3.4b).

At different rates of potential sweep ($\tau_2 - \tau_1$), the values of the ΔE difference of the initial and final sweep potentials E_1 to E_2, the mass of the sample (m), the module of the specific current (I) and the data of impedance spectroscopy on the initial capacitance.

Table 3.3. Characteristics of charge capacities of heterostructures

System	$C_{in} \cdot 10^{-3}$, F/g	Black radish	White cabbage
		C_{ef}, F/g	$C_{ef} \cdot 10^{-3}$, F/g
Bentonite + NED	0.62	1.6	26.3
Mod.bent. + NED	1.14	0.068	1.53
Kaolin + NED	1.74	51.3	0.39
Aerosil-300+ NED	0.38	95.7	3.56

a)   b)
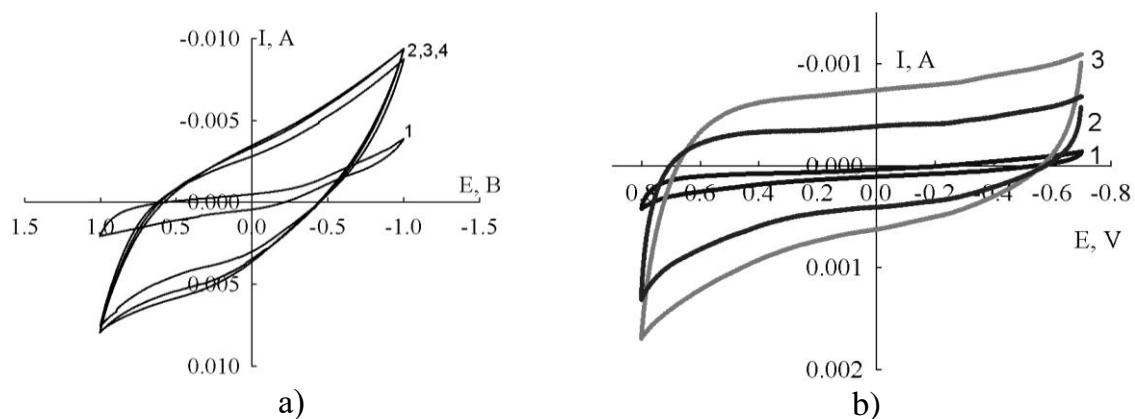
Fig. 3.4. *CVA for heterostructures aerosil 300 - NED from radish black (a), white cabbage (b) on the potential sweep rate (mV/s): 1- 5, 2-50, 3- 100. Electrolyte is a saturated solution of KCl, S_{el} = 1.5 cm², sample of heterostructure - 3 mg/cm².*

The capacitance of the studied materials (Table 3.3) are calculated according to the known ratio:

$$C = \frac{I \cdot (\tau_2 - \tau_1)}{(E_1 - E_2) \cdot m}$$

(3.1)

It has been established that the systems based on the carrier - NED (white cabbage) are characterized by low current values relative to materials based on radish black. This means the inexpediency of the use of these materials in electrochemical devices.

Different behavior can be seen in equivalent schemes obtained by impedance spectroscopy (see Figure 2). Regarding radish extract, an equivalent circuit shows the possibility of transfer of charge through two mechanisms, and hence the possibility of energy conservation. For cabbage, the scheme is an electrolyte.

Conclusions. The comparative analysis of the physicochemical properties of synthesized heterostructures, which contain an enzyme drug of black radish and white cabbage, shows different behavior of heterostructures depending on support. This is caused by different mechanisms of binding of an enzyme drug with an inorganic carrier and the possible formation of core-shell structures.

The formation of heterostructures, which are able to accumulate charge in inorganic systems of aerosol 300-enzyme-graphene, makes it possible to apply them to redox transformations. Such heterostructures can be promising materials in energy conversion devices (supercapacitors) up to 95 F/g, having commercial values. They can be also used for cheap and biocompatible current sources.

References

1. *Matthews M.A.* Green electrochemistry // Pure and Applied Chemistry. 2001. V. 73.8. P. 1305-1308.
2. *Clark J.H., Macquarrie D.J., eds.* Handbook of green chemistry and technology. John Wiley & Sons, 2008.
3. *Zhang Y., Liu X., Wang Sh., et al.* Bio-Nanotechnology in High-Performance Supercapacitors // Advanced Energy Materials. 2017. V.7. P. 1700592.
4. *Wang P., Wang Q., Zhang G. et al.* Promising activated carbons derived from cabbage leaves and their application in high-performance supercapacitor electrodes // J. Solid State Electrochemistry. 2016. V. 20(2) P. 319-325.
5. *Kaviyarasui K., Manikandan E., Kennedy J. et al.* Rice husks as a sustainable source of high quality nanostructured silica for high performance Li-ion battery requital by sol-gel method // Adv. Mater. Lett., 2016, 7(6), 100-150.
6. *Majdecka D., Draminska S., Stolarczyk K. et al.* Sandwich Biobattery with Enzymatic Cathode and Zinc Anode Integrated with Sensor // J. Electrochem. Society. 2015. V. 162 (6). P. F555-F559.
7. Wang, J. Electrochemical glucose biosensors A Review // Chemical reviews. 2008. V.108.2. P. 814-825.
8. *Vyatkina O., Lavrentieve I., Ermakova M.* Catalytic activity of peroxidase pf black radish relatively to substrates – reducing agents of different nature // Visnyk Lvivskogo Universitetu. Seriya Khimichna. 2012. № 53. P. 357–362.
9. *Khodykina M.O. Pershina E.D., Kazdobin K.A.* Electrochemical properties of immobilized ferment drugs of *Raphanus l. Var. Niger* on water insoluble substrates // Ukrainian Chemical Journal. 2015. V. 81. № 4. P. 116–119.
10. *Pershina K.D. Khodykina M.O., Kazdobin K.A.* Analysis of the activity of immobilized enzyme preparations of black horseradish using electrochemical impedance spectroscopy // Surface Engineering & Applied Electrochemistry. 2015. V. 51. №. 6. P. 572–580.

11. *Khodykina M.O. Pershina K.D., Kazdobin K.A., Trunova E.K.* Immobilization of the Raphanus sativus l. Var. Niger enzyme preparation on natural bentonite and bentonite modified by phosphate ions / // Surface Engineering & Applied Electrochemistry. 2017. V. 53, № 2. P. 196–201.
12. *Pershina K.D., Khodykina M.O., Kazdobin K.A., Shulga S.V.* Voltammetric Responses of Black radish Enzyme preparation immobilized on Kaolin and Aerosil // Surf. Engineering & Appl. Electrochemistry. 2017. V. 53, № 6. P. 542–550.
13. *Pershina K.D., Kazdobin K.O.* Impedance spectroscopy for eletrolytic materials, Osvita Ukraini, Kyiv, 2012.
14. *Singh B.K., Sharma S.R., Singh B.* Antioxidant enzymes in cabbage: Variability and inheritance of superoxide dismutase, peroxidase and catalase // Scientia Horticulturae. 2010. V.124. P. 9–13.

УДК 544.47:544.72

АДСОРБЦІЙНІ МЕХАНІЗМИ САМООРГАНІЗАЦІЇ ГЕТЕРОСТРУКТУР НЕОРГАНІЧНИЙ НОСІЙ - НАТИВНИЙ ФЕРМЕНТНИЙ ПРЕПАРАТ

К.О. Каздобін[1], К.Д. Першина[2], М.О. Ходикіна[1], О.К. Трунова[1]

*[1] Інститут загальної та неорганічної хімії ім. В.І. Вернадського НАН України,
пр. Палладіна, 32/34, Київ, 03142, Україна
E-mail: kazdobin@ionc.kiev.ua*
*[2]Міжвідомче відділення електрохімічної енергетики НАН України,
пр. акад. Вернадського, 38а, м Київ, 03142, Україна*

Встановлено вплив складу композиційного матеріалу (core-shell структури), утвореного нативним ферментним препаратом – витяжкою з редьки чорної або капусти, іммобілізованим на неорганічних носіях з різною природою поверхні на їх активність і електрохімічні характеристики. Показано, що в залежності від природи носія механізм іммобілізації ферментів, їх активність і швидкість інактивації змінюються. На основі аналізу вольтамперометрії іммобілизованого ферментного препарату на неорганічних носіях показано можливість використання таких композитних матеріалів для створення пристроїв для накопичення енергії.
Ключові слова*: нативний фермент, іммобілізація, неорганічний носій, графен, ємність.*

CHAPTER 4

POLYMER MEMBRANES WITH ENHANCED STABILITY TO BIOFOULING

P.V. Vakuliuk[1], I.M. Furtat[1], O.O.Yatseyko[1]
[1]National University of Kyiv-Mohyla Academy,
2, Skovoroda St., Kyiv, 04655, Ukraine
email *vakuliuk@ukma.edu.ua*

Abstract. *The major problem in membrane separations is biofouling as it leads to more frequent chemical cleaning, higher operating pressures, shortened membrane life, and compromised product water quality. Methods of creation of new polymer composite membranes with increased resistance to biofounling by bulk and surface modification of membranes have been developed, separation and functional properties of the received membranes have been investigated. The performed researches allowed to create a number of new functionalized membranes with a wide range of properties and to improve the technological processes of obtaining hydrophilic, charged and bactericidal polymer membranes to increase their usage for water treatment, concentration and separation of substances of different nature.*
Keywords*: polymer membranes, biofouling, bulk and surface modification.*

Introduction. The relevant issue is creation of new polymer composite membranes and improvement of modification method of commercial polymer membranes with the use of new types of bactericidal modifying agents. The modifying agents of bactericidal action must meet the requirements of high bactericidal stability and, at the same time, the ability to both effective surface and volume modification of membranes. Ultimately, it will create new types of competitive membranes with the necessary transport characteristics and long-term resistance to biofouling.

Our attention is focused on the involvement of polymer ultra- and microfiltration membranes in the process of modification, especially with ion-containing oligomers of various chemical nature and molecular architecture, as well as ion-containing polymers and their complexes. The study of the influence of chemical nature of modifying agents, as well as modification methods of surface and structure chemical nature of the resulting composite membranes, their functional properties, in particular the resistance to biofouling, has practical value in the fundamental plans and in the aspects of applied application.

Numerous studies in the field of membrane technology show that the creation of new membranes is economically unprofitable; therefore, modification is the main method of solving this problem. The attachment of bacterial cells to the membrane surface is the first step in the formation of biofilm. There are many factors that affect the ability of cells to attach. Conditionally, they can be

divided into bacterial characteristics, membrane characteristics and technological parameters. In our work, attention at membrane charge and the hydrophobicity of its surface was focused.

The aim of the work is to extend the life of the membranes due to the creation of increased resistance to biofouling by modifying the surface with substances that either prevent unwanted interactions (adhesion) between the pollutants and the membrane, or destroy the microorganisms that settle on the surface of the membrane. Conditionally these strategies can be divided into strategies of "defending" and "attacking". The strategy of "defending" provides surface characteristics that would not allow the bacteria to join the surface of the membrane, for example, hydrophilicity. The strategy of "attacking" involves the functionalization of bactericidal agents, which, in the case of cell contact, lead to their death.

The methods of bulk and surface modification for different types of polymer membranes, characterization of the influence of modification methods and the nature of modifying agents on the selective surface layer characteristics and the structure of composite membranes, selectivity , as well as creation of composite polymeric membranes with increased resistance to biofouling was also aimed.

Experimental. In this study two polymers – polyacrylonitrile (PAN) and polyethylene terephthalate (PETF) were selected for creating of the membranes. Membranes from PAN polyacrylonitrile were made by phase inversion. PETF is industrial membrane, which is a model object for study. The difference between the membranes consists in structure points: PAN - asymmetric with a selective layer, PETF membranes have cross-cut straight pores.

In our work, modifying agents are selected according to the "defending" and "attacking" strategies. N-vinyl-2-pyrrolidone and methacrylic acid have been selected to create "defending" effect. The difference between these modifiers is that methacrylic acid provides carboxyl groups of the membrane surface, and N-vinyl-2-pyrrolidone provides amide-carbonyl -N-C=O groups. In order to implement the "attacking" strategy, GO (guanidine-containing oligomer) and PVP-I$_3$ were selected.

Bactericidal agents are selected depending on the mechanism of action against bacterial cells. Guanidin-containing oligomers, penetrating through the cell wall, are embedded in the phospholipid layer of the immiscible metamorphic membrane, resulting in its defragmentation. There is a loss of vitality of the cell. The main effect of *Povidone-iodine* is the oxidation of amino acids of bacterial cell proteins by the release of iodine complex, inhibition of the synthesis of toxins (alpha-hemolysin, phospholipase C and lipase), and inhibition of the activity of enzymes (elastase, beta-glucoronidase). For example, representatives of *Pseudomonas* produce elastase, which is a factor in pathogenicity. Iodine suppresses the activity of this enzyme.

Results and discussion. Surface modification of the membranes by methacrylic acid leads to contact angle decreasing of the PAN and PETF membranes from 40° to 20°, respectively, and by vinyl pyrrolidone - from 30° to 15°. Surface recharging as a result of the modification of polyacrylonitrile and polyethylene terephthalate membranes with methacrylic acid gives the surface a negative charge that repels bacterial cells, which is associated with repulsion of charges of the same name.

Modification with polyvinylpyrrolidone does not create the phenomenon of recharging the surface. Modification with guanidinium oligomer leads to a positive charge on the surface, which promotes the contact of negatively charged bacteria (Table 4.1). While membranes with immobilized polyvinylpyrrolidone iodine complex, membrane charge does not change.

Table 4.1. Adhesion of bacteria on membrane surface,%

Membrane	*P fluorescens* 8573	*S. aureus* ATCC25923	*E. coli* ATCC 25922	*C. stationis* Ukm Ac 719
PAN	98	71	84	81
PETF	90	67	79	77
"Protection" strategy				
PAN-PMAA	38	17	25	20
PAN-PVP	41	19	20	24
PETF-PMAA	43	23	32	30
PETF-PVP	48	26	37	32
"Attack" strategy				
PAN-PMAA-GO	41	19	20	24
PAN-PVP-I_3	34	16	23	21
PETF-PMAA-GO	48	26	37	32
PETF-PVP-I_3	39	19	26	18

Conclusions. Modification of membranes with methacrylic acid and polyvinylpyrrolidone results in surface and prevents the adhesion of hydrophobic test cultures, implementing the strategy of "defending". The most effective "protective" agent is methacrylic acid.

Modifying membrane surface with more hydrophobic polymer based on polyacrylonitrile reduces the adhesion of test cultures to the surface by 50-60%, and for polyethylene terephthalate membranes with less hydrophobic properties by 40-45%.

References

1. *Zhao X., Zhang R., . Liu Y., He M., Su Y., Gao K., Jiang J.* Antifouling membrane surface construction: Chemistry plays a critical role // J. Membr. Sci. 2018. V. 551. P. 145–171.
2. *Jiang S, Li Yu., Ladewig P.B.* A review of reverse osmosis membrane fouling and control strategies // Sci. Total Envir. 2017. V. 595. P. 567–583.

3. *Ye G., Lee J., Perreault F., Elimelech M.* Controlled architecture of dual-functional block copolymer brushes on thin-film composite membranes for integrated "defending" and "attacking" strategies against biofouling // ACS Appl. Mater. Interfaces. 2015. V. 7. N 41. P. 23069–23079.

ПОЛІМЕРНІ МЕМБРАНИ З ПІДВИЩЕНОЮ СТІЙКІСТЮ ДО БІОЗАБРУДНЕННЯ

П.В. Вакулюк[1], І.М. Фуртат[1], О.О.Яцейко[1]
[1]Національний університет «Києво-Могилянська академія»,
2, вул .Сковороди, Київ, 04655, Україна
email vakuliuk@ukma.edu.ua

Резюме. *Основною проблемою в процесах мембранного розділення є біозабруднення мембран, адже це призводить до підвищення робочих тисків, скороченого терміну експлуатації мембран, необхідності очищення мембран тощо. Розроблені методики створення нових полімерних композитних мембран з підвищеною стійкістю до біозабруднення за допомогою об'ємного та поверхневого модифікування мембран та досліджені розділові та функціональні властивості одержаних мембран. Виконані дослідження дозволили створити низку нових функціалізованих мембран з широким діапазоном властивостей і удосконалити технологічні процеси одержання гідрофільних, заряджених та бактерицидних полімерних мембран для підвищення ефективності їх використання в галузях водопідготовки, концентрування та розділення речовин різної природи.*
Ключові слова: *полімерні мембрани, біозабруднення, об'ємне і поверхневе модифікування.*

CHAPTER 5

SYNTHESIS AND APPLICATION OF NANOPOROUS FUNCTIONAL MATERIALS

N.D. Shcherban

L.V. Pisarzhevsky Institute of Physical Chemistry, National Academy of Sciences of Ukraine, 31 pr. Nauky, Kiev, 03028, Ukraine

email nataliyalisenko@ukr.net

Abstract. *The available literature data and results of own investigations on the methods of preparation, structure, sorption properties and functional characteristics of micro-mesoporous zeolite-like and carbon nanoporous materials were summarized. The features and the prospect of using the mentioned systems in catalysis, photocatalysis, adsorption, electrochemistry were shown.*

Keywords: *micro-mesoporous zeolite-like materials, doped carbon, carbon nitride, silicon carbide, hard-template synthesis.*

Introduction. In recent years, creation of micro-mesoporous materials (the terms mesoporous and hierarchical zeolites are also used), combining the properties of zeolites and mesoporous molecular sieves (MMS) attracts the attention of researchers [1-4]. Such materials are characterized by an enhanced accessibility of sorption space and active sites for reagent molecules, and as a result an increase of catalytic activity in reactions involving bulk molecules. Carbon-containing nanoporous materials (carbon, silicon carbide, carbon nitride) can be functionalized in wide limits for regulation the reactivity [5-10]. For example, carbon nitride g-C_3N_4 is interesting due to unique electronic properties, photocatalytic and catalytic activity (as a result of incomplete condensation and surface defects) [11,12].

The aim of the current work is to establish a connection between composition, structure, porosity, chemical nature of the surface of micro-mesoporous zeolite-like and carbon-containing nanoporous materials and their sorption, including acid-base properties; the development of methods and the search for areas of possible application of nanoporous materials for obtaining new catalysts of acid-base transformations, in particular, involving bulk molecules, and photocatalysts, electrode materials for supercapacitors, adsorbents for carbon dioxide, hydrogen, etc.

Experimental. The detailed synthesis procedures were given in the corresponding previous papers [13-15,17-23].

Results and discussion. Zeolite-like mesoporous foams of the cellular structure were obtained by a template method on the basis of the initial products of crystallization of β zeolite. The prepared materials have high textural *(S_{BET} up to 690 m^2/g, V_{pore} up to 1.5 cm^3/g, $D_{pore}=21–23$ nm)* and acid (total concentration of Brønsted and Lewis acid sites up to 0.4 mmol/g, maximum of ammonia thermodesorption ∼ 350 ºC) characteristics [13]. Potentiometric titration shown that low-crystalline and X-ray amorphous micro-mesoporous materials contain acid sites close to beta zeolite by strength (lg *K* values 4.3 – 4.7). High content of acid sites in this kind of samples can be assigned to the acidity of zeolite precursors rather than zeolite crystals [14]. The obtained materials exhibit high catalytic activity in verbenol oxide isomerization towards a compound with p-menthol structure possessing anti-parkinson activity. The catalytic activity of the investigated materials, in particular the TOF values for the obtained low-crystalline samples, were significantly higher than for conventional zeolite, which can indicate a zeolite-like structure of the resulting samples in their entire volume [13].

Isomerization of α-pinene oxide, the products of which are important for pharmaceuticals and perfumery, was investigated over three types of ZSM-5 based micro-mesoporous aluminosilicates obtained by a dual-template method, steam-assisted conversion and dual-functional templating [15]. The highest reaction rate was observed over an X-ray amorphous micro-mesoporous aluminosilicate possessing both developed porosity and a low concentration of medium strength acid sites giving the total conversion of α-pinene oxide already in 60 min. Symbatic dependence between the yields of the main products and accessibility index of the micro-mesoporous materials indicates a crucial role of the catalyst porous structure in the investigated reaction. The most appropriate (in terms of conversion and selectivity towards trans-carveol) catalysts for α-pinene oxide isomerization were prepared via the low-temperature dual-template method using sol-precursors of ZSM-5 zeolite and a micellar template. Obviously, this approach allows formation of both developed mesoporous structure and mild acidity due to application of small building units and possibility of their recrystallization and self-organization in hydrothermal conditions.

The method of matrix or hard-template synthesis consists in the replication of the porous structure of an inorganic (in particular silica) matrix (exotemplate) with other substances (carbon, carbon nitride, etc.) [16]. For this purpose, the precursor (in particular, organic one) is subjected to pyrolysis in the pores of an inorganic matrix, – a substance (e.g. carbon) formed as a result of pyrolysis, is isolated by treatment of the resulting composite with hydrofluoric acid or alkali. The advantage of the hard-template synthesis is the possibility of obtaining materials with uniform in size and shape pores, which is due to pyrolysis performing in a kind of nanoreactor, whose reaction space is limited by the walls of the framework.

N- and B-doped carbons possessing high spatial ordering, developed surface and porosity were prepared by hard-template and bulk carbonization of sucrose in the presence of melamine and boric acid, respectively. The obtained materials exhibit high interfacial capacitance (up to 0.36 F/m^2), which enables application of synthesized samples as materials of supercapacitors [17,18].

Nonstoichiometric carbon nitride samples characterized by spatial ordering, large pore volume (up to 0.8 cm^3/g) and specific surface area (up to 585 m^2/g) were prepared via matrix pyrolysis of ethylenediamine in the presence of CCl_4 in MMS KIT-6 and MCF as hard templates. In contrast to nitrogen-doped carbons (obtained by incorporation of N into carbon structure in the result of compatible thermal treatment of the initial porous carbon with melamine) nonstoichiometric carbon nitride possesses much more nitrogen (up to 13.7 wt.% (C/N = 6), vs. 0.6 wt.%) and an increased concentration of basic nitrogen-containing groups – up to 0.68 mmol/g (vs. 0.46 mmol/g). An increase of adsorption capacity towards hydrogen and carbon dioxide, namely adsorption potential, differential heat of CO_2 adsorption, specific adsorption on the pore surface – from 5.4 to 7.3 $\mu mol\ H_2/m^2$ and from 2.2 to 5.4 $\mu mol\ CO_2/m^2$ for carbon and synthesized nonstoichiometric carbon nitride, respectively, due to the incorporation of nitrogen atoms into the carbon framework was revealed [19].

Silicon carbide samples with a developed surface (up to 410 m^2/g) and large pore volume (up to 1.0 cm^3/g) were prepared by carbothermal reduction of carbon-silica composites base on silica MMS (SBA-15, KIT-6, MCF, SBA-3). The formation of SiC with high porosity parameters is facilitated by an application of MMS KIT-6 of the 3-dimensional structure with mutually intersecting mesoporous system, C/SiO_2 ratio close to the stoichiometric one, and an increased level of the pore filling of silica MMS with carbon. High hydrogen adsorption capacity (energy $|\Delta\mu_o|$, specific adsorption on the pore surface ρ) of nanoporous silicon carbide samples was demonstrated. The maximal among the investigated porous materials specific adsorption of H_2 by SiC (ρ – up to 15 $\mu mol/m^2$, 1.2 wt.% H_2 at S_{BET} = 400 m^2/g) was observed [20].

Porous carbon nitrides were obtained via bulk and hard template (SBA-15 and MCF) pyrolysis of melamine. It was shown that carbon nitride obtained by the hard-template method in MCF has a higher band gap (2.87 eV), compared with a bulk sample (2.45 eV), and, accordingly, exhibits a higher photocatalytic activity in photoreduction of carbon dioxide (to acetaldehyde 8.0 $\mu mol \cdot g^{-1}$ and methane 0.78 $\mu mol \cdot g^{-1}$) [21].

Incorporation of sulfur into C_3N_4 leads to a significant increase of the light absorbance intensity especially in the UV region compared to undoped sample. Doping C_3N_4 with sulfur during thermal treatment of melamine and sulfuric acid which is also accompanied with the porosity enhancement increases the catalytic activity in CO_2 photoreduction almost tenfold [22].

It has been shown that melamine-derived g-C_3N_4 can act as an effective catalyst for the Knoevenagel condensation between benzaldehyde and

ethylcyanoacetate to form ethyl-α-cyanocinnamate (conversion of benzaldehyde up to 100%, yield of the desired product up to 51%), which is important for creation of potentially biologically active compounds and fine organic synthesis. The highest yield of the desired product was achieved over carbon nitride obtained using silica as a hard template. Weak basic sites assigned as C-N=C species contribute to an increase of selectivity towards the desired product, while the conversion of benzaldehyde is increased as a result of an increase of tertiary nitrogen content [23].

Conclusions. Thereby, formation of micro-mesoporosity for zeolite structures contributes to an increase the accessibility of catalytically active sites for reactants. Such structures can be considered as nanoreactors, where the transformation of molecules takes place in micro- and mesopores, providing transport of reagents to the active sites of the catalyst, which allows to perform catalytic reactions with the participation of relatively bulk molecules and to regulate the selectivity of the process.

In the case of carbon-containing nanoporous materials, application of the hard-template method and purposeful functionalization (with certain elements, etc.) allows to regulate porosity, acid-base properties influencing the catalytic and photocatalytic (for C_3N_4) activity.

References

1. *Perego C., Millini R.* Porous materials in catalysis: challenges for mesoporous materials // Chem. Soc. Rev. 2013. V. 42. P. 3956-3976.
2. *Linares N., Silvestre-Albero A. M., Serrano E., Silvestre-Albero J., García-Martínez J.* Mesoporous materials for clean energy technologies // Chem. Soc. Rev. 2014. V. 43. P. 7681-7717.
3. *Schwieger W., Machoke A. G., Weissenberger T., Inayat A., Selvam T., Klumpp M., Inayat A.* Hierarchy concepts: classification and preparation strategies for zeolite containing materials with hierarchical porosity // Chem. Soc. Rev. 2016. V. 45. P. 3353-3376.
4. *Feliczak-Guzik A.* Hierarchical zeolites: Synthesis and catalytic properties // Micropor. Mesopor. Mater. 2018. V. 259. P. 33-45.
5. *Li Y., Wang G., Wei T., Fan Z., Yan P.* Nitrogen and sulfur co-doped porous carbon nanosheets derived from willow catkin for supercapacitors // Nano Energy. 2016. V. 19. P. 165-175.
6. *Borchardt L., Zhu Q. L., Casco M. E., Berger R., Zhuang X., Kaskel S., Feng X., Xu Q.* Toward a molecular design of porous carbon materials // Mater. Today. 2017. V. 20. P. 592-610.
7. *Borchardt L., Hoffmann C., Oschatz M., Mammitzsch L., Petasch U., Herrmann M., Kaskel S.* Preparation and application of cellular and nanoporous carbides // Chem. Soc. Rev. 2012. V. 41. P. 5053-5067.
8. *Duong-Viet C., Ba H., El-Berrichi Z., Nhut J. M., Ledoux M. J., Liu Y., Pham-Huu C.* Silicon carbide foam as a porous support platform for catalytic applications // New J. Chem. 2016. V. 40. P. 4285-4299.
9. *Lakhi K. S., Park D. H., Al-Bahily K., Cha W., Viswanathan B., Choy J. H., Vinu A.* Mesoporous carbon nitrides: synthesis, functionalization, and applications // Chem. Soc. Rev. 2017. V. 46. P. 72-101.

10. *Zhang J., Zhang M., Lin S., Fu X., Wang X.* Molecular doping of carbon nitride photocatalysts with tunable bandgap and enhanced activity // J. Catal. 2014. V. 310. P. 24-30.

11. *Liu J., Wang H., Antonietti M.* Graphitic carbon nitride "reloaded": emerging applications beyond (photo) catalysis // Chem. Soc. Rev. 2016. V. 45. P. 2308-2326.

12. *Zheng Y., Lin L., Wang B., Wang X.* Graphitic carbon nitride polymers toward sustainable photoredox catalysis // Angew. Chem. Int. Ed. 2015. V. 54. P. 12868-12884.

13. *Torozova A., Mäki-Arvela P., Shcherban N. D., Kumar N., Aho A., Stekrova M., Valkaj K. M., Sinitsyna P., Filonenko S. M., Yaremov P. S., Ilyin V. G., Volcho K. P., Salakhutdinov N. F., Murzin D. Yu.* Effect of acidity and texture of micro-, mesoporous and hybrid micromesoporous materials on the synthesis of paramenthanic diol exhibiting anti-Parkinson activity // Catal. Struct. React. 2015. V. 1. P. 146-154.

14. *Shcherban N. D., Filonenko S. M., Barakov R. Yu., Sergiienko S. A., Yu K., Heinmaa I., Ivaska A., Murzin D. Yu.* New insights in evaluation of acid sites in micro-mesoporous zeolite-like materials using potentiometric titration method // Appl. Catal. A Gen. 2017. V. 543. P. 34-42.

15. *Shcherban N. D., Barakov R. Yu., Mäki-Arvela P., Sergiienko S. A., Bezverkhyy I., Eränen K., Murzin D. Yu.* Isomerization of α-pinene oxide over ZSM-5 based micro-mesoporous materials // Appl. Catal. A Gen. 2018. V. 560. P. 236-247.

16. *Ryoo R., Joo S. H., Jun S.* Synthesis of highly ordered carbon molecular sieves via template-mediated structural transformation // J. Phys. Chem. B. 1999. V. 103. P. 7743-7746.

17. *Shcherban N. D., Filonenko S. M., Yaremov P. S., Dyadyun V. S.* Synthesis and physical–chemical properties of N-containing nanoporous carbons // J. Mater. Sci. 2014. V. 49. P. 4354-4362.

18. *Shcherban N., Filonenko S., Yaremov P., Dyadyun V., Bezverkhyy I., Ilyin V.* Boron-doped nanoporous carbons as promising materials for supercapacitors and hydrogen storage // J. Mater. Sci. 2017. V. 52. P. 1523-1533.

19. *Shcherban N. D., Filonenko S. M., Yaremov P. S., Skoryk M., Ilyin V. G., Aho A., Murzin D. Yu.* Synthesis, structure and adsorption properties of nonstoichiometric carbon nitride in comparison with nitrogen-containing carbons // J. Ind. Eng. Chem. 2016. V. 34. P. 292-299.

20. *Shcherban N. D., Filonenko S. M., Yaremov P. S., Sergiienko S. A., Ilyin V. G., Murzin D. Yu.* Carbothermal synthesis of porous silicon carbide using mesoporous silicas // J. Mater. Sci. 2017. V. 52. P. 3917-3926.

21. *Ovcharov M., Shcherban N., Filonenko S., Mishura A., Skoryk M., Shvalagin V., Granchak V.* Hard template synthesis of porous carbon nitride materials with improved efficiency for photocatalytic CO_2 utilization // Mater. Sci. Eng., B. 2015. V. 202. P. 1-7.

22. *Shcherban N. D., Filonenko S. M., Ovcharov M. L., Mishura A. M., Skoryk M. A., Aho A., Murzin D. Yu.* Simple method for preparing of sulfur-doped graphitic carbon nitride with superior activity in CO_2 photoreduction // ChemistrySelect. 2016. V. 1. P. 4987-4993.

23. *Shcherban N. D., Mäki-Arvela P., Aho A., Sergiienko S. A., Yaremov P. S., Eränen K., Murzin D. Yu.* Melamine-derived graphitic carbon nitride as a new effective metal-free catalyst for Knoevenagel condensation of benzaldehyde with ethylcyanoacetate // Catal. Sci. Technol. 2018. V. 8. P. 2928-2937.

СИНТЕЗ ТА ЗАСТОСУВАННЯ НАНОПОРИСТИХ ФУНКЦІОНАЛЬНИХ МАТЕРІАЛІВ

Н.Д. Щербань

Інститут фізичної хімії ім. Л.В.Писаржевського НАН України, пр. Науки 31, 03028, Київ, Україна,
email nataliyalisenko@ukr.net

Резюме. *Узагальнено наявні в літературі відомості та результати власних досліджень про способи одержання, структуру, сорбційні властивості та функціональні характеристики мікро-мезопористих цеолітоподібних та вуглецьвмісних нанопористих матеріалів. Відмічено особливості та показана перспективність використання зазначених систем в каталізі, фотокаталізі, адсорбції, електрохімії.*

Ключові слова: *мікро-мезопористі цеолітоподібні матеріали, допований вуглець, нітрид вуглецю, карбід кремнію, матричний синтез.*

UDC 544.726.3

CHAPTER 6

ELECTRODEIONIZATION OF Li-CONTAINING SOLUTIONS USING ION EXCHANGE MATERIAL BASED ON TiO$_2$-MnO$_2$

M.O. Chaban, L.M. Rozhdestvenska, Y.S. Dzyazko

V.I. Vernadsky Institute of General and Inorganic Chemistry of the Ukrainian National Academy of Sciences, Kyiv, Ukraine.
e-mail mary.chaban@gmail.com

Abstract. *In this work the problem of selective extraction of Li$^+$ ions from combined solutions by electromembrane method is being solved. Sorbent based on lithium-substituted titanium manganese oxide was used. It is established that the function of the sorbent in the membrane system is reduced to the turbulization of the solution flow, but under the influence of alkalization of the solution near the surface of the sorbent granules, its sorption capacity increases with an increase in voltage from 3 to 20 V.*
Keywords: *electrodialysis, electrodionization, ion-exchange membrane, lithium-titanium-manganese spinel.*

Introduction. Due to the ever-increasing production of electronic portable devices, particularly gadgets, raw materials needs for lithium-ion batteries rise. As a rule, lithium is extracted from minerals. A promising area is the processing of brines that are formed after desalination of seawater and mine waters [1], as well as directly from seawater, where its content reaches 0.17 mg dm^{-3} (0.024 mmol dm^{-3}) [2]. In this case, it is advisable to use sorption [2] (TiO$_2$-MnO$_2$ oxide is the promising material for this purpose) or electromembrane [3] methods, combination of which, in contrast to the membrane methods, makes it possible to remove ionic components from solutions of very low concentration. The first stage of the process of extracting ions from the solution is their sorption by intermembrane filler, and the second one is the transfer of ions directly into the ion-exchanger phase affected by an electric field [4]. The advantage of the combined method comparing to sorption is reagentless continuous removal of species, since regeneration occurs due to the transfer of ions in the lion-exchanger bed and through the membranes.

Thus, the purpose of the work is to evaluate the possibility of using a double TiO$_2$-MnO$_2$ oxide for electromembrane extraction of Li$^+$ ions from combined solutions.

Experimental. Composite titanium-manganese sorbents were synthesized according to the method [5]. Sorption of cations was investigated using the method described *ibid.*

For electrochemical studies, the sorbent was heated at 600 °C and following membranes were used: cation exchange (KM) Nafion-117 (DuPont) and anion exchange (AM) AMI-7001 (Membrane International). The electromembrane extraction of Li^+ and Na^+ ions was performed using a five-chamber cell. A 0.1 M KNO_3 solution was circulated through the cathode compartment (the first liquid line), through the concentration chamber (the second line), and through the anode compartment (the third line). The fourth line provided the passage of a model two-component solution through the desalination compartment under once-through operation. The composition of the model solution was (mmol dm^{-3}):) Li^+ − 3; Na^+ − 400 K^+ − 9, chloride salt of these metals were used for the solution preparation. Sorbent or glass particles were located in the desalination compartment. The process was carried out under variation or voltage (3-20 V) or at 30 A m^{-2}. At the end of the experiment, the sorbent was regenerated and the eluate was analyzed.

In the next series of experiments, the sorbent was located in both concentration and desalination compartments. A model solution circulated through the cathode and concentration compartments (first liquid line), passed through the desalination compartment (second line). KNO_3 solution circulated through the anode compartment (third line).

Results and discussion. According to the data of the X-ray diffraction analysis, a sample of titanium manganese oxide treated at 500° C contains phases of TiO_2 (rutile) and MnO_2 in approximately equal amounts [5, 6]. A crystalline spinel $Li_{0.75}Mn_{0.25}Ti_2O_4$, which coexists with the rutile phase, is formed at 600-700°. Both phases determine the sorption properties of materials that are characterized by sufficiently developed surface (Table 6.1). It is worth noting that the values of a specific surface decrease with the increase in the temperature of heat treatment.

Table 6.1. Effect of heat treatment of sorbent on sorption of ions from seawater

Temperature of treatment, degrees C	Surface area, m^{2}g^{-1}	Sorption capacity, mmol g^{-1}				
		Li^+	Na^+	K^+	Ca^{2+}	Mg^{2+}
500	126	0.009	0.217	0.026	0.153	0.073
600	122	0.026	0.109	0.026	0.074	0.042
700	86	0.024	0.109	0.015	0.014	0.027

Sorption of metal cations from seawater was studied. In the case of the sample obtained at 500° C, its sorption capacity towards Na^+ and Ca^{2+} ions are values of the same order. Regarding K^+ and Mg^{2+} ions, these values are smaller by one order of magnitude. The ratio of the content of Na^+ and Li^+ ions in the

sorbent reaches 25. The increase in the temperature of the heat treatment of the sorbent leads to an increase in the Li^+ capacity and to a decrease in this value for other ions. The ratio of the content of Na^+ and Li^+ in sorbents treated at 600 and 700 ˚C is 4.1 and 4.5, respectively.

Taken the data of Table 1 into consideration, the optimum calcination temperature of the sorbent is 600 ºC: while maintaining a sorption high rate of Li^+ ions, a considerable selectivity of the sorbent to these ions is achieved. Consequently, for the electromembrane removal of these ions from the model solution, the material obtained under these conditions was applied.

In a five-chamber cell, the scheme of transfer of ions under the conditions, which provide lower current than limiting value, looks as shown in Figure 6.1. Water is decomposed in the cathode compartment, the solution is alkalized. OH^- and NO_3^- anions migrate through the AM to the concentration compartment that is closer to cathode. Here cations of alkaline metals are transported from the desalination compartment. Cl^- anions are removed from the same compartment to the concentration chamber, which is located closer to anode. The solution in the anode compartment is acidified. H^+ and K^+ ions are transported to the concentration chamber. The concentrate is gradually saturated with KNO_3, its pH remains at the level of 7, since H^+ ions are neutralized with OH^- anions.
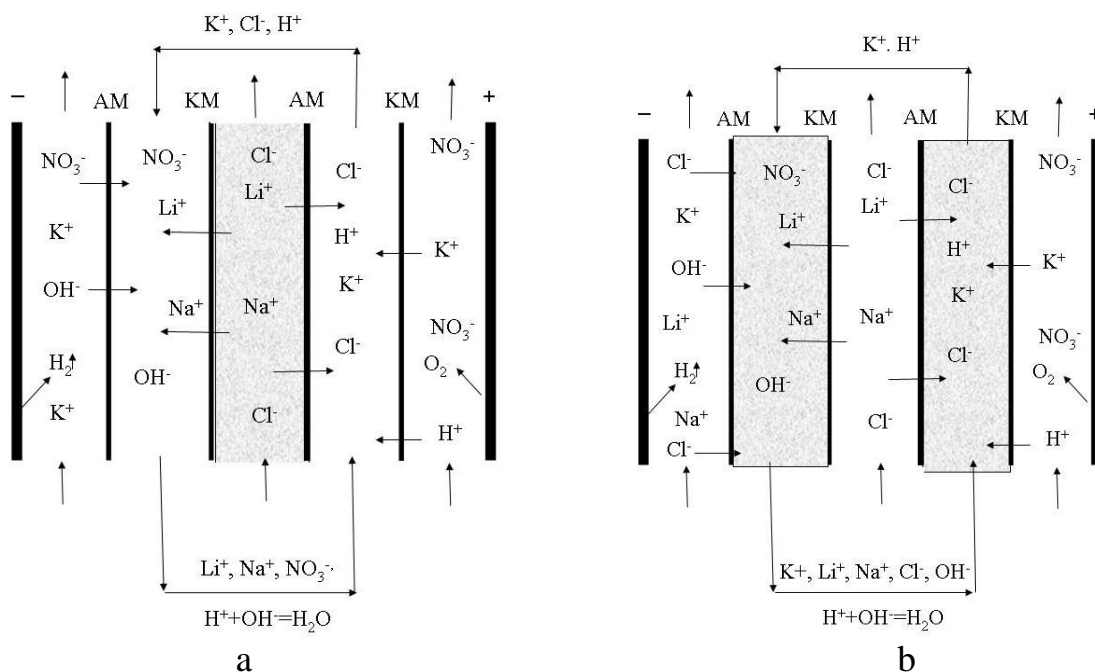
Fig. 6.1. *Schemes for the transfer of ions in the membrane system, consisting of two KM and two AM (a, b): the sorbent is located in the desalting compartment (a) and in the concentration compartment (b).*

Figure 6.2 illustrates the dependence of the content of Li^+ and Na^+ (n) ions in the concentrate on the time of electrodialysis at 30 A m^{-2}, which corresponds to the limiting current of cations. Each value of n shown in the graphs represents the difference between the value of n, which is reached for a certain period of

time, and the initial value (τ=0). When the desalination compartment was filled with glass particles, linear $n-\tau$ dependences were obtained. The flux of Na$^+$ ions through the cation exchange membrane was 3.01×10^{-4} mol m^{-2}s^{-1}, while it is 8.06×10^{-6} mol m^{-2}s^{-1} for Li$^+$ ions. The ratio of the fluxes is 373, the ratio of the initial concentrations is 133. Thus, predominantly Na$^+$ ions pass through the membrane. The current efficiency for ions is 2.6 % (Li$^+$) and 96% (Na$^+$).
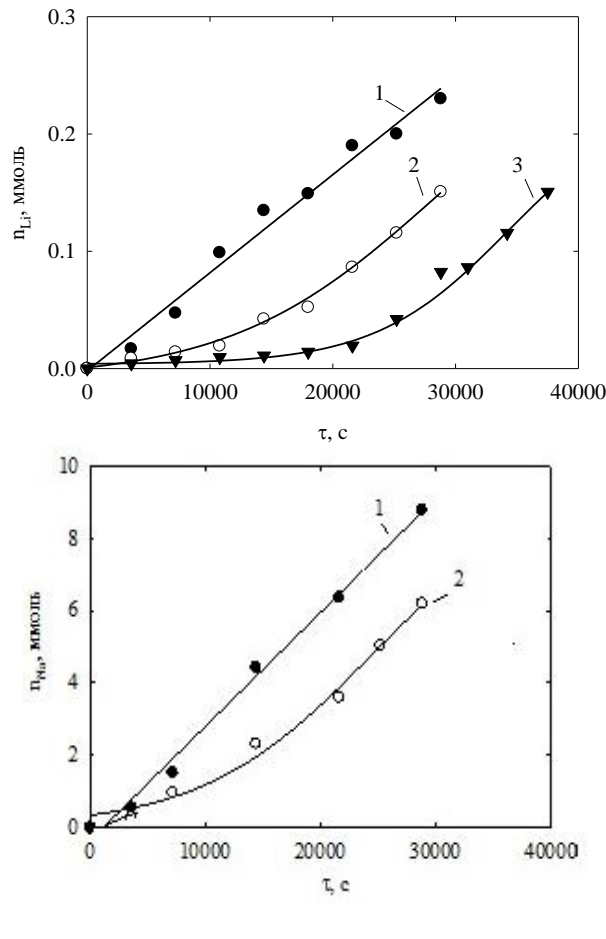
Fig. 6.2. *The content of Li$^+$ (a) and Na$^+$ (b) ions in the concentrate as a function of time. The desalination compartment was filled with glass (1, 3) or sorbent (2), and the concentration compartment remained empty (1, 2) or was filled with sorbent (3).*

When the membrane system included a sorbent in the desalination compartment, the $n-\tau$ curves show the regions of slow (corresponds to the sorbent saturation) and the rapid growth of the content of ions in the concentrate. The region of the rapid growth is parallel to the line obtained for inert glass. This means that the function of the sorbent is turbulization of the fluid, and the transfer of ions occurs mainly through the solution. Indeed, Li$^+$ and Na$^+$ ions in the sorbent are moving slowly: the order of magnitude of the diffusion coefficient of sorbed ions has been found to reach only 10^{-13}-10^{-12} m^2 s^{-1}.

When the concentration chamber is filled with the ion exchanger, a longer period of time is required to achieve a steady flux of Li$^+$ ions than in the case when the ion exchanger is in the desalination department. This is due to larger

amount of sorbent in the membrane system. A similar dependence on Na^+ ions was impossible due to their high initial content in the concentrate.

With an increase in voltage from 3 to 5 V, a slight increase in the electrical resistance of the membrane system is observed, indicating an approximation of the current, corresponding to the transfer of cations, to the limiting value (Figure 6.1a). The growth of the resistance is explained by the depletion of the hydrodynamically immobile layer of the solution near the surface of the cation exchange membrane from the side of the desalination compartment (concentration polarization) [4]. In the future, the near-surface layer of the solution collapses, as a result of which the resistance decreases − the transfer of cations and anions occurs due to overlimiting current.

At the end of the electrodialysis, the ion content in the intermembrane filler was determined and its sorption capacity was calculated. In all cases there is an increase in the capacity with voltage (Figure 6.3b). This, of course, is due to the dissociation of water on the surface of sorbent [4]. Hydrogen ions are involved into ion transport in the sorbent phase, and the OH^- ions remain in the near-surface layer of the solution near the granules. This additional factor promotes the solution alkalization. As a result, the equilibrium of sorption is shifted towards the formation of the substituted forms of sorbent. In all cases, sorbents exhibit the largest capacity of Li^+ ions, despite the Na^+ ions dominated in the solution. It was found that the smallest capacity is achieved for K^+ ions.
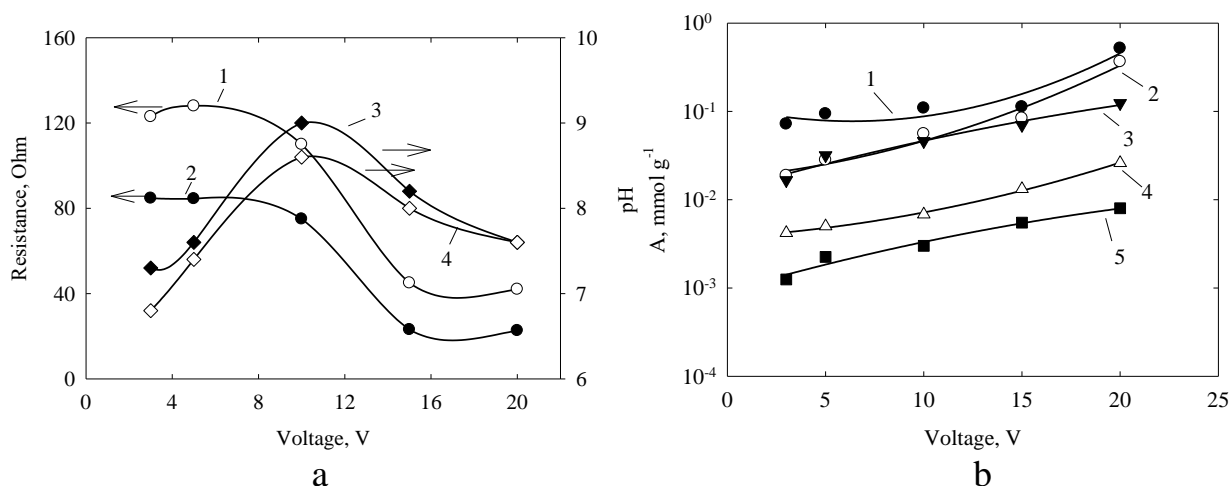
Fig. 6.3. *Resistance of membrane system (a1, a2), pH of the solution at the outlet of desalination compartment (a3, a4), sorbent capacity towards Li^+ (b1, b3), Na^+ (b2, b4) and K^+(b5) ions. Sorbent was placed in desalination (a1, b1, b2, b5) and concentration (a2. a4, b2, b4) compartments.*

Thus, under conditions of electromembrane separation, the sorption capacity of materials based on titanium-manganese oxides increases. After treatment of the sorbent with a 1 M HNO_3 solution (mass ratio of sorbent and liquid was 1:5) followed by neutralization of the eluate with a Na_2CO_3 solution, a precipitate of Li_2CO_3 was obtained.

Conclusions. It should be noted that the purposeful recovery of lithium ions from seawater using the electromembrane method is economically unprofitable, but lithium salt can be obtained as a by-product during the electrodialytic desaltination of seawater. Sorbent can be used as spacers for turbulization of the solution flow through the desalination compartments. In order to prevent the formation of a sediment of insoluble inorganic compounds in the membrane system and the competing influence of hardness ions upon precipitation of lithium carbonate, preliminary water softening with the use of nanofiltration method is recommended.

References

1. *Kesler S., Gruber P., Medina P., Keoleian G., Everson M., Wallington T*. Global lithium resources: Relative importance of pegmatite, brine and other deposits // Ore Geology Reviews. 2012. V.. 48. P. 55-69.
2. *Chitrakar R., Kanoh H., Miyai Y, Ooi K*. Recovery of lithium from seawater using manganese oxide adsorbent ($H_{1.6}Mn_{1.6}O_4$) derived from $Li_{1.6}Mn_{1.6}O_4$. // *Ind. Eng. Chem. Res.* 2001. V. 40. N 9. P. 2054–2058.
3. *Bunani S., Arda M., Kabay N., Yoshizuka K., Nishihama S*. Effect of process conditions on recovery of lithium and boron from water using bipolar membrane electrodialysis (BMED) // *Desalination.* 2017. V. 416. P. 10-15.
4. *Mulder J*. Basic principles of membrane technology, Dordrecht, Boston, London, 1996.
5. *Chaban M.O., Rozhdestvenska L.M., Palchyk O.V., Dzyazko Y. S., Dzyazko O. G.* Structural characteristics and sorption properties of lithium-selective composite materials based on TiO_2 and MnO_2// Appl. Nanosci. 2018. V. 8. P. .1-9. Available at: https://link.springer.com/article/10.1007/s13204-018-0749-1
6. *Helfferich F*. Ion Exchange, Dover, New York, 1995.

ЕЛЕКТРОДЕІОНІЗАЦІЯ ЛІТІЙ-ВМІСНИХ РОЗЧИНІВ З ВИКОРИСТАННЯМ ІОНІТУ НА ОСНОВІ TiO₂-MnO₂

М.О. Чабан, Л.М. Рождественська, Ю.С. Дзязько
Інститут загальної та неорганічної хімії ім.В.І. Вернадського НАН України, Київ
e-mail mary.chaban@gmail.com

Резюме. *У роботі вирішується проблема селективного вилучення іонів Li⁺ з комбінованих розчинів електромембранним методом. Використовували сорбент на основі літій-заміщеної форми титан-марганцевого оксиду. Встановлено, що у мембранній системі функція сорбенту зводиться до турбулізації потоку розчину. Проте під впливом підлуження розчину біля поверхні гранул сорбенту, його сорбційна ємність зростає при збільшенні напруги з 3 до 20 В.*
Ключові слова: *електродіаліз, електродеіонізація, іонообмінна мембрана, літій-титан-марганцева шпінель.*

CHAPTER 7

LABORATORY AND INDUSTRIAL TESTING OF MEMBRANE ELECTROCHEMICAL DEVICES FOR PURIFICATION AND REGENERATION OF CHROMIUM-CONTAINING GALVANIC SOLUTIONS

V.O. Serdiuk[1], K.O. Zaytseva[1], V.I. Sklabinsky[1], V.D. Ivchenko[2], L.M. Ponomarova[1]

*[1]Sumy State University, 2, Rymsky-KorsakovStr., Sumy 40007, Ukraine
email mikishasumy@gmail.com*
[2]Sumy National Agrarian University, 160, M. Kondratiev Str., Sumy 40021, Ukraine

Abstract. *The regeneration process of galvanic solutions by transferring the contaminating Cd^{2+} and Zn^{2+} cations through a cation exchange membrane RALEX®CM-PES 11-66 in a two-chamber electrolyser has been researched. The cathode processes that are associated with the migration of ions through the membrane and the cathodic deposition have been investigated. Laboratory and industrial testing of devices was carried out. Cathode products were studied using scanning electron microscopy with X-ray phase microanalysis functions to determine the elemental composition of cathodic deposits. This process allows to regenerate galvanic solutions and maintain stable composition of passivation baths.*
Keywords: *electrolysis, cation-exchange membrane, chromium-containing solution, cadmium cations, zinc cations.*

Introduction. The use of Cr(VI) compounds for the applying protective conversion films on galvanic coatings to significant environmental hazard due to waste water pollution. These compounds possess toxic properties, they have mutagenic and carcinogenic effect on living organisms [1, 2]. Cr(VI)-containing solutions are applied to brightening and passivation baths, the main component of which is sodium dichromate, chromic anhydride and other aggressive reagents. The chrome plating process is accompanied by the reduction of Cr(VI), the solutions also accumulate heavy metal ions. The ratio of the essential components in these baths changes that entails the need for adjustment of the solution composition by adding new portions of reagents. This leads to instability of bath operation and declining quality of a coating. The problem could be solved by the development and implementation of membrane-type electrochemical devices, which provide simultaneous return of valuable components into a technological cycle (in the form of commercial products and secondary raw materials). Electrolysis with ion-exchange membranes is the most perspective method for the wastewater purification [3-5].

Membrane and Sorption Materials and Technologies: Present and Future

Experimental. In order to study the regeneration of chromium-containing solutions using a membrane system, laboratory and industrial membrane electrochemical electrolysers were produced [6, 7]. Electrochemical reactions were studied using a laboratory membrane system (LME), whereas an industrial membrane electrolyser (IME) was used to study the effectiveness of the process under real operation conditions (Table 7.1, Fig.7.1).

Table 7.1: Comparative characteristics of membrane electrolysers

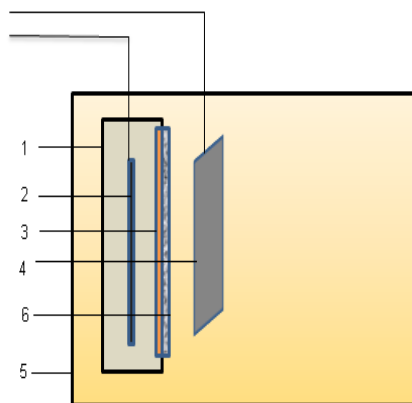| Electrolyser characteristic	LME	IME
Material of the cathode	Titanium BT-1	Titanium BT-1
Cathode area S, дм^2	0,3	0,7
Membrane	RALEX®CM-PES 11-66	RALEX®CM-PES 11-66
Catholyte	1% sulphuric acid solution	1% sulphuric acid solution
Anode material	Lead C2	Lead C2
Anode area S, dm^2	0,72	2,1
Anolyte, g/l	Sodium dichromate $Na_2Cr_2O_7$ – 50 Sulfuric acid H_2SO_4 – 10 Ions Zn^{2+}, Cd^{2+} and Cr^{3+} 2,5 g/l each	1) brightening bath: Chromium trioxide $CrO3$ …80-110 H_2SO_4 …3-5 2) passivation bath: Sodium dichromate $Na_2Cr_2O_7$ …150-200 Sulfuric acid H_2SO_4 …8-12 Content of ions Zn^{2+}, Cd^{2+}, Cr^{3+} was not determined
Catholyte volume, dm^3	1	4,5
Anolyte volume, dm^3	10	150
Voltage, V	3-9	3-9
Current density, A/dm^2	0,3-3	1-5

Fig. 7.1. *Scheme of membrane electrolyser. 1 –cathode chamber body; 2 – inner electrode - cathode; 3 – ion exchange membrane; 4 – external electrode - anode; 5 – chamber with chromium-containing solution; 6 – filtering cloth.*

Cathodic deposit was investigated by using the method of raster electron microscopy and X-ray diffraction analysis.

Results and discussion. While studying electrode reactions, we can assume the resulting products. Thus, the following reactions can occur:

$$Zn^{2+} + 2e = Zn; \tag{7.1}$$
$$Cd^{2+} + 2e = Cd; \tag{7.2}$$
$$2H_3O^+ + 2e = H_2 + 2H_2O; \tag{7.3}$$
$$2H_2O + 2e = H_2 + 2OH^-. \tag{7.4}$$

Reactions 7.3 and 7.4 cause the change in catholyte pHm. Change in catholyte acidity (its shift towards the alkaline side), leads to the drop of electroconductivity of solution and formation of flaked insoluble metal hydroxides that results in module efficiency decrement.

X-ray diffraction analysis, conducted on an automated diffractometer DRON-4-07, and an electron microscopy were used to determine the elemental composition of products deposited on the cathode. X-ray microanalysis conducted using the scanning electron microscope "REM-106-i" allowed determination of mass fraction of elements in the samples of the studied cathodic deposits and average from field of view on the basis of energy values of the characteristic X-ray peaks of each chemical element. The results are shown in Figures 7.2, 7.3. As can be seen, among the compounds in the cathodic deposits there are metallic cadmium, cadmium carbonate $CdCO_3$, a small amount of mixed ferrous oxide Fe_3O_4, as well as insignificant (less than 3%) amount of amorphous impurities and sand.

Simultaneously with the removal of ions that contaminated technological solutions of passivation and brightening baths, regeneration of chromate and dichromate ions was observed.
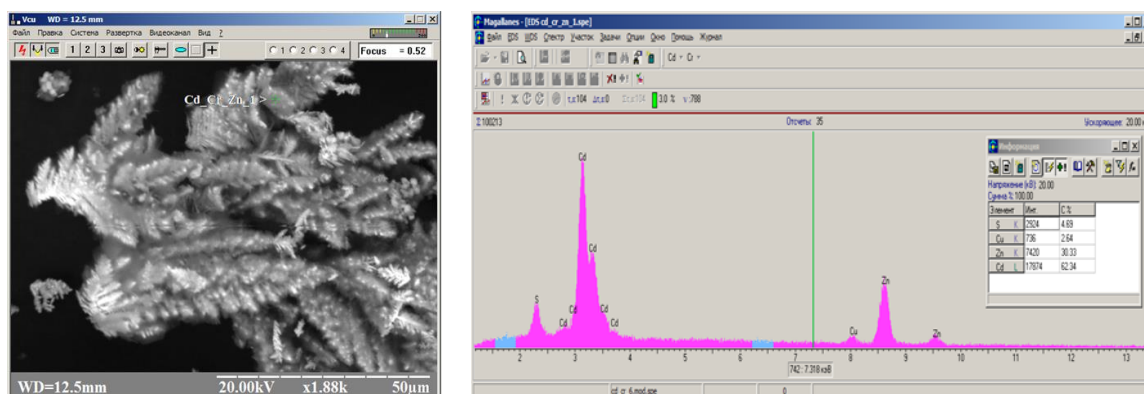

Fig. 7.2. *a) A REM photograph of cathodic deposit samples when the module is operated: the anolyte contains Zn^{2+} ions (2.5 g / l) and Cd^{2+} (2.5 g / l), x1880;*
b) Spectrograms of cathodic deposit samples and the results of microanalysis: the anolyte contains Zn^{2+} ions (2.5 g / l) and Cd^{2+} (2.5 g / l).
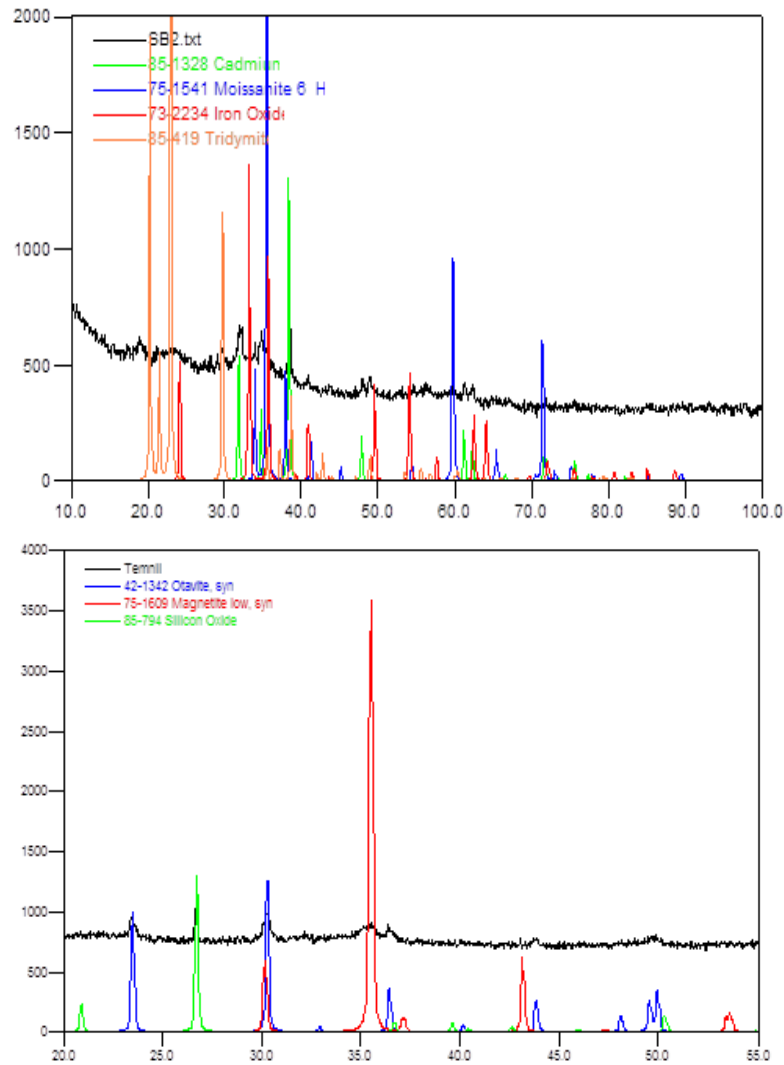
Fig. 7.3. *X-ray diffraction analysis of cathodic deposits samples conducted on IME.*

This process was provided by the ability of Cr^{3+} ions to be easily oxidized on a lead anode in accordance with the scheme of the process (7.5):

$$2Cr^{3+} + 7H_2O \rightarrow Cr_2O_7^{2-} + 14H^+ + 6e^-$$ (7.5)
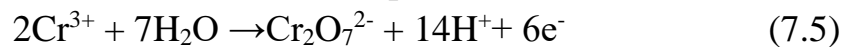
To evaluate the performance of the device, its efficiency was determined at different intervals of time in the passivation bath with 150 liters bath volume. The efficiency of the Cr^{3+} ion oxidation in Cr(IV) was evaluated by monitoring the change in the concentration of Cr(IV) ions in this bath, as shown in Fig. 4. The testing stages were related to the selection of operating and structural parameters of the membrane electrolyser and the production conditions. Characteristics of IME, shown in Table. 7.1, meet the requirements of the third stage of industrial testing. The regeneration efficiency of the content of hexavalent chromium ions in the solution is 52 grams per hour.

It is known that the recovery process in the cathode chamber is significantly influenced by the acidity of the catholyte medium [8, 9]. During laboratory studies, range of pH value (from 1.5 to 1.8) of a catholyte solution were determined, in which the most effective metal deposit on a cathode and regeneration of a chromium-containing solution are observed. At pH less than

1.5, hydrogen actively forms on the cathode, which interferes with the metal deposition process. And at a pH of more than 1,8-2, insoluble metal hydroxides are formed in areas close to the cathode. These conclusions were confirmed by industrial testing.
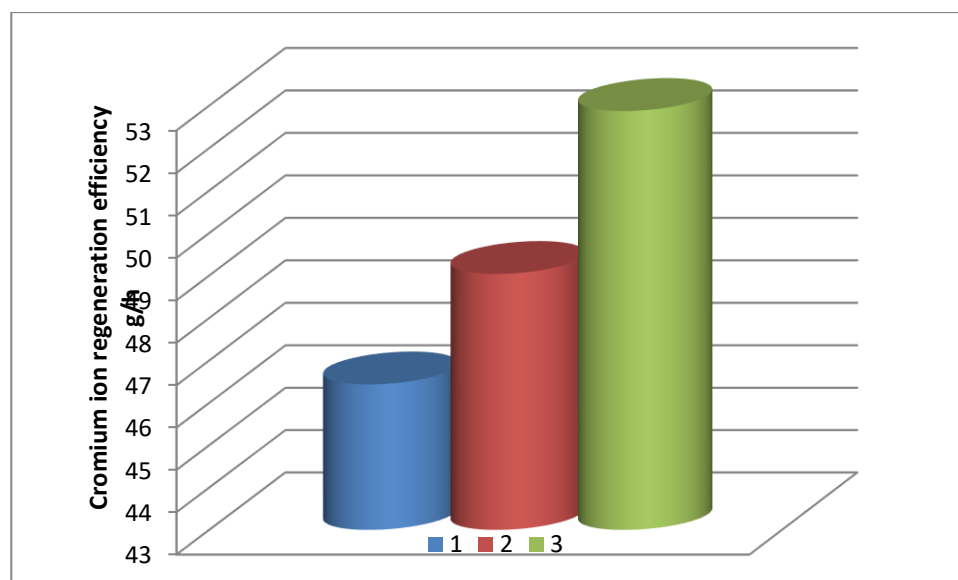

Fig. 7.4. *Effectiveness of IME at different stages: 1, 2, 3 - stages of testing in the factory passivation bath with 150 liters bath volume.*

Conclusions. This research has shown that the electrolysis of chromium-containing solutions using a laboratory model of electrolyser with a cation exchange membrane allows to regenerate the solution by removing the metal ions that contaminate it. Using an electron microscopy with X-ray phase microanalysis functions, it was found that cathode deposits contain cadmium and zinc atoms that were present in anolyte as impurities. Due to the use of the IME, optimal operating modes were selected in production conditions. As a result of implementation of IME, hexavalent chromium can be returned to the brightening and passivation baths (up to 50 grams per hour). Thus, the exploitation period of the brightening and passivation baths is significantly increased, and the costs of preparing new solutions are reduced

References

1. *Yao Y., Wei Q., Sun M., Chen Y., Ren X.* Environmentally friendly chromium electrodeposition: effect of pre-electrolysis on a Cr(III) bath in an anion-exchange membrane reactor // RSC Adv. 2013. V.**3**. P. 13131-13136.
2. *Zhitkovich A.* Chromium: exposure, toxicity and biomonitoring approaches. In: *Wilson SH, Suk WA* (eds.) Biomarkers of Environmentally Associated Disease: Technologies, Concepts, and Perspectives, CRC Press LLC, New York, 2002, P. 269–287.
3. *Benvenuti T., Krapf R.S., .Rodrigues M.A.S , Bernardes A.M., Zoppas-Ferreira J.* Recovery of nickel and water from nickel electroplating wastewater by electrodialysis // Separ. Purif. Technol. 2014. V. 129. P. 106-112.

4. *Kruglikov S.S., Kolotovkina N.S.* The use of immersed electrochemical modules for the removal of iron and other cationic impurities from chromium plating solutions // Electroplating and surface treatment, 2013, V. 21. N 3. P. 63-67. (in Russian)
5. *Marder L., Bernardes A.M., Zoppas Ferreira J.* Cadmium electroplating wastewater treatment using a laboratory-scale electrodialysis system // Separ. Purif. Technol. 2004. V. 37. P. 247-255,
6. *Bolshanina S.B., Serdyuk V.A., Vorobyova I.G.* Chromium-containing technological wastes. Increase of regeneration efficiency // Himicheskaya promyshlennost Ukrainy. 2016, N 1. P. 13-18. (in Russian)
7. *Bolshanina S.B., Abljejeva I.Ju., Kyrychenko O. M., Altunina L. L., Klimanov O. B., Serdiuk V.* Ukrainian Patent 109623,
8. *Kruglikov S.S., Kolotovkina N.S., Kazakova K.V., Kruglikova E.S.,Romanenkova A.A.* The use of three-chamber electrolytic cells for the recuperation of chromic acid // Electroplating and surface treatment. 2008. V. 16. N 1.P. 34-38. (in Russian)
9. *Kruglikov S.S., Nekrasova N.E., Nevmyatullina Kh.A., Kharin P.A., Kruglikova E.S.* The Use of Two-chambers Immersed Electrochemical Modules (IEM) to Improve the Stability of Lead Anodes in Aggressive Media // // Electroplating and surface treatment. 2016. V. 24. N 1. P. 22-25.

УДК 54.058+544.725.2

ЛАБОРАТОРНІ ТА ПРОМИСЛОВІ ВИПРОБУВАННЯ МЕМБРАННИХ ЕЛЕКТРОХІМІЧНИХ ПРИСТРОЇВ ДЛЯ ОЧИЩЕННЯ ТА РЕГЕНЕРАЦІЇ ХРОМОВМІСНИХ ГАЛЬВАНІЧНИХ РОЗЧИНІВ

В.О. Сердюк [1], К.О. Зайцева[1], В.І. Склабінський[1], В.Д.Івченко [2], Л.Н.Пономарьова [1]

[1]*Сумський державний університет, Україна, 40007 м.Суми, вул. Римського-Корсакова, 2. email mikishasumy@gmail.com*
[2]*Сумський національний аграрний університет, Україна,40021 м.Суми, вул.Г.Кондратьєва 160*

Резюме. *Досліджено процес регенерації гальванічних розчинів, шляхом перенесення забруднюючих катіонів Cd^{2+} та Zn^{2+} через катіонообмінну мембрану RALEX®CM-PES 11-66 в двокамерному електролізері. Вивчені катодні процеси, що пов'язані із міграцією йонів крізь мембрану та виділенням металів на катоді. Проведені лабораторно-промислові випробування пристроїв та досліджено катодні продукти за допомогою методу скануючої електронної мікроскопії з функцією мікроаналізу та рентгенофазового аналізу для визначення елементарного складу катодних осадів. Даний процес дозволяє регенерувати гальванічні розчини та підтримувати стабільний склад ванн пасивування..*
Ключові слова: *електроліз, катіонообмінна мембрана, хромовмісний розчин, катіони кадмію, катіони цинку.*

CHAPTER 8

HYBRID ORGANIC-INORGANIC NANOCOMPOSITES FOR ION-EXCHANGE PROCESSES

Yu. S. Dzyazko[1], L. N. Ponomarova[2]

V.I. Vernadskii Institute of General & Inorganic Chemistry of the NAS of Ukraine, Palladin Pr. 32/34, 03142, Kiev, Ukraine; email dzyazko@gmail.com
[2]Sumy State University, 2 Rymskogo-Korsakova St., 40007, Sumy, Ukraine, email ponomarouva@gmail.com

Abstract. *Two types of composite ion-exchangers, which are based on strongly acidic gel-like cation-exchange resin and weakly acidic cation exchange resin have been obtained by modification with nanoparticles of zirconium hydrophosphate. Removal of the dye from deionized water and Ni(II) ions from water containing also hardness ions was studied under dynamic conditions. The composites show higher break-through capacity than that of the pristine resin.*
Keywords: *nanocomposite, ion-exchanger, polymer matrix, zirconium hydrophosphate,*

Introduction. Ion-exchangers that combine constituents of different nature are in a focus of attention. The combination of organic and inorganic ion exchangers gives a possibility to obtain sorbents with a wide spectrum of functional properties. As a rule, organic-inorganic materials are characterized by considerable exchange capacity and high rate of ion exchange. Their selectivity is more expressed than that for organic components. In comparison with inorganic sorbents, some composites show better granulometric properties that makes them suitable for the application in column under dynamic conditions [1].

Organic polymer also provides better mechanical properties for the sorbents.

Strongly acidic polymers were applied mainly to preparation of organic-inorganic ion exchangers. In swollen state, ion-exchange polymers are characterized by complex porous structure. This structure involves hydrophilic pores (nanosized clusters and channels), where ions move. These pores are formed from heterogeneities of air-dry polymers [2-3]. The heterogeneities are caused by fragments of polymer chains, which contain functional groups. During swelling, these fragments form so-called gel regions penetrated by a continuous system of hydrophilic clusters and channels (transport pores). Ion-exchange polymers contain also hydrophobic pores (voids between gel regions, structure defects). Depending on location, the embedded particles change size and volume of one or other pores. This affects functional properties of the composites [4].

Weakly acidic ion-exchange resins show better selectivity toward toxic ionic components due to formation of complexes with functional groups [5]. However, the composites based on these resins are practically unknown. The aim of the research involves obtaining nanocomposite using weakly acidic resin as a polymer matrix. Another purpose is to compare porous structure and functional properties of the composites based on strongly and weakly acidic resins [4].

The organic-inorganic materials can be applied to water softening, separation and preconcentration of metal ions, nuclear separations, catalysis, redox systems, electrodeionization, hydrometallurgy, effluent treatment, production of ion selective electrodes and membranes. The composite sorbents are most often used for removal of toxic metal ions from water.

Experimental. Following reagents were used for the investigation: NaOH, HCl, $NiSO_4 \cdot 7H_2O$, H_3PO_4, $ZrOCl_2 \cdot 8H_2O$ (lab or synthesis grade, Ukrkhimsyrie LTD), Brilliant Green (BG) (hydrogen sulphate) (Merck).

Following cation exchange resins that are produced by Dow Chemical Company were used for modification with nanoparticles of zirconium hydrophosphate (ZHP): Dowex MAC-3 (weakly acidic macroporous resin) and Dowex HCR-S (strongly acidic gel-like resin). The weakly acidic resin is polyacrylic polymer containing -COOH groups, and the strongly acidic ion exchanger is styrene-divinylbenzene polymer with -SO$_3$H groups.

The organic-inorganic ionites were obtained by impregnating the cation-exchange resins (below CR, the polymer matrix) with a solution containing $ZrOCl_2$ (1000 mol m^{-3}). ZHP in the matrix was deposited with an H_3PO_4 solution (1000 mol m^{-3}). The ionites were washing with deionized water, drying at room temperature, and treatment with ultrasound to remove the precipitate from the outer surface of the grains. ZHP powder, which was obtained by this manner, was investigated further for comparison. Synthesis of ZHP inside polymers procedure was carried out one (weakly acidic resin) or eight times (strongly acidic resin). In the last case, the nanocomposite containing large amount of ZHP shows much faster proton transport than the pristine resin.

TEM images were obtained with a JEOL JEM 1230 transmission electron microscope (Jeol, Japan). Preliminarily the ion exchangers were milled and treated with ultrasound.

A method of standard contact porosimetry (MSCP) [6], which had been accepted by the IUPAC [7], was applied to study porous structure of the polymers. Preliminarily the tested samples were dried at 80ºC under vacuum. Water was used as a working liquid.

The adsorption of BG and Ni^{2+} was investigated. The samples were tested in ion-exchange columns. A diameter of the column was 0.7 cm, a volume of the bed was 5 cm^3, and the solution velocity was 5 cm^3 min^{-1}. The solutions containing 1–7 mg·dm^{-3} (0.02–0.15 mmol dm^{-3}) of the dye was used. The effluent was analyzed by Shimadzu UV-mini 1240 spectrophotometer 89

(Shimadzu, Japan) at 625 nm. Ni(II) removal from tap water was also performed using ion exchange column, the conditions were the same. The solution contained (mmol dm^3): Ni(II) – 0.1, Ca(II) – 1.3, Mg(II) – 0.4. The effluent was analyzed by atomic absorption method using an S9 Pye Unicam spectrophotometer (Philips).

Results and discussion. Morphology of the composite was investigated using TEM microscopy (Figure 8.1). As seen from the image the resins contain globular non-aggregated nanoparticles with size of 5-15 nm (Dowex MAC-3) and 4-20 nm (Dowex HCR-S). Larger globular particles (from ≈250 to 600 nm) and irregular formations of micron size are seen in the image of higher resolution. The particles of different size can occupy one or another type of pores of the ion exchange polymer affecting its porous structure.
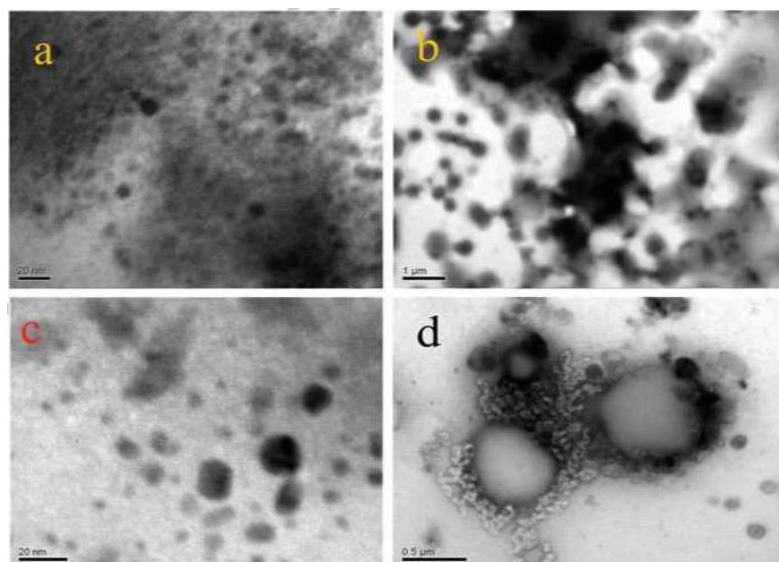

Fig. 8.1. *TEM images of ZHP particles embedded to weakly (a, b) and strongly (c, d) acidic resins*

A method of water adsorption isotherm was used to research the porous structure of composite ion exchange polymers. Single nanoparticles are located in pores containing functional groups; aggregates occupy inert pores. From the formal point of view, non-aggregated nanoparticles can be considered as a cross-linking agent, which increases swelling pressure. Swelling pressure provides stretching of transport pores. As a result, porous structure of the polymer constituent is transformed: some regions of the polymers, which are able to interact with species, become unavailable for them. However, embedded ZHP particles evidently expand the range of pores, where adsorption is possible [4].

Porous structure of the polymer constituent affects adsorption capability of the composite, since pore size determines availability of adsorption centers. In order to fix this effect, BG and Ni^{2+} adsorption was investigated. The samples were tested in ion-exchange columns. Figure 8.2 illustrates the capacity of ion exchangers toward BG and Ni^{2+}. Despite slower rate of BG adsorption on the

composite, this material shows higher break-through capacity towards the dye comparing with the pristine resin. This is evidently due to higher adsorption capacity of the modified ion exchange resin.
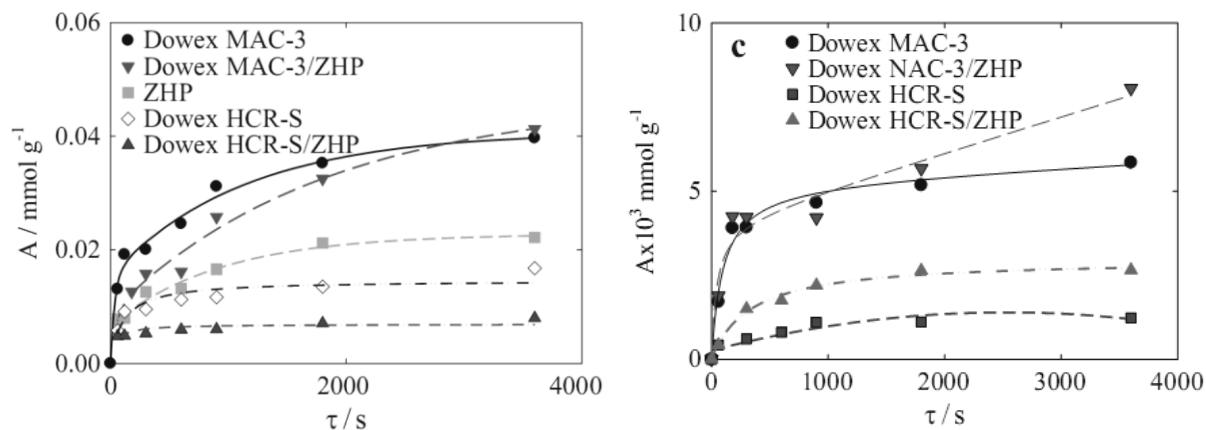

Fig. 8.2 *Capacity of ion exchangers toward BG (a) and* Ni^{2+} *(b)*

Indeed, lower values of Ni(II) diffusion coefficients have been found for composite ion-exchangers than those for pristine ion exchange resin. The composites show preferable sorption of Ni(II) ions in comparison with Ca^{2+} and Mg^{2+}.

Conclusions. Modification of ion-exchange resins causes transformation of porous structure of labile polymer matrix. The transformation occurs both at nano- and micro-levels. However, embedded ZHP particles evidently expand the range of pores, where adsorption is possible. This is valid both for BG adsorptions on weakly and strongly acidic resins. It is the same for Ni^{2+} ion sorption on strongly acidic resins. The particles decrease sorption rate by this manner. At the same time, strong interaction with Ni^{2+} ions is attributed to the structure of the weakly acidic resin. Partial screening of the polymer with particles causes acceleration of ion exchange.

References
1. *Naushad M.* Inorganic and composite ion exchange materials and their applications (Review). Ion Exch. Lett. 2(1): 1. 2009.
2. *Berezina N.P., Kononenko N.A., Dyomina O.A. et al* Characterization of ion-exchange membrane materials: properties vs structure. // Adv Colloid Interf Sci. 2008. V. 139 (1-2). P. 3-28
3. *Yaroslavtsev A.B., Nikonenko V.V., Zabolotsky V.I.* Ion transfer in ion-exchange and membrane materials. // Russ Chem Rev. 2003. V. 72(5). P. 393-421
4. *Ponomarova L., Dzyazko Yu., Volfkovich Yu., Sosenkin V., Scherbakov S.* Effect of Incorporated Inorganic Nanoparticles on Porous Structure and Functional Properties of Strongly and Weakly Acidic Ion Exchangers.: Springer Proceedings in Physics, 2018. V. 214. P. 63-77.
5. *Saha B., Streat M.* Adsorption of trace heavy metals: application of surface complexation theory to a macroporous polymer and a weakly acidic ion-exchange resin. // Ind Eng Chem Re. 2005. V. 44(23). P. 8671-8681

6. *Volfkovich Y.M., Sosenkin V.E.* Porous structure and wetting of fuel cell components as the factors determining their electrochemical characteristics. Russ Chem Rev. 2012. V. 86(6). P. 936-959.
7. *Rouquerol J., Baron G., Denoyel R. et al* Liquid intrusion and alternative methods for 408 the characterization of macroporous materials (IUPAC technical report). Pure Appl Chem. 2012. V. 409 84(1). P. 107-136.

УДК 544.022.537+544.726

ГІБРИДНІ ОРГАНІЧНО-НЕОРГАНІЧНІ НАНОКОМПОЗИТИ ДЛЯ ІОНООБМІННИХ ПРОЦЕСІВ

Ю.С. Дзязько[1], Л.М. Пономарьова[2]

Інститут загальної та неорганічної хімії ім. В.І. Вернадського Національної академії наук України просп. Академіка Палладіна, 32/34, 03142, Київ, Україна, email dzyazko@gmail.com

[2] Сумський державний університет, вул. Римського-Корсакова 2, 40007, Суми, Україна, email ponomarouva@gmail.com

Резюме. *Синтезовані композиційні іонообмінники на основі сильнокислотної гелевої катіонообмінної смоли та слабокислотної катіонообмінної смоли, шляхом модифікації їх наночастинками цирконій гідрофосфату. У динамічних умовах досліджено вилучення барвника із деіонізованої води та іонів Ni (II) з води, у присутності йонів жорсткості. Композити демонструють більшу іонообмінну ємність, ніж у немодифікованих смол.*

Ключові слова: нанокомпозит, іонний обмін, полімерна матриця, цирконій гідрофосфат.

UDC 544.726+544.723.3+546.791.6

CHAPTER 9

POLYMER-INORGANIC CATION-EXCHANGERS CONTAINING ZIRCONIUM HYDROPHOSPHATE.
REGENERATION OF URAIUM-LOADED FORM

O.V. Perlova[1], Yu.S. Dzyazko[2], N.O. Perlova[1], I. S. Ivanova[1],

A.V. Palchik[2]

[1]Odessa I.I. Mechnikov National University, 2 Dvoryanska Str., 65082, Odesa, Ukraine,

email olga_perlova@onu.edu.ua

[2]V.I. Vernadskii Institute of General and Inorganic Chemistry, NAS of Ukraine, 32/34 Palladin ave., 03142, Kyiv, Ukraine,

email dzyazko@gmail.com

Abstract. *It has been found that polymer-inorganic cation-exchangers, which contain nanoparticles of zirconium hydrophosphate, can be used many times for sorption of uranyl cations from diluted solutions. This is due to the possibility of practically complete regeneration of the loaded sorbents with diluted solutions of $NaHCO_3$ or EDTA. The sample that includes the smallest embedded particles shows the highest regeneration rate.*

Keywords: *organic-inorganic cation-exchangers, zirconium hydrophosphate, uranyl, regeneration of sorbent, polymer-based composite*

Introduction. In practice, sorption is the main effective method for the recovery of valuable and toxic components from water. As opposed to membrane separation, the choice of selective sorbent allows us to extract one or other ionic component from the solutions containing high amount of salts. Economical efficiency of sorption processes is determined particularly by optimal conditions for regeneration of sorption materials and processing of effluents. This is necessary for the repeated use of sorbents on the one hand and, in the case of processing of liquid industrial wastes, to return valuable components back to the technological process.

Last years organic-inorganic ion-exchangers are used for sorption of heavy metal ions [1]. These ion-exchangers are characterized by selectivity towards heavy metal ions comparing with commercially available ion exchange resins. In comparison with inorganic sorbents, much higher sorption rate is attributed to the composites of mentioned type.

As shown in [2-3], the composites based on gel-like strongly acidic ion exchange resin, which contains both non-aggregated and aggregated nanoparticles of zirconium hydrophosphate (ZHP), effectively extract uranyl

cations. The main advantage of these composites is the possibility of multiply usage after regeneration with a 1 M H_2SO_4 solution. The disadvantages of this reagent is its significant danger and high chemical activity providing equipment corrosion. Moreover, the use of sulfuric acid is limited at the legislative level.

The aim of the work is to establish some regularities of the regeneration of uranyl-loaded forms of polymer-based ion-exchangers containing ZHP nanoparticles. The solutions of $NaHCO_3$ and EDTA were applied to investigations. .The choice of these low-cost reagents is due to their availability and low selfishness. Moreover, they form strong complexes with uranyl-iions in solutions [4].

Experimental. Aqueous solutions of uranium (VI) acetate were used ($2.0 \cdot 10^{-4}$ mol dm^{-3}). Additionally the solutions contained 0.02 M HNO_3. Полученные растворы имели pH 2.2-2.5. Under these experimental conditions, uranium was in a form of cations in the nitrate solution (98.3% of UO_2^{2+} and 1.7% of $[UO_2NO_3]^+$) [4].

As sorbents, the samples based on Dowex HCR-S resin were used. The polymer was modified with ZHP particles according to [1-3]. The samples marked as *1, 2* and *3*, they differed in synthesis conditions (concentrations of $ZrOCl_2$ and H_3PO_4, Table 9.1), which determine diameter of grains, and the size of embedded aggregated and non-aggregated particles. The composition of sorbents affects their functional properties, namely .sorption ability towards uranyl ions and facility of regeneration of uranium forms.

Table 9.1. Synthesis conditions and some characteristics 0f polymer-inorganic cation-exchangers [2-3]

Sample	Synthesis conditions		Size of embedded ZHP particles, nm	Average diameter of grains, μm
	$C(ZrOCl_2)$, M	$C(H_3PO_4)$, M		
1	1	0,01	10-20; 400-600	800
2	1	1	50; 200-300	624
3	0.3	1	2-10;<100	640

Sorption experiments were performed under static conditions with continuous shaking at 20±2^{0}C during 30–180 min. The sorbent dosage was 2 g dm^{-3}. The solutions after sorption were analyzed with a photometric method using arsenazo III [5]. Sorption degree was calculated as:

$$S = \frac{C_0 - C}{C_0} \times 100, \%$$
(9.1)

where C_0 and C are the initial and final concentration of uranium (VI).

Membrane and Sorption Materials and Technologies: Present and Future

The sorbent loaded with uranyl-ions was separated from liquid, washed with deionized water and dried down to constant mass. utanyl-loaded forms of ion-exchanger was obtained by this manner. Namely these sorbents were regenerated for 30-240 min shaking with 0.01-1 M $NaHCO_3$ solutions or 0.01-0.4 M EFTA solutions. These reagents were well proven for the regeneration of uranium forms of other ion exchangers of different nature, particularly composites [6, 7]. The efficiency of sorbent regeneration was estimated as uranium desorption degree ($S_{des.}$):

$$S_{des.} = \frac{C_{des}}{C_0 - C} \times 100, \% ,\qquad(9.2)$$

where C_{des} is the concentration of uranium (VI) in the solution after desorption. The rate constant for uranyl desorption ($k_{des.}$) was found by graphically solving the equation:

$$\ln(C_{ads.} - C_{des.}) = \ln C_{ads.} - k_{des.} \times t ,\qquad(9.3)$$

where $C_{ads.}$ $(C_{ads.} = C_0 - C)$ is the concentration of uranium in a sorbent.

Results and discussion. The investigations have shown that the efficiency of regeneration (degree of uranium desorption, time and rate of sorbent regeneration) depends on properties of organic-inorganic ion-exchangers, as well as nature and concentration of the solution for regeneration (Figures 9.1).

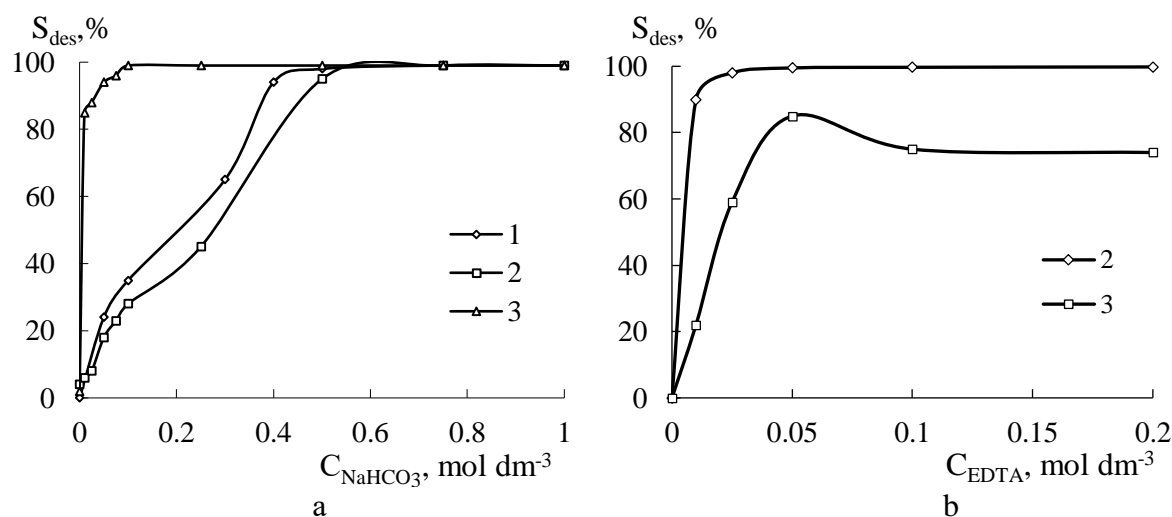**Fig. 9.1.** *Degree of desorption ($S_{дес.}$) for uraniun (VI) from uranium forms of polymer-inorganic cation-exchangers as a function of concentration of $NaHCO_3$ (a) and EDTA solutions (b).*

Increasing in the concentration of $NaHCO_3$ and EDTA solutions up to a certain value, which is determined by the properties of sorbent, causes the efficiency of uranium desorption (Table 9.2). Regeneration of samples *1* and *2*

requires 0.5 M $NaHCO_3$ solution. Less concentrated solution (0.1 M) is desirable for regeneratiion of sample *3*. Even a 0.05 M EDTA solution allows us to reach high desorption degree of uranyl ions and maximal desorption rate. It is necessary to note that EDTA is the most effective reagent for sample *2*: higher quantitative desorption rates were found in this case. Regarding sample 3, s $NaHCO_3$ solution is more desirable.

Table 9.2. Kinetics of uranium (VI) desorption with $NaHCO_3$ and EDTA solutions

C, M	Sample *1*			Sample *2*			Sample *3*		
	t, min	k $\times 10^4$, s^{-1}	R^2	t, min	k $\times 10^4$, s^{-1}	R^2	t, min	k $\times 10^4$, s^{-1}	R^2
NaHCO$_3$									
0.01	—	—	—	210	0.05	0.98	150	2.53	0.94
0.025	—	—	—	180	0.03	0.97	120	2.93	0.89
0.05	180	0.25	0.94	180	0.15	0.98	150	3.54	0.89
0.075	—	—	—	180	0.20	0.99	150	4.11	0.97
0.10	180	0.48	0.97	180	0.25	0.99	150	4.43	0.99
0.25	180	0.88	0.99	180	0.55	0.99	120	4.90	0.92
0.50	90	3.97	0.88	150	4.51	0.96	90	5.53	0.99
0.75	90	4.55	0.95	120	5.50	0.99	90	5.68	0.98
EDTA									
0.01	—	—	—	210	2.50	0.98	180	0.23	0.99
0.02	—	—	—	210	2.41	0.99	180	0.75	0.97
0.05	—	—	—	210	3.48	0.99	150	2.07	0.99
0.10	—	—	—	—	—	—	150	0.83	0.99
0.20	—	—	—	—	—	—	150	1.15	0.96
0.40	—	—	—	—	—	—	150	1.05	0.95

* *t* is the desorption time, R^2 is the correlation coefficient of line (3).

The sorbents, which are completely regenerated with a 0.5 M $NaHCO_3$ solution, completely restore their original form and the sorption capacity for uranium (the degree of sorption of uranium reaches $99.9 \pm 0.5\%$) after 5th cycles of sorption-regeneration. During further cycles, the degree of sorption decrease Further cycles reduce the degree of uranium sorption by 3-5%. The sorbents regenerated with a 1 M $NaHCO_3$ solution save their sorption capacity after 10th cycle of sorption-regeneration.

Conclusions. The obtained results are explained with composition and properties of organic-inorganic materials being regenerated. The samples *1* and *2* contain larger non-aggregated and aggregated ZHP particles. they are located in void between gel field of polymer blocking them. This evidently makes it difficult diffusion of exchanged ions inside the grains. Moreover, the modifier particles are also able to sorb ions. In the case of particle diffusion, increase of the size of embedded particles slow down the sorption rate. When the movement of ions is limited by chemical reaction, the deceleration is caused by high

amount of functional groups of ZHP. Smaller embedded particles accelerate ion exchange (sample 3), this is most expressed in the case of $NaHCO_3$ solutions.

References

1. *Dzyazko Yu.S., Ponomaryova L.N., Volfkovich Yu.M., Sosenkin V.E., Belyakov V.N.* Polymer Ion-exchangers modified with zirconium hydrophosphate for removal of Cd^{2+} ions from diluted solutions// Separ. Sci. Technol. 2013. V. 48. P. 2140-2149.
2. *Dzyazko Yu. S., Perlova O. V., Perlova N. A., Volfkovich Y.M., Sosenkin V.E., Trachevskii V.V., Sazonova V.F., Palchik **A.V.*** Composite cation-exchange resins containing zirconium hydrophosphate for purification of water from U(VI) cations // Desalination and Water Treatment. 2017. V. 69. P. 142-152.
3. *Perlova N., Dzyazko Yu., Perlova O., Palchik O., Sazonova V.* Formation of zirconium hydrophosphate nanoparticles and their effect on sorption of uranyl cations // Nanoscale Res. Lett. 2017. V. 12. 209.
4. *Gapel G.* Speciation of actinides // Handbook of elemental speciation II. Species in the environment, food, medicine and occupational health / Eds. R. Cormelis, J.A. Caruso, H. Crews, K.G. Heumann, Chichester, Wiley, 2005, P.509–563.
5. *Khan* M.H., *Warwick* P., *Evans* N. Spectrophotometric determination of uranium with arsenazo-III in perchloric acid // Chemosphere. 2006. V. 63. P. 1165-1169.
6. *Sazonova V. F., Perlova O.V., Perlova N.A., Polikarpov A.P.* Sorption of Uranium(VI) Compounds on Fibrous Anion Exchanger Surface from Aqueous Solutions // Colloid J. 2017. V. 79. P. 270–277.
7. *Tan L., Wang Y., Liu Q., Wang J., Jing X., Liu L., Liu J., Song D.* Enhanced adsorption of uranium (VI) using a three-dimensional layered double hydroxide/graphene hybrid material // Chem. Eng. J. 2015. V. 259. P. 752-760.

ОРГАНО-НЕОРГАНИЧЕСКИЕ КАТИОНИТЫ, СОДЕРЖАЩИЕ ГИДРОФОСФАТ ЦИРКОНИЯ: ОСОБЕННОСТИ РЕГЕНЕРАЦИИ УРАНОВОЙ ФОРМЫ

О.В. Перлова[1], Ю.С. Дзязько[2], Н.О. Перлова[1], І.С.Іванова[1], О.В. Пальчик[2]

[1]Одеський національний університет імені І.І. Мечникова, вул. Дворянська, 2, 65082, Одеса, Україна
email olga_perlova@onu.edu.ua
[2]Інститут загальної та неорганічної хімії ім. В.І. Вернадського НАН України, Пр. Академіка Палладіна, 32/34, 03142, Київ, Україна
email dzyazko@gmail.com

Резюме. *Встановлено, що полімер-неорганічні катіоніти, що містять наночастинки гідрофосфату цирконію, можуть бути використані багаторазово для сорбції катіонів уранілу з розбавлених розчинів. Це зумовлено ефективною регенерації уранової форми цих сорбентів розбавленими розчинами $NaHCO_3$ або ЕДТА. Найвищу швидкість десорбції знайдено для композиту, який містить найменші частинки модифікатору.*

Ключові слова*:органо-неорганічні катіоніти, гідро фосфат цирконію,ураніл-іони, регенерація сорбенту, композит на основі полімеру.*

UDC [628.161.2+ 546.711+ 546.27+ 546.19] 621.359.7+66.081.63

CHAPTER 10

PECULIARITIES OF REMOVAL OF NATURAL WATER MICROCOMPONENTS WITHIN THE PROCESS OF MEMBRANE DESALINATION (THE CASES OF ARSENIC, BORON, AND MANGANESE)

L.O. Melnyk

A.V. Dumansky Institute of Colloid Chemistry and Water Chemistry of NAS of Ukraine, Vernadsky ave., 42, 03142, Kyiv, Ukraine

email lumel2903@gmail.com

Abstract. *The removal of microcomponents during electrodialysis down to the norms of drinking water has been established to require deeper desalination than that provided by traditional techniques (0.2-0.3 g/dm³). The concentration range, within which the growth of the coefficient of microcomponent retention by nanofiltration and reverse osmosis membranes is observed, is individual for each component and depends on the nature of the membrane.*

Keywords: *microcomponents, natural water, removal, membrane desalination*

Introduction. Over recent decades membrane methods such as reverse osmosis (RO), nanofiltration (NF) and electrodialysis (ED) have gained wide practical use in the process of desalination of brackish ground- and marine waters as well as the treatment of wastewater and polluted water resources. The intensification of the use of membrane desalination methods and the diversity of natural waters in terms of chemical composition make it urgent to study the behavior of a number of microcomponents within membrane processing. In particular, it is necessary to remove As, B, and Mn, concentration of which in ground- and surface water often exceeds the standards for drinking water due to both natural and anthropogenic intake. A number of modern studies [1-3] has established the carcinogenic and genotoxic effect of arsenic, the gonadotoxic and embryotoxic effects of boron, the neurological, general toxic, embryotoxic and mutagenic effects of manganese. Therefore these microcomponents components are among the priority toxicological indicators of water quality. The analysis of scientific literature shows that it is difficult to remove As, B, and Mn down to the level that corresponds to the quality of drinking water.

Experimental. The model solutions containing microcomponents (arsenic, boron, manganese) were used in the processes of electrodialysis, nanofiltration and reverse osmosis. Ion exchange MK-40 and MA-40 (Schekinoazot, Russia) were applied to electrodialysis, OPMN-P nanofiltration membrane (Vladipor, Russia) and ESPA-1 reverse osmosis membrane (Hydranautics, USA) were used

for baromembrane separation. The feed solution was supplied to the desalination chambers in a circulating mode in the process of electrodialysis, and a dead-end cell was used for baromembrane processes.

Results and discussion. The dependence of the degree of electrodialytic manganese removal on the degree of solution desalination differs significantly from the curves obtained for borate- and arsenate-ions (Figure 10.1). The main amount of manganese is removed from water down to 30% of initial content. In the case of boron and arsenic, intensive electromigration is observed only with an increase in the desalination degree up to 82.9 and 90.0%, respectively (with a decrease of value of the total salinity of dialysate down to ≈ 1.0 and 0.5 g/dm^3).
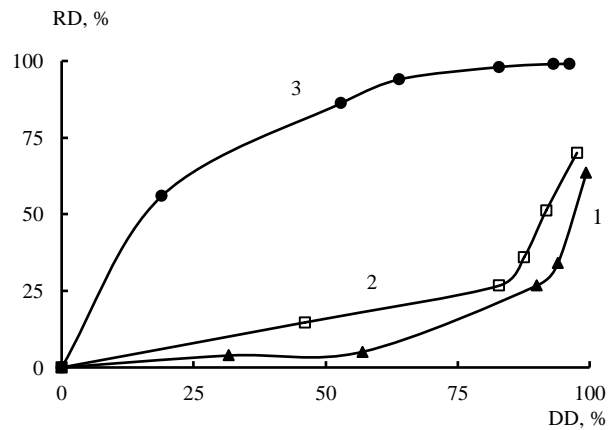

Fig. 10.1. *The dependence of the degree of arsenicic (1), boron (2) and manganese (3) removal on the degree of the model solution desalination in the process of electrodialysis using MC-40 and MA-40 membranes.*
The model solution contained 0,1 mg/dm^3 As(V), 5,85 g/dm^3 NaCl (1); 1,6 mg/dm^3 B, 8,5 g/dm^3 NaCl (2); 5,0 mg/dm^3 Mn(II), 11,7 g/dm^3 NaCl (3).

The results obtained during desalination of boron- and arsenic-containing waters can be explained by analyzing the following equation:

$$\bar{t}_1 = \frac{\overline{C_1}\,\overline{U_1}}{\overline{C_1}\,\overline{U_1} + \overline{C_2}\,\overline{U_2}}$$
(10.1)

where $\overline{C_1}$, $\overline{C_2}$, $\overline{U_1}$, $\overline{U_2}$ are the concentration and mobility of the micro- and macrocomponents in the membrane respectively. Indeed, as the equation (10.1) suggests, the transport number of $\bar{t}_1$ microcomponent in the membrane can reach high values only with the concentration of the macrocomponent decreasing significantly.

In the case of electrodialytic desalination of a model manganese-containing solution, the removal of manganese is intensive already at the initial stages of desalination. This is explained by selectivity of the MK-40 cation exchange membrane towards double-charged cations, which reduces the competing effect

of the macrocomponent (Na^+) on the transport of manganese ions. The presence of Ca^{2+} and Mg^{2+} cations has been shown to have a competing effect on the electromigration of Mn^{2+}, but this effect slightly affects the rate of manganese removal.

Taking into account that the maximum allowable concentration (MAC) of arsenic in drinking water is very low (10 $\mu g/dm^3$), obviously it is problematic to achieve this value in the process of electrodialysis, since it requires almost complete desalination of the solution.

In the case of electrodialytic treatment of manganese-containing solutions (owing to the selectivity of the cationic membrane to Mn^{2+} ions), the concentration of manganese decreases to the MAC, when the total salinity of the dialysate reduces down to 0.2-0.3 g/dm^3. This is despite the fact that the maximum permissible concentration of manganese in drinking water is also fairly low and reaches 50 $\mu g/dm^3$.

The boron concentration in dialysate also reduced down to the MAC with the reducing salinity of dialysate down to 0.2-0.3 g/dm^3, despite the fact that the rates of removal of borate and arsenate anions are close to each other. Obviously, this is due to the fact that the limit for boron content in drinking water is less stringent (500 $\mu g/dm^3$) than the one for the content of manganese and arsenic.

The analysis can be used to predict the prospects for removing other microcomponents of natural and waste water by electrodialysis down to the standards for drinking water. This analysis has to take into consideration the MAC magnitudes for any microcomponent and the shape of the kinetic curve of its removal during desalination.

The retention coefficient of borate-anion (pH 11) by ESPA-1 reverse osmosis membrane has been established to be bot higher than 93% within the range of boron concentration of 1.2-20.0 mg/dm^3 (Figure 10.2). The increase in boron retention is observed within the concentration range of 1.2-2.0 mg/dm^3, which is explained on the basis of capillary-filtration model of the selective permeability of reverse osmosis membranes.

The arsenate-anion retention coefficient for ESPA-1 reverse osmosis membrane and OPMN-P nanofiltration membrane reaches 95-99% within the wide range of pH, operating pressure, concentration and nature of background electrolyte with a permeate recovery of up to 90% (Table 10.1). The coefficient of arsenate retention by OPMN-P nanofiltration membrane increases within the range of arsenate concentrations of 50-100 $\mu g/dm^3$, whereas the arsenate retention coefficient is constant and reaches 99% in this concentration range using ESPA-1 reverse osmosis membrane.

The reliable data on the radius of the hydrated ion $HAsO_4^{2-}$ (as well as its heat of hydration) are absent. However, the diffusion coefficients of arsenate-ion and other ions, which are typical for water, are compared. Besides, they stress correlation between the diffusion coefficient of ion and its hydrated radius [4, 5].
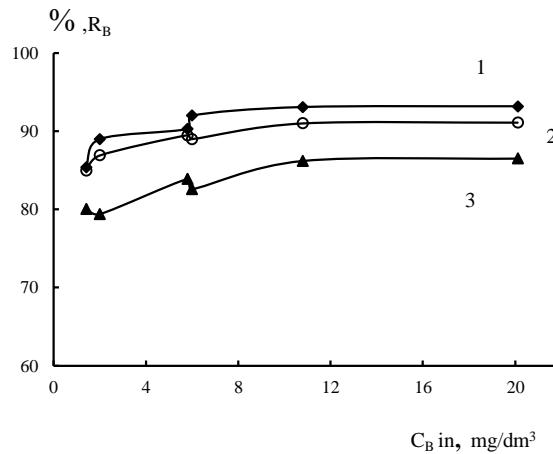
Fig. 10.2. The coefficients of boron retention using ESPA-1 membrane at different boron concentrations in the initial solution and 25 (1), 50 (2), 75% (3) permeate recovery. The model solution contained 1,0 g/dm³ NaCl; pH – 11,0; P – 3,0 MPa; T – 18-20 ºC.

Table 10.1. Removal of As(V) compounds using OPMN-P nanofiltration membrane at different operating pressure and permeate recovery

Permeate recovery, %	0.5 MPa			1.0 MPa			1.5 MPa		
	$C_{As}perm$, µg/dm³	R,%	J, dm³/ m²·h	$C_{As}perm$, µg/dm³	R,%	J, dm³/ m²·h	$C_{As}perm$, µg/dm³	R,%	J, dm³/ m²·h
25	1.5	98.3	15.2	-	-	28.5	2.6	97.1	40.5
50	1.8	98.0	15.1	1.8	98.0	27.8	2.5	97.2	39.8
75	1.6	98.2	15.1	1.9	97.9	27.7	2.4	97.3	39.8
90	2.2	97.5	14.9	2.3	97.4	27.1	2.9	96.7	39.1

Note. The solution contained 90 µg/dm³ As(V) and 1 g/dm³ NaCl; pH 7,5; T=15-16 ºC.

Table 10.2 shows that the diffusion coefficient of the anions in the solution decreases within the following series: $Cl^- > HCO_3^- > SO_4^{2-} > HAsO_4^{2-}$. The coefficient of ion retention by the NF membranes increases within this series as well: $SO_4^{2-} > HCO_3^- > Cl^-$.

Table 10.2. The heat of hydration (ΔH) and diffusion coefficient (D) of anions typical for natural waters [4, 5]

Ion	Cl^-	HCO_3^-	SO_4^{2-}	$HAsO_4^{2-}$
ΔH, kJ/mol	351	381	1109	-
$D·10^9$, m²/s	2,030	1,185	1,065	0,323

Conclusions. Electrodialytic removal of microcomponents of manganese, boron, arsenic down to the standards for drinking water requires a deeper procedure of water desalination (0.2-0.3 g/dm³) comparing with traditional desalination. This is caused by the competing influence of macrocomponents on the process as well as low MAC of microcomponents in water. It has been proposed to forecast the prospects of removal of microcomponents from natural

and waste waters by electrodialysis to the standards for drinking water based on the analysis of the kinetic peculiarities of the microelement removal from water in the process of electromembrane desalination and the value of its MAC.

Increase of the concentration of a microelement (boron and arsenic) improves its retention by reverse osmosis and nanofiltration membranes. However, the concentration range, within which this growth is observed, is individual for each component and depends on the nature of the membrane. The obtained results correspond to the capillary-filtration model of selective permeability of reverse osmosis membranes.

References

1. *Halem D., Bakker S.A., Amy G.L.,* van *Dijk J.C.* Arsenicic in drinking water: not just a problem for Bangladesh // Drinking Water Engineering and Science Discussions. 2009. N 2. P. 51-64.
2. Guidelines for drinking water quality, V. 1, Recommendations, 3rd edition, WHO, Geneva, 2004.
3. *Bouchard M.F., Sauve S., Barbeau B., Legrand M., Brodeur M.E., Bouffard T., Limoges E., Bellinger D.C., Mergler D.* Intellectual impairment in scool-age children exposed to manganese from drinking water // Environmental Health Perspectives. 2011. V. 119, N 1. P. 138-143.
4. *Saitua H., Gil R., Padilla A.P.* Experimental investigation on arsenicic removal with a nanofiltration pilot plant from naturally contaminated groundwater // Desalination. 2011. 274. P. 1-6.
5. *Vrijenhoek E.M., Waypa J.J.* Arsenicic removal from drinking water by a "loose" nanofiltration membrane / E.M. Vrijenhoek, Desalination. 2000. V. 130. P. 265-277.

ОСОБЛИВОСТІ ВИДАЛЕННЯ МІКРОКОМПОНЕНТІВ ПРИРОДНИХ ВОД У ПРОЦЕСАХ МЕМБРАННОГО ОПРІСНЕННЯ (НА ПРИКЛАДІ АРСЕНА, БОРУ, МАРГАНЦЮ)

Л.О. Мельник

Інститут колоїдної хімії та хімії води ім. А.В. Думанського НАН України, просп. Вернадського, 42, 03142, м. Київ, Україна
email: lumel2903@gmail.com

Резюме. *Встановлено, що видалення мікрокомпонентів в процесі електродіалізу до норм питного водопостачання вимагає більш глибокого знесолення води (0,2-0,3 г/дм³), аніж за традиційного опріснення. Інтервал концентрацій, в якому спостерігається зростання коефіцієнта затримки мікрокомпонента нанофільтраційними та зворотноосмотичними мембранами, для кожного компонента є індивідуальним і залежить від природи мембрани.*
Ключові слова: *мікрокомпоненти, природні води, видалення, мембранне опріснення*

CHAPTER 11

DEEP PROCESSING OF PERMEATE AFTER NANO-FILTRATION (NF) OF MILKY WHEY

V.V. Zakharov[1], Yu.G. Zmievskii[1], O.A. Ustinov[1], Yu.S. Dzyazko[2],
V.G. Myronchuk[1]

[1]*National University of Food Technologies of the MES of Ukraine,
Vladimirskaya str. 48, 01601, Kyiv, Ukraine.*
[2]*V.I. Vernadskii Institute of General & Inorganic Chemistry of the NAS of
Ukraine, Palladin Ave. 32/34, 03142, Kyiv, Ukraine.*
email *saharoff.911@gmail.com*

Abstract. The method of deep processing of nano-filtration permeate of milk whey is proposed and scientifically substantiated, using ozonation and electrodialysis processes. The ozonation station can remove up to 96 % of organic compounds of NF permeate, and the amount of dissolved ozone in this case should be 20...28 mg/dm^3. This treatment allows us to fully utilize NF permeate in the future. It has been established that in order to achieve the posteffect of the impossibility of microflora in the ozone-treated nanofiltration permeate, the minimum amount of dissolved ozone should not be less than 2,5 mg/dm^3.
Keywords: membrane separation, ozone, ozone-gas mixture, nanofiltration permeate, organic pollution.

Introduction. During the production of cheeses, a large amount of whey is produced, which in most cases is processed at the nanofiltration station (NF). The essence of the process implies in concentrating of milk whey to the content of dry matter of 20±3 % while simultaneously desalting it by 25-.30 %. The thus obtained concentrate is preferably dewatered during spray drying and has improved organoleptic properties. Nevertheless, the formation of NF permeate requires further processing due to the high value of chemical oxygen demand (COD) and the content of monovalent ions, which can be further used in remineralization and mineralization of drinking water. This required appropriate research, due to the lack of effective processing technologies for NF permeate. The purpose of this work was to develop a scheme for maximally deep processing of nano-filtration permeate of milk whey.

Experimental. The installation for experimental studies is shown in Figure 11.1. Its principle of action is the following. The compressor, which is mounted in the body of the concentrator of oxygen 1, is absorbed by air from the environment. First, the air goes through a coarse filter for separating large

suspended impurities, and then into a dehumidifier, to reduce the moisture content. Further, there is concentration of oxygen in the air to 90-95 %. The resulting oxygen concentrate enters the ozonator 2. Due to the electrical discharge in the discharge chamber, the ozonator is produced by ozone. Its content in the gas mixture was about 4-6 %.
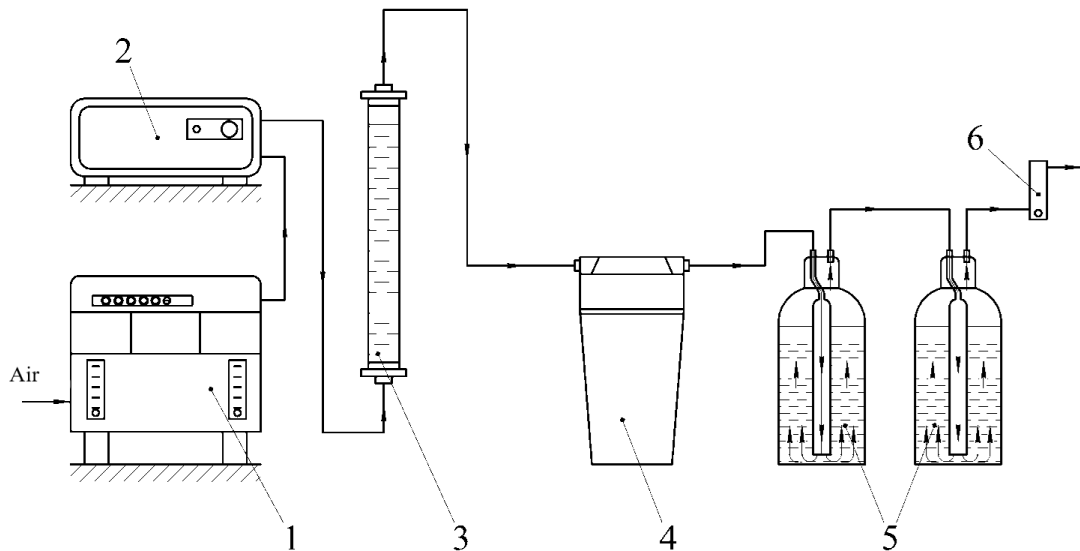

Fig. 11.1. *Scheme of laboratory installation for ozonation.*

The ozonation process took place in the contact capacitance 3. This is a cylindrical reactor with a body height of 0,34 m, an internal diameter of 0,032 m. The total volume of the contact capacity is 0,5 dm^3, the working volume is 0,4 dm^3. Through the connecting tube, the ozone-gas mixture came to the bottom of the contact tank, where the grid-distributor was installed, and fell into the working volume of the apparatus. Passing through the layer of the processed solution, the residual ozone proceeded from the upper part of the apparatus, passed through the foam trapper 4 and two glasses of Drexel 5 with a solution of potassium iodide (KI). The amount of ozone was determined by the iodometric method. Its essence is captured in determining the amount of iodine, which in the equivalent amount (I:O$_3$ = 1:1) is formed when the ozone-gas mixture passes through the KI solution.

Results and discussion. The application of the ozonation station is due to the following:

1. Ozone is a very powerful oxidant.

2. The production of ozone occurs at the place of its use and without the use of any additional reagents.

3. The main product of the decay of ozone is oxygen, which is safe for humans.

On the basis of new experimental data and previous studies the hardware-technological scheme of NF permeate processing was proposed [1]. The principle of the proposed scheme is as follows.

After the baths, the milk serum is sent to the NF station, where it is divided into NF permeate and concentrate. The latter, with a content of dry matter of 20±3 %, is sent to the final condensation in vacuum evaporators and dried to further obtain valuable components from it. The resulting NF permeate is fed to an ozonation station, where it is treated with ozone in the contact capacity. It contributes to the oxidation of organic compounds and the disinfection of the solution. It was found that the combination of ozonation and subsequent sorption purification reduces the COD in NF permeate by 96 % (Figure 11.2) [2, 3].
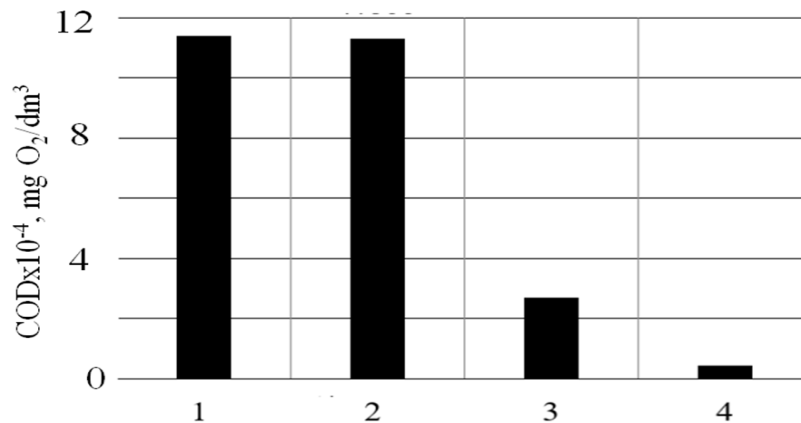

Fig. 11.2. *Chemical oxygen demand. 1 – output NF permeate; 2 – NF after ozonation; 3 – NF permeate after sorption; 4 – NF permeate after ozonation and sorption (adapted from [4]).*

The treated solution after the ozonation and filtration through the layer of activated carbon is concentrated to the state, which is needed for reverse osmosis. Due to the preliminary removal of organic components, the performance of reverse osmosis membranes rises by 25-30 % (Figure 11.3) [4], in comparison with the processing method without the ozonation station. This increases the amount of purified water obtained, and the amount of concentrate is reduced twice.
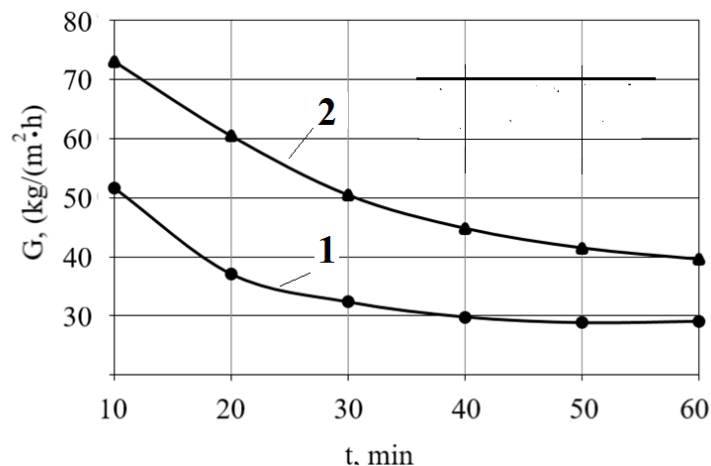

Fig. 11.3. *Change the productivity of the reverse osmotic membrane. G, over time, t (adapted from [4]). The permeate is before (1) and after (2) ozonation.*

The resulting concentrate goes to the electrodialysis station (ED), where the concentration of salts occurs, which can then be used for the mineralization and remineralization of potable water. The use of ED is due to the lack of phase transition of treated substances and direct action on mineral salts during the process of their concentration. The filtrate after reverse osmosis and after ED diluent mixes with residual ozone, which can reach 40-70 % of the initial values at the ozonation station, and is used for washing the equipment. Mixing with residual ozone is necessary for two reasons: first, such a scheme allows to save on the establishment of an ozone destructor for the residual gas mixture; second, such an operation allows the solution to saturate with ozone with a residual concentration of 0,1 mg/dm^3, which makes it impossible to develop pathogenic microflora in such water for 30-60 minutes [5-8] and allows it to be used for washing the equipment. According to the results of experiments (Figure 11.4), in order to determine the required minimum values of the transferred ozone dose (TOD), the total transmitted ozone dose is 2,5 mg/dm^3 in order to achieve the minimum required ozone dose of 0,1 mg/dm^3.
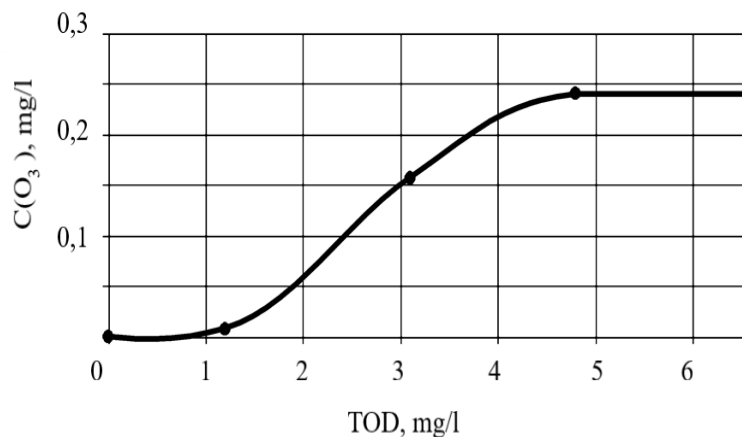

Fig. 11.4. *Dependence of changes in the residual concentration of ozone C(O₃) from transferred ozone dose (TOD).*

Conclusions. According to the results of the work, rational parameters were determined during the processing of NF of milk whey in the ozonation station and the hardware and process scheme of NF permeate treatment was proposed. The ozonation station allows removal of up to 96 % of organic compounds of NF permeate, TOD = 20...28 mg/dm^3. It was established that the ozone using factor, in the case of ozonation of NF permeate, is within 40...60 %. The TOD should be 2,5 mg/dm^3 for a minimum required ozone dose of 0,1 mg/dm^3. The significant benefit of the proposed scheme is the deep processing of NF permeate of milk whey.

References

1. *Zmievskii Y.G., Zaharov V.V., Kornienko L.V., Myronchuk V.G. Ukrainian Patent* 113724.

2. *Zakharov V., Zmievskii Yu., Biletska I., Myronchuk V.* Ozonation of milk industry fluids// Scientific Works of National University of Food Technologies. 2017. V. 23, №5, P. 124-130.

3. *Zakharov V., Zmievskii Yu., Myronchuk V.* Treatment of industrial wastes of dairy industry with ozone. Preliminary results // Visnyk Petro Vasilenko Kharkiv national agrarian university. 2016. V. 179. P. 167-173.

4. *Zmievskii Y.G., Zaharov V.V., Rudenko O.S.* and other. Ozonation of nanofiltration permeate of whey before processing by reverse osmosis // Acta periodica technologica. 2017. N 48. P. 315-323.

5. *Kozhenov V.F.* Devices for water ozonation, Stroyizdat, Moscow, 1968.

6.   SUEZ's Degremont Water Handook, SUEZ's, Paris, 2007.

7. *Shigezo N., Takahara H.* Ozone Contribution in Food Industry in Japan // Ozone: Science and Engineering. 2006. № 28. P. 425-429.

8. *Desvignes C., Chaurand, M., Dubois M., Sadoudi A., Abecassis J., Lullien-Pellerin V.* Changes in common wheat grain milling behaviour and tissue mechanical properties following ozone treatment // J. Cereal Sci. 2008. № 47. P. 245-251.

УДК 664+628.3

ГЛИБОКА ПЕРЕРОБКА ПЕРМЕАТУ ПІСЛЯ НАНОФІЛЬТРАЦІЇ (НФ) МОЛОЧНОЇ СИРОВАТКИ

В.В. Захаров[1], Ю.Г. Змієвський[1], О.А. Устінов[1], Ю.С. Дзязько[2], В.Г. Мирончук[1].

[1]Національний університет харчових технологій, вул. Володимірська 48, 01601, м. Київ, Україна.
[2]Інститут загальної та неорганічної хімії ім. В.І. Вернадського НАН України, проспект Палладіна 32/34, м. Київ, Україна.

Резюме. *В роботі запропоновано і науково обґрунтовано спосіб глибокої переробки нанофільтраційного пермеату молочної сироватки, шляхом використання процесів озонування та електродіалізу. Станція озонування дозволяє видаляти до 96 % органічних сполук НФ пермеату, кількість розчиненого озону має складати 20…28 мг/дм³ Встановлено, що для досягнення постефекту унеможливлення розвитку мікрофлори у обробленому озоном нанофільтраційному пермеаті мінімальна кількість TOD не повинна бути меншою 2,5 мг/дм³.*

Ключові слова*: мембранне розділення, озон, озоно-газова суміш, нанофільтраційний пермеат, органічне забруднення.*

UDC 664+004.94

CHAPTER 12

MATHEMATICAL MODELING OF MASS TRANSFER IN BAROMEMBRANE PROCESSES

O.A. Ustinov[1], V.V. Zakharov[1], O.M. Obodovich[2]

[1]*National University of Food Technologies of the MES of Ukraine, Vladimirskaya str. 48, 01601, Kyiv, Ukraine.*

[2]*Institute of Engineering Thermophysics of NAS of Ukraine, Zhelyabov str. 2a, 03057, Kyiv, Ukraine.*

email: *hokalextyr@gmail.com*

Abstract. *To determine the optimal modes of rational exploitation of membranes the phenomena of concentration polarization was researched. To simulate the real processes of separation, we used geometric, physical and mass-exchange characteristics of real membrane systems. Depending on the pressure, membrane characteristics and flow turbulence, the concentration polarization may exceed the value of 10, which must be taken into account in order to prevent the formation of sediment on the surface of the membrane.*

Keywords: *membrane, modeling, separation, concentration polarization, mas transfer.*

Introduction. The problem of the use of membrane technology is complicated by membrane contamination, since the operation modes are sometimes far from optimal. As a result, the concentration of solutes at the membrane surface increases significantly (the phenomenon of concentration polarization). When the solution concentration i high, some components may form insoluble compounds, gel-like sediment etc. When the concentration in the layer near the membrane surface becomes higher comparing with the feeding solution, diffusion streams are directed in the opposite direction relative to the flow of the filtering solution. Such effects significantly reduce the membrane productivity, during separation processes [1, 2].

Therefore, it is advisable to investigate the phenomenon of concentration polarization, studying the distribution of concentrations and its change over time in the channel, to determine the optimal modes of rational operation of membranes. Since experimental determining concentration distribution during the filtration process is very difficult, methods of mathematical modeling are used. Unfortunately, there is no single theory capable of fully describing the processes that take place near the surface of the membrane for the processes of separation (concentration) of multicomponent solutions [3], so this task remains relevant. Among modern works, there are stochastic approaches [4], various semi-empirical models [3, 5], but in most cases the theoretical study of mass

transfer processes is carried out by methods of continuum mechanics using finite difference approximation [3, 5-7].

The purpose of this work was to determine the level of concentration polarization in the membrane channels of barometric apparatus with methods of mathematical modeling.

Experimental. The phenomenon of concentration polarization related to mass transfer processes, namely the distribution of the concentration C (x, t) of the dissolved substance in solvent through height of the channel of baromembrane apparatuses is studied.

For one-dimensional models, the concept of linear concentration, kg/m, is introduced, that is, the mass of the dissolved substance per unit length of the segment on x-coordinate:

$$C_{line} = \frac{dM}{dx}, \tag{12.1}$$

For explicit schemes of finite-difference approximation the stability conditions are formulated by the Courant's criterion [6]. Physical meaning of this criterion is followng: the speed of movement along the grid should be less than the transmission rate of perturbations in the system. For this case, the relation determines the Courant's criterion:

$$\Delta t < \frac{\Delta x^2}{2D}, \tag{12.2}$$

where D is the diffusion coefficient, Δx, Δt is the spatial and temporal step according to the scheme, respectively. The concentration of the dissolved substance in the point x at time t is $C = C(x,t)$, kg/m. Change of its mass in volume $S \cdot dx$ for time dt equals $\frac{\partial C}{\partial t} \cdot dx$. Because of the movement of convective and diffusion streams, the concentration of the target component in the considered elemental volume changes (Figure 12.1) [7, 11, 12].

Diffusive fluxes are:

$$q_1^{diff} = -D\frac{\partial C}{\partial x}, \tag{12.3}$$

$$q_2^{diff} = -D\frac{\partial C}{\partial x} - \frac{\partial}{\partial x}\left(D\frac{\partial C}{\partial x}\right)dx, \tag{12.4}$$

Convective fluxes are:

$$q_1^{conv} = C \cdot v, \tag{12.5}$$

$$q_2^{conv} = C \cdot v + \frac{\partial (C \cdot v)}{\partial x}dx, \tag{12.6}$$

$q_e \cdot dx$ is the mass flow from external sources, kg/s, q_e is the flow density, kg/m s. Taking into account the balance of masses in the allocated volume, we obtain the equation of convective diffusion with an external source:

$$\frac{\partial C}{\partial t} = -\frac{\partial (C \cdot v)}{\partial x} + \frac{\partial}{\partial x}\left(\frac{D \cdot \partial C}{\partial x}\right) + q_e, \tag{12.7}$$

The solution $C=C(x,t)$ must satisfy the initial and boundary conditions set at the boundaries of the interval [0, h] at the points $x=0$, $x=h$ and set the upper

boundary of the channel and the surface of the membrane. $C(x,0)=C_0(x)$ - initial conditions, concentration of feeding solution [13].

Results and discussion. Consider a one-dimensional system simulating a portion of space (vertical line, with width $w \to 0$) of the channel of length l, height h, with a membrane with area S is completely filled with a flow of solution (carrier) in which the target component is present (Figure 12.1). From the bottom there is a membrane that completely passes by the carrier (solvent), but does not pass by the target component (Figure 12.2).
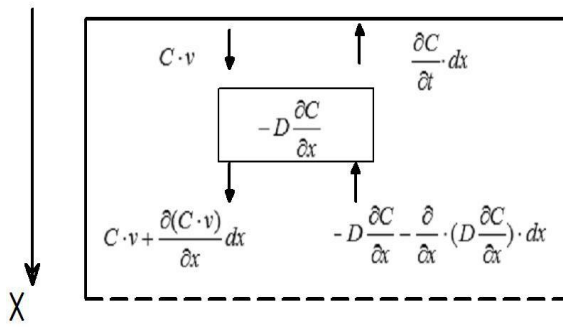

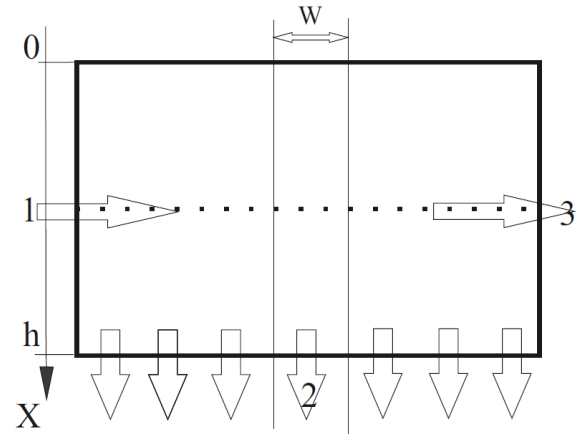*Fig. 12.1.* Scheme of flows in the membrane channel: X – spatial coordinate.

Fig. 12.2. Scheme of the pressure channel: 1 – the flow of feeding solution; 2 – flow of permeate (filtrate); 3 – the flow of concentrate.

For a numerical solution of equation (12.7), we apply the finite difference method. It is necessary to switch from continuous variables to discrete ones:

$$x \to x_j, j = 0,1,...,n, \qquad t \to t_i, i = 0,1,...,m \qquad (12.8)$$

$$\Delta x = \frac{h}{n}, \qquad \Delta t = \frac{t_{max}}{m}, \qquad (12.9)$$

Similarly for concentration:

$$C(x,t) \to C(x_j, t_i) = C_{i,j} . \qquad (12.10)$$

We apply marginal and initial conditions. At the initial moment of time (at t=0) the concentration is equal to the concentration of feeding solution:

$$C(x,0) = C_0, \qquad (12.11)$$

The key component does not pass through the membrane and the upper boundary of the channel:

$$C(0,t) = C(h,t) = 0, \qquad (12.12)$$

we approximate derivatives by difference schemes:

$$\frac{\partial C}{\partial t} \approx \frac{C_{i+1,j} - C_{i,j}}{\Delta t}, \qquad D\frac{\partial^2 C}{\partial t^2} \approx D\frac{C_{i,j+1} - 2C_{i,j} + C_{i,j-1}}{\Delta x^2}; \qquad (12.13)$$

Consequently, by substituting expressions (12.13) into equation (12.7), we obtain the one-dimensional equation in discrete variables with initial and boundary conditions:

Membrane and Sorption Materials and Technologies: Present and Future

$$C_{i+1,j} = C_{i,j} + D \frac{\Delta t \cdot (C_{i,j+1} - 2C_{i,j} + C_{i,j-1})}{\Delta x^2} \,,$$

(12.14)

$$C_{0,j} = C_0 \,, \qquad C_{i,0} = C_{i,n} = 0$$

(12.15)

Using an explicit finite-difference scheme, with a given concentration value $C_{i,j}$ at a given point for fixed i,j, we can calculate $C_{i+1,j}$ and, thus, obtain the distribution of concentrations along the entire height of the pressure channel, and its change over time (Figure 12.3).
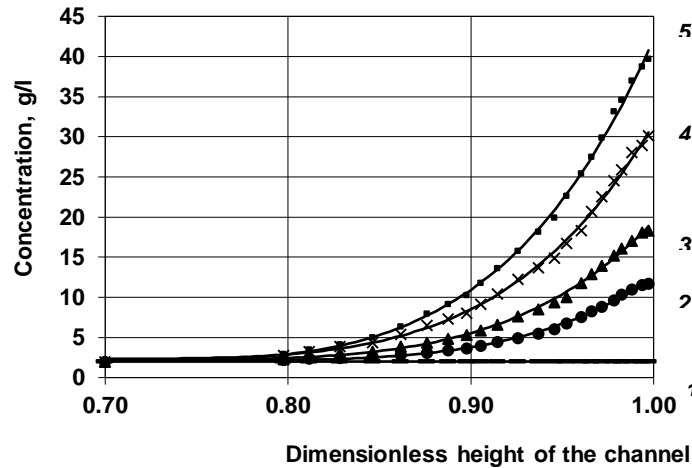

Fig. 12.3. *Distribution of concentrations by the height of the channel: 1 – 0 sec, 2 – 32 sec, 3 – 384 sec, 4 – 448 sec, 5 – 512 sec.*

Conclusions. The distributions of concentrations of the target component by height of the membrane channel were obtained and analyzed. The character of the curves coincides with physical representations of the process, with the exception of the region located near surface of the membrane. This is explained by the fact that in real systems the convective flow, having a turbulent flow pattern, makes the distribution of concentrations more uniform, diverting the mass flows of the target component into the volume of the channel from membrane surface. As a result, the effect of concentration polarization decreases and the sediment is formed less intensively.

The one-dimensional model that is presented does not consider the effects associated with turbulence, but can be applied to a dead-end separation scheme.

The scientific novelty consists in the determination of the kinetic changes in the level of concentration polarization in the membrane channels of barometric apparatus in the separation of food industry liquids.

References

1. *Davydova E.B., Il'in M.I., Tarasov A.V.*, Simulation of the unsteady-state filtration of suspensions in a dead-end channel // Theor. Found.Chem. Eng. 2013. V. 47. P. 295-.297.
2. *Morao A., Nunes J.C., Sousa F., Amorim M.T.P., Escobar I.C., Queiroz J.A.*, Development of a model for membrane filtration of long and flexible macromolecules: application to predict dextran and linear DNA rejections in ultrafiltration // J. Membr. Sci. 2009. V. 336. P. 61–70.

Membrane and Sorption Materials and Technologies: Present and Future

3. *Kumar V.*, Computer simulation of membrane processes: ultrafiltration and dialysis units// Comp. Chem. Eng. 2000. V. 23. P. 1713–1724.
4. *Foulkes W. M. C., Mitas L., Needs R. J., Rajagopal G.* Quantum Monte Carlo simulations of solids // Rev. Modern Phys. 2001. V. 73. P. 33-83.
5. *Natwar S.R., Kundariya N., Sadistap S., Narain A.* Mathematical modeling and simulation of concentration polarization layer in reverse osmosis process, // Engineering and System 2013, DOI:10.1109/SCES.2013.6547547.
6. *Courant R., Friedrichs K.O., Lewy H.*, Uber Differenzengleichungen die mathematischen Physik, // Mathematsche Annalen. 1928. V. 100. P. 32–74.
7. *Deinega A., Valuev I.*, Long-time behavior of PML absorbing boundaries for layered periodic structures // Comp. Phys. Commun. 2011. V. 182. P. 149–153.
8. *Poliakov Y.S.*, Pore Constriction in Ultrafiltration: A Discrete Multilayer Deposition Model with Steric Exclusion of Solutes at the Pore Inlet, // Theor. Found. Chem. Eng. 2014. V. 48. N 4. P. 382–396.
9. *Kim S., Hoek M.V.*, Modeling concentration polarization in reverse osmosis processes, // Desalination. 2005. V. 186. P. 111–128.
10. *Ahmad A.L., Chong M.F., Bhatia S.* Mathematical Modeling and simulation of the multiple solutes system for nanofiltration process // J. Membr.Sci. 2005. V. 253. P. 103-115.
11. *Lapisova K., Vlcek R., Klozova J., Rychtera M., Melzoch K.*, Separation techniques for distillery stillage treatment // Chez. J. Food Sci. 2006. V. 24. P. 261–267.
12. *Jayanti V.K., Rai P., Dasgupta S., De S.*, Quantification of flux decline and design of ultrafiltration system for clarification of tender coconutwater // J. Food Proc. Eng. 2010. V. 33. P. 128–143.
13. *Kanani, D.M., Fissell, W.H., Roy S., Dubnisheva A., Fleischman A., Zydney A.L.*, Permeability–Selectivity Analysis for Ultrafiltration: Effect of Pore Geometry // J. Membr. Sci. 2010. V. 349. N 1-2. P. 405-410.

МАТЕМАТИЧНЕ МОДЕЛЮВАННЯ МАСООБМІНУ В БАРОМЕМБРАННИХ ПРОЦЕСАХ

О.А. Устінов[1], В.В. Захаров[1], О.М. Ободович[2]
[1]Національний університет харчових технологій, вул. Володимірська 48, 01601, м. Київ, Україна.
[2] Інститут технічної теплофізики Національна академія наук України, вул. Желябова, 2а, 03057, м. Київ, Україна

Резюме. *Застосовуючи відповідні граничні умови, що характеризують фізичну сутність баромембранних процесів, а також чисельні методи розв'язку диференціальних рівнянь, отримано систему алгебраїчних кінетичних рівнянь, які дозволяють визначити розподіл концентрації розчиненої речовини по висоті напірних каналів, що практично неможливо зробити експериментально. Встановлено, що залежно від тиску, характеристик мембрани та турбулізації потоку, величина концентраційної поляризації може перевищувати значення 10, що необхідно враховувати з метою унеможливлення утворення осаду на поверхні мембрани.*

Ключові слова: *мембрани, моделювання, розділення, концентраційна поляризація, масообмін.*

CHAPTER 13

SORBENT ON THE BASIS OF Ti/Mn OXIDE AND Co CYANOFERRATE FOR ^{90}Sr AND ^{137}Cs SELECTIVE REMOVAL

T.V. Maltseva[1], O.V. Palchik[1], G.M. Bondarenko[2]
[1]*V.I. Vernadskii Institute of General and Inorganic Chemistry of the NAS of Ukraine*
[2]*Institute of Geochemistry of Environment of the NAS of Ukraine*
email: maltseva@ionc.kiev.ua

Abstract. *The complex oxides of $M_xMn_{1-x}O_2 \cdot nH_2O$ composition, (M-Zr, Ti, Sn) have been synthesized. Their surface was modified with phosphoric acid. phosphoric-molybdic acid and cobalt hexacyanoferrate. The sorption isotherms of Sr^{2+}, Cs^+ ions, as well as isotherms of sorption-desorption of such radionuclides as ^{90}Sr and ^{137}Cs were obtained. It was found that the most suitable sorbents for Sr^{2+} removal are $M_xMn_{1-x}O_2 \cdot nH_2O$ complex oxides. ZrO_2 modified by phosphate and molybdophosphate anions is effective towards Cs^+. The sorbent consisting of titanium dioxide and cobalt hexacyanoferrate can be recommended for extraction of both Sr^{2+} and Cs^+ ions.*
Keywords: *sorbent, composite, double oxides, hexacyanoferrate, strontium, cesium.*

Introduction. Radioactive waste from nuclear power plants (NPP) is one of the major problems, both in the field of NPP safety and industrial ecology. Today the objects of interest are full-cycle technologies. They give a recycled product that is suitable for disposal without any additional processing. The main chemical components of liquid radioactive wastes are borate and nitrate of Na^+ (~98%). The remaining 2 percents are the objects of our research, namely radioactive Cs^+ and Sr^{2+}. Cesium makes a major contribution to the amount of gamma activity, which is characterized by considerable radioactive toxicity. Strontium is of particular concern, because, it emits no gamma radiation (similarly to iron-55, carbon-14, tritium and plutonium), which is easy detectable. During the transfer from the original liquid radioactive wastes to the evaporator concentrates and further to solutions after deep evaporation plants, the salt content, alkalinity of the solutions (pH) and radioactivity increase in the first approximation according to the degree of concentration. Such salt content significantly increases the requirements for filtering material in the case of sorption and/or filtration technologies for their processing. Sorption technologies using selective inorganic ion exchange sorbents are the most promising for such applications. The relevant research is aimed at the development of technologies for the processing of radioactive waste that provides minimal disposal volumes [1]. Our investigations are devoted to synthesis and adsorption properties of double M/Mn and M/Al hydrated oxides

with various metals ratio (M – Zr(IV), Sn(IV), Ti(IV). In addition, the modification of oxide surface with phosphates (*Ph*), ammonium molybdophosphate (*Mo-Ph*) and hexacyanoferrate (*HCF*) of Co(II) was made.

Experimental. Sol-gel synthesis was applied to preparation of a composite oxide sorbents [2]. Addition of anions of phosphates and molybdo-phosphates to oxide surface was performed by impregnation of oxide sorbents with solution of phosphoric acid and ammonium molybdo-phosphate [3]. Modification of oxide surface with hexacyanoferrate of Co(II) was performed by two way: classic precipitation and with usage of gel technology. Sorption capacity and distribution coefficients (K_d) were calculated from changing the concentration of Cs^+ and Sr^{2+} ions in model solutions (0.1 M Na^+, the concentration of Cs^+ and Sr^{2+} was varied) before and after sorption. Sorption was performed from the solutions containing radionuclides in an amount that corresponds to gamma-activity of 371 Bq for strontium-90 and of 16000 Bq for cesium-137. The sorbents were regenerated using a 1 M solution of ammonium acetate.

Results and discussion. The insertion of manganese dioxide to the hydrated oxides of metals of IV group leads to decrease of absorption capacity in relation to single charged K^+ ions compared with one-component oxides. This effect can be caused by increase of microporosity. The absorption capacity of synthesized oxides was determined towards ^{90}Sr radionuclides. The model solutions with a very low initial concentration of this component was used. It was found that the change of magnitudes of the distribution coefficients for double hydroxides is from 71200 (Sn/Mn) and 95000 (Zr/Mn). A very high level of radionuclides removal was found. The advantage of double oxides in comparison with manganese dioxide is follows: (i) coarse grains allowing us to reduce hydrodynamic resistance, (ii) much higher values of the coefficient of distribution of strontium ions, which indicate the possibility to use the sorbents for decontamination of very diluted solutions.

Figure 13.1 represents sorption data for $Ti_{0.3}Mn_{0.7}O_2 \cdot nH_2O$ double oxide and $Ti_{0.3}Mn_{0.7}O_2 \cdot nH_2O/Co\text{-}HCF$ composite sorbent. Ti/Mn double oxide was chosen for surface modification due to the best sorption-desorption results concerning ^{90}Sr radionuclides (Tables 13.1 and 13.2). Modification of double oxide surface by hexacyanoferrate of Co(II) should increase sorption ability towards ^{137}Cs.

Table 13.1 gives sorption characteristics of the investigated composites iand some other ion exchange materials for comparison. Table 13.2 shows desorption results for some sorption materials loaded with radionuclides.

According to the Tables, manganese-containing sorbents are promising materials for the removal of ^{90}Sr radionuclides, and *Zr-Ph*, *Zr-Ph-Mo* sorbents are promising sorbents for the removal of ^{137}Cs radionuclides from water and liquid waste solutions. Ion exchange is the main mechanism of sorption, this provides high degree of regeneration with ammonium acetate. After surface modification

with hexacyanoferrate of Co(II), the $Ti_{0,3}Mn_{0,7}O_2 \cdot nH_2O$ sorbent can remove both ^{137}Cs and ^{90}Sr.
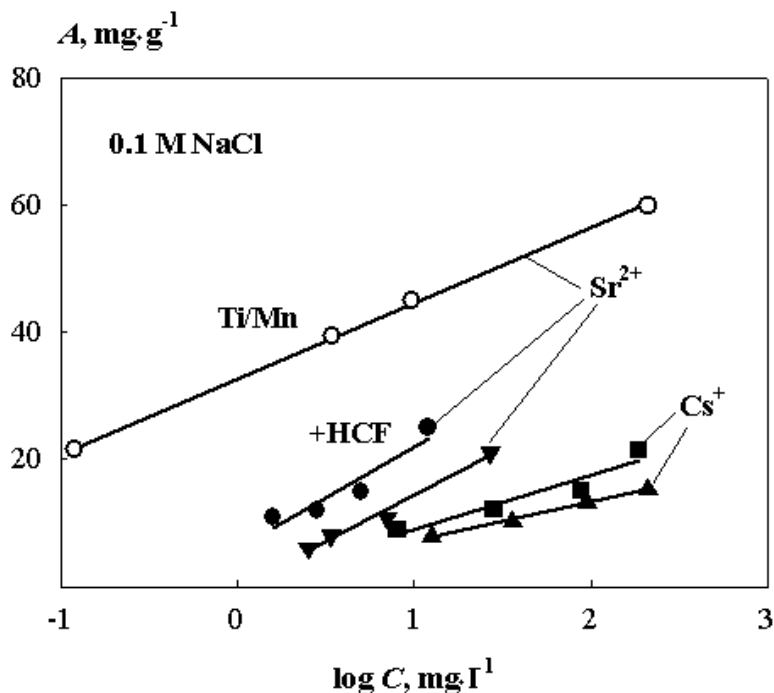

Fig. 13.1. *Sorption of Sr^{2+} and Cs^+ ions from model solution with 0.1 M NaCl with $Ti_{0,3}Mn_{0,7}O_2 \cdot nH_2O$ double oxide and $Ti_{0,3}Mn_{0,7}O_2 \cdot nH_2O$/Co-HCF composite sorbent:•,■ - synthesis using gel formation, ▼▲- synthesis by means of classic technique.*

Table 13.1. Sorption from model solutions containing Sr^{2+} and Cs^+ ions

Sorbent	$K_d \cdot 10^{-3}$	
	Sr^{2+}	Cs^+
Dowex 50WX-2	2	0.1-1
Dowex HCR-S	23	0.3
$M_{0,6}Mn_{0,4}O_2 \cdot nH_2O$	71-95	до 1.2
$TiO_2 \cdot nH_2O$/ *Dowex HCR-S*	50	4
Zirconium phosphate (*Zr-Ph*)	-	33
Zirconium phosphate modif. (*Zr-Ph-Mo*)	-	123
$Ti_{0,3}Mn_{0,7}O_2 \cdot nH_2O$ (+0.1M Na(I))	53	-
$Ti_{0,3}Mn_{0,7}O_2 \cdot nH_2O$/*HCF* (+0.1M Na(I))	20	7

Table 13.2. Degree of radionuclide desorption

Sorbent	Degree of regeneration, %	
	^{90}Sr	^{137}Cs
Zirconium phosphate (*Zr-Ph*)	-	67
Zirconium phosphate modif.(*Zr-Ph-Mo*)	-	47
$M_xMn_{1-x}O_2 \cdot nH_2O$	85-93	-

Conclusions. $M_xMn_{1-x}O_2 \cdot nH_2O$ oxides (M - Zr, Ti, Sn) of complex composition wre synthesized. Modification of their surface with various compounds such as phosphates, ammonium molybdophosphate and hexacyanoferrate was performed. The results for sorption-desorption concerning ^{90}Sr and ^{137}Cs confirm a suggestion about good perspective of the obtained materials for radionuclide removal from the solution containing high amount of salts.

References
1. *R. Koivula, R. Harjula, J. Lehto.* Selective removal of radionuclides from nuclear waste effluents with inorganic ion exchangers. In: J. M. Loureiro. M.T. Kartel (eds.) Combined and hybrid adsorbents. Fundamentals and application, Springer, Dordrecht, 2006, P. 37-47.
2. *T.V. Yatsenko, T.V Maltseva, A.V. Palchik, Yu.S. Dzyazko, G.N. Bondarenko* Influence of the introduction of manganic dioxide in the Zr, Sn, Ti oxygidrates on the adsorption of lead ions, strontium ions and radionuclides ^{90}Sr // Ukrainskii Khimicheskii Zhurnal. 2017. V. 83(11). P. 26-32.
3. *Maltseva T.V., Palchik O.V.* Influence of the pore size of the inorganic ion exchange adsorbents on the basis of complex oxide compounds Zr(IV)-P(V), Zr(IV)-P(V)-Mo(VI) on the mobility of Cs$^+$ ions adsorbed // Ukrainskii Khimicheskii Zhurnal. 2017. V. 82(6). P. 87-93.

СОРБЕНТ НА ОСНОВІ Ti/Mn ОКСИДУ І ГЕКСАЦІАНОФЕРАТУ Co ДЛЯ СЕЛЕКТИВНОГО ВИДАЛЕННЯ ^{90}Sr ТА ^{137}Cs

Т.В. Мальцева[1], О.В. Пальчик[1], Г.М. Бондаренко[2]
*[1]Інститут загальної nf неорганічної хімії ім. В.І. Вернадського НАН України,
пр. акад. Палладіна 32/34, 03142, Київ, Україна
email:maltseva@ionc.kiev.ua*
*[2] Інститут геохімії навколишнього середовища НАН України,
пр. акад. Палладіна 34А, 03142, Київ, Україна*

Резюме. *Синтезовано складні оксиди $M_xMn_{1-x}O_2 \cdot nH_2O$,(M - Zr, Ti, Sn). Поверхню оксидів модифіковано фосфорною та фосфорно-молібденовою кислотою, а також гексаціанофератом кобальту. Отримано ізотерми сорбції іонів Sr^{2+}, Cs^+, а також ізотерми сорбції-десорбції раділнуклідів ^{90}Sr та ^{137}Cs. Знайдено, що найбільш ефективними сорбентами для іонів Sr^{2+} є складні оксиди $M_xMn_{1-x}O_2 \cdot nH_2O$, а для Cs^+ - ZrO_2, модифікований фосфат- та молібдофосфат- аніонами. Сорбент $Ti_{0,3}Mn_{0,7}O_2 \cdot nH_2O$/Co-HCF селективно поглинає Sr^{2+}, Cs^+.*
Ключові слова*: сорбент, композит, подвійні оксиди, гексаціаноферат, стронцій, цезій.*

CHAPTER 14

ION EXCHANGE MEMBRANES FOR REGENERATION OF HYDROCHLORIC ACID FROM ETCHING SOLUTIONS

S. Bolshanina, V. Serdiuk, L. Ponomarova, A. Yanovska, A. Ableev
Sumy State University, 2, Rymsky-Korsakov Str., Sumy 40007, Ukraine
email svet.bolshansna@gmail.com

Abstract. *The process of regeneration of utilized hydrochloric acid etching solutions using electrochemical equipment with ion exchange membranes was examined. The products of cathode reactions were studied. It was proved that the waste solution was not only purified from contaminate ions, but the acid content increased during the electrolyzer operation.*
Keywords: *membrane, ion exchange membrane, electrodialysis, chloride acid, regeneration.*

Introduction. One of main stages of production of metallic devices before the deposition of galvanic coating is cleaning of their surface from corrosion products and other contaminants. For this goal the etching with solutions of various acids (mainly HCl or H_2SO_4) is used. Rust and shruff are dissolved during the etching and metal surface is purified. At the same time the etching solution is polluted, the acid concentration is reduced the solution cannot be used further. After the etching the acid solution is neutralized with calcium hydroxide before dropping in the sump. Soluble metal chlorides obtained by neutralization are dissolved in ground waters polluting the environment. Thus, hydrochloric acid is lost.

Known methods for acid regeneration are energy consuming processes and require additional expensive equipment. For instance, the waste acid is thermally treated in the air stream in a reactor under the temperature of 600–800 °C [1].

Electrodialysis is the economically efficient technique for regeneration of acidic etching solutions. Two- or three-compartment electrolyzers and various alternation of cation exchange and anion exchange membranes are used for such purpose.

However, these methods are used for sulfuric acid baths [2]. It is caused by the fact that the anodic process is provided by water molecules during sulfuric acid electrodialysis, which is accompanied by oxygen evolution. In the case of electrolysis of hydrochloric acid, gaseous chlorine is generated on anode, its evolution is undesirable. The trapping released gas seems to be a very difficult process, which requires special equipment. The ways of regenerations using bipolar membranes for saline solutions are also proposed [3-5]. However, there is no information about their application for regeneration of etching solutions. Furthermore, bipolar membranes are not economically effective for this process.

Experimental. In this work, we discussed the possibility of regeneration of the utilized etching solutions of hydrochloric acid by means of electrochemical equipment with ion exchange membranes. For regeneration of the solutions, we used an electrolyser consisting two modules (cathode chamber and anode chamber) that were divided from the etching solution with a RALEX®CM-PES 11-66 cation exchange membranes. A 1 wt.% solution of sulfuric acid filled each chamber, where cathode and anode were placed. The anode was made of lead (grade C2), the cathode was manufactored from titanium (BT1-0). Electrolysis was carried out at current density of 5-10 A/dm^2.

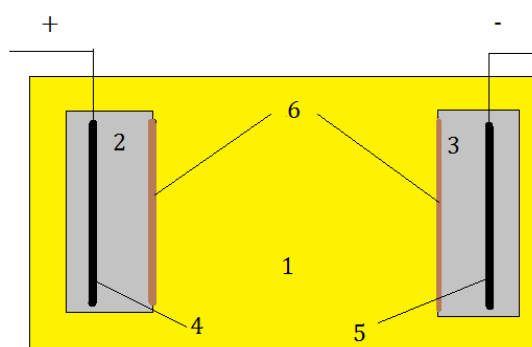The scheme of experimental setup is presented in the Figure 14.1

Fig. 14.1. *The scheme of experimental setup for regeneration of etching solution.*
1 – bath with utilized etching solution; 2 – anode chamber; 3 – cathode chamber; 4 – anode; 5 – cathode; 6 – cation exchange membrane.

Results and discussion. When a cation exchange membrane is placed both near cathode and anode, such system is able to remove metal ions from the solution of hydrochloric at the side of cathode, furthermore migration of chloride anions towards anode and chlorine generation are suppressed. This excludes the transfer of H$^+$ and Cl$^-$ ions from the cathode solution to the anolyte, and provides accumulation of these species in the solution of technological bath. As seen from the results of obtained experimental data, the acidity of a cathode solution has a great impact on this process. During the process, metal cations from the etching solution migrate to the cathode solution, which is neutralized by OH$^-$ ions (they are generated on the cathode during electrochemical reaction of oxygen evolution). As a result the cathode medium is transformed from acidic to alkaline. Precipitation of insoluble compounds of metals as well as pure metals is observed in cathode solution (Figure 14.2). In this case, the cathode is coated with a thick layer of deposit.

Due to decrease of membrane conductivity, the resistance of the system increases followed by reducing current density. As found, the highest conductivity value is related to the solution pH of 1-2.

The cation exchange membrane performs isolation function and preventing the transfer of chloride ions to the anode space.

Membrane and Sorption Materials and Technologies: Present and Future
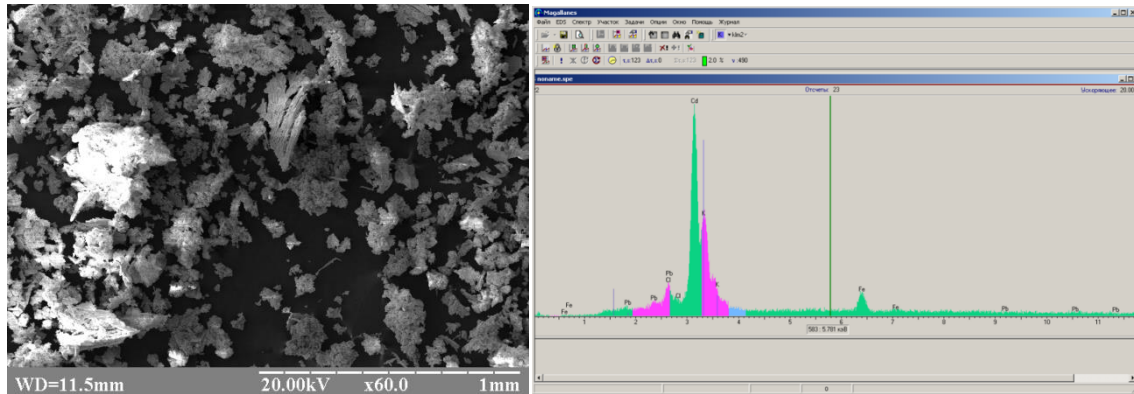
a
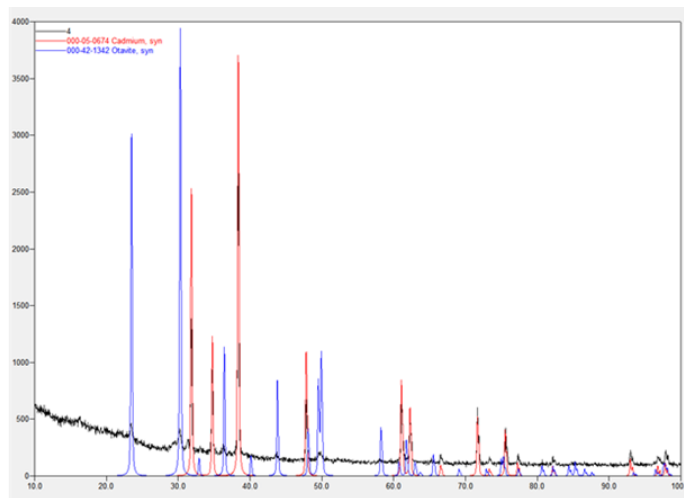
b

Fig. 14.2. *a) SEM – Morphology of the cathode deposit and average EDX analysis of the sample; b) XRD analysis of cathode slime (main fraction is cadmium and its compounds (cadmium carbonate).*

Instead of chloride ions, water molecules are discharged on anode according to the following scheme:

$$2H_2O - 4\,\bar{e} \rightarrow O_2\ + 4H^+ \tag{14.1}$$

Nevertheless, oxygen releases and acidification of the anode solution occurs. This process keeps the necessary level of the pH in the anode chamber to maintain the inertness of lead as anode material. Otherwise it will be dissolved very fast.

During operation of the electrolyzer, the etching solution was not only purified from ion impurities but the concentration of acid was also increased. The concentration of hydrochloric acid was estimated by potentiometric titration using a 0.1 M NaOH solution up to pH 3.7. During operation of the membrane system, the concentration of acid increases from 0.9 g/L to 1.4 g/L. This means the effectiveness of the membrane devise in the process of acid regeneration.

Conclusions. Hence, the proposed experimental setup provides not only extraction of metal cations from the utilized etching solution, but promotes the increase of acid concentration in this medium. Since no chlorine evolution at the anode occurs, the proposed method is related to ecologically safe.

References

1. *Aksenov V.I.* (ed,) Etching-regenerating complexes, Teplotekhnika, Moscow, 2006.
2. Gomelya M.D., Trus I.M., Vasylenko I.A. Mathematical modeling of the sulfuric acid concentration process' kinetics in electrochemical treatment of sulphate-containing eluates// Odes'kyi Politechnyi Universytet. Pratsi. 2015. N 1. P. 146-151.
3. *Campione A*. Electrodialysis for water desalination: A critical assessment of recent // Desalination. 2018. V. 434. P. 121-160.
4. *Strathmann H*. Electrodialysis, a mature technology with a multitude of new applications// Desalination. 2010. V. 264. P. 268–288.
5. *Pourcelly G*. Electrodialysis with bipolar membranes: principles, optimization, and applications// Russ. J. Electrochem. 2002. V. 38. P. 919–926.

ІОНООБМІННІ МЕМБРАНИ В РЕГЕНЕРАЦІЇ ХЛОРИДНОЇ КИСЛОТИ З ТРАВИЛЬНИХ РОЗЧИНІВ

С. Большаніна, В. Сердюк, Л. Пономарьова, А. Яновська, О. Аблєєв

Сумський державний університет, вул. Римського-Корсакова 2, 40007, Суми, Україна, email svet.bolshansna@gmail.com

Резюме. *Розглядається процес регенерації відпрацьованих травильних розчинів на основі хлоридної кислоти з використанням електрохімічних пристроїв з іонообмінними мембранами. Вивчено продукти реакцій на катоді. Доведено, що при роботі електролізера відпрацьований травильний розчин не тільки очищується від забруднюючих його іонів, але і збільшується вміст кислоти.*

Ключові слова*: мембрани, іонообмінні мембрани, електродіаліз, хлоридна кислота, регенерація.*

CHAPTER 15

CAPACITIVE DEIONIZATION OF WATER (REVIEW)

Yu.M. Volfkovich

A.N. Frumkin Institute of Physical Chemistry & Electrochemistry of the RAS,

Leninskii pr. 31, Moscow, 119071, Russia

email: yuvolf40@mail.ru

Abstract. *The method of capacitive deionization of water (CDI) is to pump brackish water or seawater though an electrochemical cell, where certain potential difference is kept between carbon electrodes, which are characterized by high specific surface area. This method is sufficiently more attractive from the economical point of view in comparison with other desalination techniques, particularly with reverse osmosis that is widely used in industry. Different modifications of CDI have been developed, for instance, membrane capacitive deionization of water (MCDI) with cation and anion exchange membranes, CDI with ion-selective carbon electrodes, CDI with flow electrodes, CDI with Na-intercalating electrodes, CDI with cation-exchange and anion exchange mixed membrane of mosaic structure, which is used instead of conventional porous separator.*

Keywords: *capacitive deionization, mosaic membrane, carbon electrode, Na-intercalating electrode, membrane capacitive deionization.*

Introduction. Capacitive deionization of water (CDI) is an effective new method for desalination of brackish water [1]. Its stream flows between pairs of carbon electrodes, which are characterized by high surface area (HSACE). For example, activated carbon electrodes (ACE) are applied to CDI processes, the electrodes are kept at a potential difference of > 1.2 V. Ions and other charged species are attracted to the opposite charged electrode, which keeps them. The negative electrode adsorbs cations, while the positive electrode adsorbs anions. Eventually the electrodes become saturated with ions and must be regenerated. When the electrical circuit is opened, ions are removed from the electrodes producing more concentrated brine stream. In practice, CDI processes produce deionized potable water and concentrated brine solution, the ratio of their volumes is 4:1. The concentrate contains all salts, which were present in the feeding solution. The main advantage of CDI is low operating cost, this is three times less comparing with the main competitor − reverse osmosis. The mechanism of the CDI processes is based on charging - discharging of electric double layer (EDL) similarly to EDL of supercapacitor.

Results and discussion. Different modifications of CDI processes are known, for instance, the method of membrane capacitive deionization (MCDI) [2]. In this case, the anion exchange membrane is adjacent to the positively charged

electrode, and the cation exchange membrane borders on the cathode [Fig. 1]. The anion exchange membrane prevents cation transport to the anode, while the cation exchange membrane makes impossible anion movement towards the cathode. This provides more complete separation of cations and anions in the MCDI cell. When the HSACE, which are characterized by high specific surface area, are used and no membranes are applied to the CDI process, separation of oppositely charged ions occurs due to EDL charging inside pores of the electrodes. However, the membranes provide additional hydrodynamic resistance (increasing energy consumptions).This is a disadvantage of the MCDI method in comparison with CDI.

Nitrate-selective composite carbon electrodes (NSCCEs) were manufactured for capacitive deionization to remove nitrate ions selectively from the solution containing different anions. The NSCCEs were fabricated by coating the surface of the carbon electrode with BHP 55 anion exchange resin, this sorbent is known to be selective towards nitrate ions. The resin was ground to a fine powder. The mixed solution containing 5.0 mM NaCl and 2.0 mM NaNO$_3$ was applied to desalination process using the NSCCE system that involved the fabricated electrode. Selective removal of nitrate ions using the NSCCE and MCDI systems (the last one involved ion exchange membranes and carbon electrodes) was performed, the results have been compared. In the case of the NSCCE system, adsorption of nitrate ions was 19 mmol/m^2, This is 2.3-times higher than adsorption in the MCDI system. These results showed that ions were initially adsorbed due to electrostatic force, then the species from the solution are sorbed by resin particles of the surface according to ion exchange mechanism.

Another modification of CDI is flow-electrode capacitive deionization (FCDI)[3]. FCDI is novel technology that exhibits continuous deionization and high efficiency ion removal. The flow-electrode possess high capacitance and low resistance, this is necessary to achieve low energy consumptions. In order to develop high-performance flow-electrode, its constituents, such as porous solids, conductive additives and electrolyte, have to be considered. Desalting performances of flow-electrodes containing spherical activated carbon and aqueous electrolyte (NaCl solution of various concentration)has been confirmed (Figure 15.1), the effect of salt concentration in the feeding solution has been found. It has been shown that moderate amount of the salt in the flow-electrode is necessary in order to compensate reduced productivity of the flow-electrode, attributed to decrease of water resistance.

Interesting modification of CDI is membrane-free cation intercalation desalination (CIDI) [4]. In this case, the electrochemical desalination devices involve redox-active cation intercalation electrodes. The stacks are prospective for desalination of salty water, they show high water recovery and low energy consumption. Previous modeling and experiments, which involve ion-exchange membranes to maximize charge efficiency, show rather low capital cost of the processes. At the same time, CIDI (membrane-free alternative) allows us to

reduce the capital cost even more. Porous diaphragm was used to separate *NaNiFe(CN)₆*electrodes:

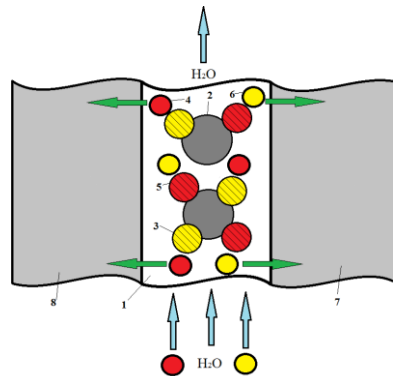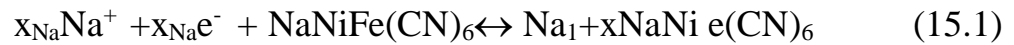$$x_{Na}Na^+ + x_{Na}e^- + NaNiFe(CN)_6 \leftrightarrow Na_1 + xNaNi\ e(CN)_6 \qquad (15.1)$$

Fig. 15.1. *Flow electrode.*

The energy consumptions for CDI and MCDI are sufficiently lower comparing with other deionization methods. This is mainly due to resulting energy consumptions. This parameter is equal to difference of energy consumptions between deionization stage (charging) and concentrating stage (discharging), since the energy is returned to the CDI and MCDI stack during the last stage (Figure 15.2 [2]).
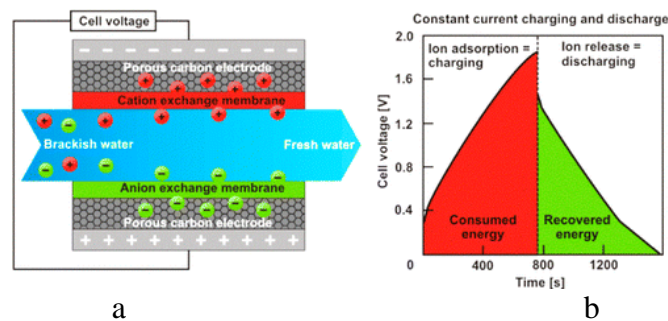

a   b

Figure 15.2. *MCDI scheme (a). Consumed energy costs in the deionization stage and the energy released in the regeneration stage [2] (b).*

Recently a large number of papers, which dealt to investigation and optimization of CDI processes, has been published. Many of them were devoted to investigation of effect of porous structure of carbon electrodes, methods of BET and standard contact porosimetry (MSCP) were used in order to research the effect of their porous structure [5]. The MSCP technique allows us to estimate also hydrophilic and hydrophobic properties of the electrodes. It has been shown that meso-microporous carbon electrodes are more effective for deionization than microporous materials. It was shown that hydrophilization of carbon results in increase of deionization degree. For this purpose, the materials are treated with oxides of titanium, manganese or zinc. Preliminary treatment of the electrodes with KOH, HNO_3 and nitrogen provides desalination

improvement. Activated carbon (AC) is the most common electrode material. However, carbon nanotubes (CNT), graphene and aerogels. In addition to symmetric electrochemical cells, for instance, AC – AC, asymmetrical cells are also used, for instance, CNT–composite CNT with polyaniline.

Many studies are devoted to removal of different ionic impurities from water, for instance, sodium, chloride, fluoride, chromate, iron, copper, arsenic, zinc, uranium, thiosulfate, organic salts and so on. Special types of carbon electrodes for selective removal of one of other ions are selected. Mathematical modeling and optimization of CDI processes are also considered [6 -8].

The approach that allows one to decrease energy consumptions of water purification was considered in [9]. The method provides usage of mosaic membrane (MM) containing both cation and anion exchange fragments instead of glass spacer. Counter-ions inside the membrane ensure rather high ionic conductivity even in pure water. Mosaic membranes based on phenol-formaldehyde matrices were studied, their electric conductivity and exchange capacity were determined. Deionization in static and dynamic electrochemical cells, which were filled with deionized water and 0.005 M KCl solution respectively, was researched. The mechanism of EDL charging inside pores of the electrodes, which are impregnated with pure water, has been proposed. Specific energy consumptions for deionization of very diluted solutions are sufficiently lower for the cell containing mosaic membrane than those for the cell with inert glass spacer. Minimum energy consumptions and maximum deionization degree are reached at cell voltage of 1.4 V. Thus, the idea about optimal composition of the MEA for obtaining pure water has been confirmed experimentally. The MEA has to contain MM and AC electrodes. Highly dispersive AC electrodes have to possess both cation and anion exchange capacity. The other important requirement is high surface conductivity [10]. Thus, MM application to CDI for obtaining pure water is one way to solve the problem of minimizing of the energy cost.

Conclusions. CDI and MSD technologies possess huge potential possibilities for water desalination. Due to the lowest energy consumptions and the largest energy recovery, these technologies are very attractive for practical usage.

References
1. *Oren Y.* Capacitive deionization (CDI) for desalination and water treatment — past, present and future (a review) // Desalination. 2008. V. 228. P. 10–29.
2. *Strathmann H.* Ion-exchange membrane processes in water treatment sustainability science and engineering. In: *Escobar I.C., Schäfer A.I.* Sustainable water for the future: water recycling versus desalination. Amsterdam, Boston, Heidelberg, London, New York, Oxford, Paris, San Diego, San Francisco, Singapore, Sydney, Tokyo: Elsevier, 2010. P. 141-199.
3. *Yang S.C., Choi J., Yeo J., Jeon S.-il, Park H.-ran, Dong K.K.* Flow-electrode capacitive deionization using an aqueous electrolyte with a high salt concentration // Environ. Sci. Technol. 2016. V. 50 . N 11. P. 5892–5899.

4. *Smith K.C*. Theoretical evaluation of electrochemical cell architectures using cation intercalation electrodes for desalination // Electrochim. Acta. 2017. V. 230. P. 333–341.

5. *Volfkovich Yu.M., Filippov A.N., Bagotsky V.S.* Structural properties of porous materials and powders used in different fields of science and technology. London, Heidelberg, New York, Dordrecht: Springer, 2014.

6. *Mani A., Bazant M. Z.* Deionization shocks in microstructures // Phys. Rev. E. 2011. V. 84. N 6. 61504.

7. *Biesheuvel P.M., Porada S., Levi M., Bazant M.Z.*, Attractive forces in microporous carbon electrodes for capacitive deionization // J. Solid State Electrochem. 2014. V. 18. N 5. P. 1365–1376.

8. *Volfkovich Yu.M., Bograchev D.A., Mikhalin A.A., Rychagov A.Yu., Sosenkin V.E., Park D.* Capacitive deionization of aqueous solutions: modeling and experiments // Desalination and water treatment. 2017. V. 69. P.130- 141.

9. *Volfkovich Yu.M., Rychagov A.Yu. Mikhalin A.A., Kardash M.M., Kononenko N.A., Ainetdinov D.V., Shkirskaya S.A., Sosenkin V.E.* Capacitive deionization of water using mosaic membrane // Desalination. 2018. V. 426. P. 1–10.

10. *Volfkovich Yu. M., Mikhalin A. A., Rychagov A. Y.* Surface conductivity measurements for porous carbon electrodes // Russ. J. Electrochem. 2013. V. 49. N 6. P. 594–598.

ЄМНІСНА ДЕІОНІЗАЦІЯ ВОДИ (ОГЛЯД)

Ю.М. Вольфкович
¹Інститут фізичної хімії та електрохімії ім. О.Н. Фрумкіна РАН,
Ленінський пр. 31, Москва, 119071, Росія
email: yuvolf40@mail.ru

Резюме. *Метод ємнісної деіонізації води (ЄДВ) полягає у прокачуванні солоноватої або морської води через електрохімічну комірку, де створюється певна різниця потенціалів між вугільними електродами з великою питомою поверхнею. Цей метод є суттєво більш економічним у порівнянні з іншими опріснювальними методами, зокрема з методом зворотного осмосу. Розроблено різні модифікації ЄДВ, наприклад: мембранна ємнісна деіонізація води (МЄДВ) з катіонообмінними та аніонообмінними мембранами, ЄДВ з іонселективними вугільними електродами, ЄДВ з проточними електродами, ЄДВ з Na- інтеркалюючими електродами, ЄДВ з катіоно- аніонообмінною змішаною мембраною мозаїчної структури, яка використовується замість звичайного пористого сепаратора.*

Ключові слова: *ємнісна деіонізація, мозаїчна мембрана, вугільний електрод, Na-інтеркалюючий електрод, мембранна ємнісна деіонізація.*

UDC 542.06+542.8

CHAPTER 16

SORPTION PROPERTIES OF HYDROXYAPATITE-BASED COMPOSITES IN ALGINATE SHELL

G.O. Yanovska[1], S.B. Bolshanina[1], V.D. Ivchenko[2],

Y.L. Sydorenko[1], L.M. Ponomarova[1]

[1]Sumy State University, 2, Rymsky-Korsakov Str., Sumy 40007, Ukraine,
e-mail: yanovskaanna@gmail.com

[2]Sumy National Agrarian University, 160, H.Kondratiev Str., Sumy 40021,
Ukraine

Abstract. *Hydroxyapatite-based composite materials are widely used for treatment of bone defects due to their biocompatibility and osteoconductivity. In this work they were successfully combined with alginate – biopolymer with gel forming ability. Sorption properties of the composite materials towards Cu^{2+} and Zn^{2+} ions were compared. It was shown that sorption of Zn^{2+} ions is more effective due to ion exchange properties and formation of new insoluble phase after contact with microsphere surface.*

Keywords: *hydroxyapatite, sorption, alginate, composite.*

Introduction. Millions of people all over the world suffer from bone injuries and orthopedic problems. They usually need total or partial replacement of the bone tissue [1]. Composite materials based on calcium phosphates and biopolymers are widely used for bone replacement [2]. Hydroxyapatite (HA) ($Ca_{10}(PO_4)_6(OH)_2$) is widely applied as a biomaterial to the substitution of human bone tissues due to its excellent biocompatibility and bioactivity [3].

Polysaccharides perform different physiological functions and have various applications for regenerative medicine and tissue engineering [4]. Polysaccharides are generally more stable than nucleic acids and proteins and are usually not irreversibly denatured on heating [5]. Alginate (Alg) is natural polysaccharide extracted from algae, linear polymer consisting of (1→4) α-L-guluronic (G) and (1→4) β-D-mannuronic acid blocks (M). Alginate found several applications in tissue repair and regeneration, in particular, as a bulking agent, for drug delivery, as a carrier for cell therapies, and as a model of extracellular matrix [6]. Alginates are widely used due to their ability to form beads, films, fibers, hydrogels and composite materials. Divalent metal ions better interact with zones rich in G-blocks comparing with zones rich in M-blocks and MG-blocks [7]. Nanocomposite beads (Alg/HA) are used as drug-controlled release matrices [8]. HA is an ideal material for the preparation of drug scaffolds because of its excellent properties, such as the ability to adsorb a variety of chemical species and biocompatibility. The release of drugs from HA

is very fast, owing to the weak interaction between the drugs and the HA particles [9]. The combination of biopolymer and HA seems to be a feasible way to prolong the release of drugs to make the biopolymer/HA composites applicable for long-term controlled release carriers. In this work sorption ability of HA/Alg composite materials to Cu^{2+} and Zn^{2+} ions were compared. \

Experimental. Hydroxyapatite is synthesized by following reaction:

$$10\ Ca(NO_3)_2 \cdot 4H_2O + 6\ (NH_4)_2HPO_4 + 8\ NH_3 \cdot H_2O \rightarrow \qquad (16.1)$$
$$\rightarrow Ca_{10}(PO_4)_6(OH)_2 + 20NH_4NO_3 + 46\ H_2O.$$

As-prepared HA is mixed in a relation of 1:1 with aqueous solutions of 1.5% sodium alginate to obtain microspheres with alginate concentration of 0.75%. The mixture of HA/Alg was added drop by drop to 0.1 M $CaCl_2$ solution for microspheres formation with calcium alginate shell. An experimental setup for HA/Alg microspheres production is shown in Figure 16.1.
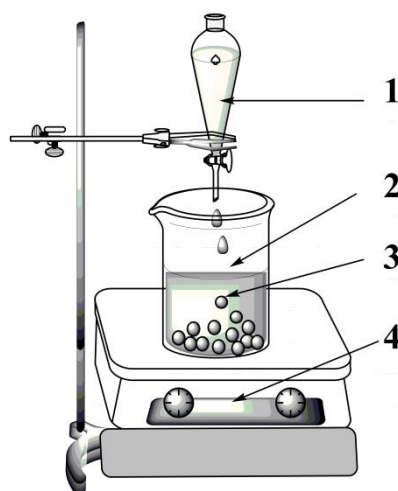

Fig. 16.1. *Experimental setup for HA/Alg microspheres formation: 1) solution of alginate mixed with as-prepared HA, 2) 0.1 M CaCl₂ solution, 3) formation of HA/Alg microspheres, 4) magnetic stirrer [10]*

A part of microspheres was triple washed with distilled water followed by immersion with 0.2 N $ZnSO_4$ solution for 24 hours. Another part was immersed with 0.2 N $CuSO_4$ solution. The obtained microspheres were removed after 24 hours from the solutions, dried down to constant mass and weight for calculation of adsorption value of Me^{2+} ions in the dry weight.

The concentration of Me^+ ions in the filtrate was determined via their complex formation with ethylene diamine tetraacetate (EDTA). This is polydentate ligand that forms complexes with Me^{2+} in a relation of 1:1. Eriochrome black (for Zn^{2+}), and murexide (for Cu^{2+}) were used as indicators, because they also form complexes with Me^{2+} ions. Titration was provided in alkaline medium using ammonium buffer solution at pH 10. A small amount of

Membrane and Sorption Materials and Technologies: Present and Future

indicator was added. The titration was performed before changing the color of investigated solution.

Adsorption value was calculated by following equation:

$$A = \frac{(C_0 - C) \cdot V \cdot m_{eqMe^{2+}} \cdot 1000}{m_{microspheres}}, \quad (16.2)$$

where C_o is the initial concentration of adsorbate in mol-eq.$\cdot$L^{-1}; C is a equilibrium concentration of adsorbate in mol-eq.$\cdot$L^{-1}; V is an adsorbate solution volume in L; $m_{eq.Me2+}$ – mass equivalent of Me in 1 g (mol-eq); m – weight of microspheres in g, A – adsorption capacity, mg$\cdot$g^{-1} [11].

Morphology of obtained microspheres was investigated using a Scanning Electron Microscopy (SEM) (REM-106, SELMI, Ukraine). The phase composition of the coatings was examined using an X-ray diffractometer DRON-4-07 ("Burevestnik", Russia) connected to a computer-aided system for the experiment control and data processing. Phase identification was performed using a JCPDS card catalog (Joint Committee on Powder Diffraction Standards).

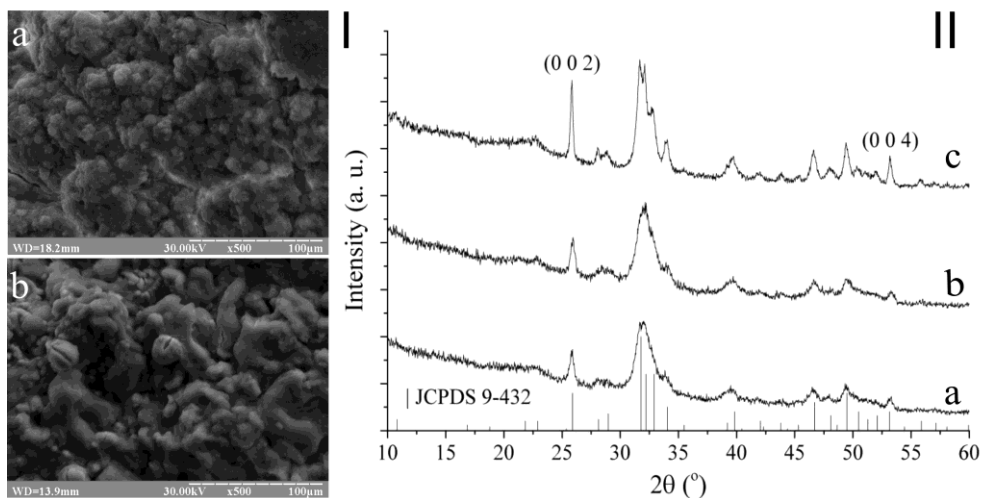**Results and discussion.** Surface morphology and phase composition is presented in Figure 16.2.

Fig. 16.2. *I) Morphology of Zn^{2+} loaded (a) and Cu^{2+} loaded microspheres (b). II) XRD patterns of a) Zn^{2+} loaded HA, b) Cu^{2+} loaded HA, c) pure HA.*

The microspheres have very developed surface that promote adsorption by HA. The main phase in the microspheres is HA (Figure 16.2. II). Calcium alginate shell of samples permits the passage of ions, further they are adsorbed by HA. To characterize the adsorption capacity, the graphical dependence of adsorption (at 22° C) on contact time is plotted in Figure 16.3.

For understanding sorption mechanism of Zn^{2+} and Cu^{2+} ions on HA/Alg microspheres, solutions of ZnSO$_4$ and CuSO$_4$ with initial concentration of 0.1 M were analyzed to estimate not only amount of mentioned ions, but also Ca^{2+} concentration and pH of the media after contact with adsorbents [10, 12].
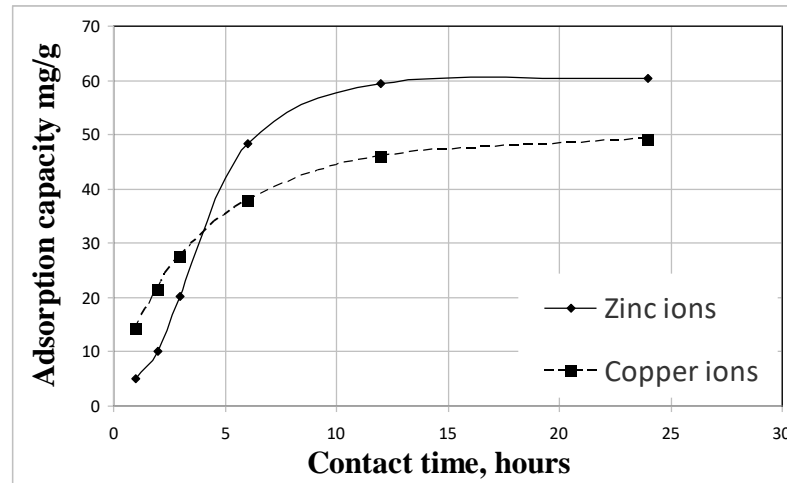
Fig. 16.3. *Adsorption capacity of HA/Alg composite materials.*

The obtained results show mixed character of adsorption. Analysis of filtrate after adsorption of Zn^{2+} and Cu^{2+} ions shows the presence of Ca^{2+} ions in amount of 1/4 from Zn^{2+} ions and 1/3 from Cu^{2+} ions due to ion exchange that accompanies adsorption. The possible substitution of surface cations is due to replacement of Ca^{2+} by Zn^{2+} or Cu^{2+} ions in hydroxyapatite structure. The difference between sorption of ions is caused by ability of metal ions to be embedded to crystal lattice of HA sorbent and formation of insoluble compounds with the HA surface. Product solubility of copper (II) orthophosphate $Cu_3(PO_4)_2$ is $1.3 \cdot 10^{-37}$, while it is $1.0 \cdot 10^{-32}$ for zinc orthophosphate $Zn_3(PO_4)_2$. The difference in solubility product of the phases on the HA surface leads to more intensive adsorption for Cu^{2+} ions at the first hours that is caused by lower solubility product of copper (II) orthophosphate. Besides, the fast formation of insoluble phases leads to blocking of adsorbent active centers with copper (II) orthophosphate with the decrease of adsorption. As a result, adsorption capacity of HA towards Cu^{2+} ions is slightly lower comparing with Zn^{2+} ions.

Conclusions. HA and HA/Alg materials can be used as excellent low-cost natural adsorbents. According to the results of adsorption kinetics, HA has the main contribution to adsorption by HA/Alg composites. Therefore, the mechanism of Cu^{2+} and Zn^{2+} ions adsorption on HA is mixed. It involves the ability of HA immobilize various metal ions due to ion exchange, and formation of insoluble phases of metal phosphates on the surface of sorbent.

References

1. *Ferreira A. M., Gentile P., Chiono V., Ciardelli G.* Collagen for bone tissue regeneration // Acta Biomaterialia. 2012. V.8. P. 3191-3200.
2. *Haroun A. A., Migonney V.* Synthesis and in vitro evaluation of gelatin / hydroxyapatite graft copolymers to form bionanocomposites // International Journal of Biological Macromolecules. 2010. V. 46. P. 310-316.

3. *Babaei Z., Jahanshahi M., Rabiee S. M.* The fabrication of nanocomposites via calcium phosphate formation on gelatin–chitosan network and the gelatin influence on the properties of biphasic composites // Materials Science and Engineering C 2013. V. 33. P. 370-375.

4. *Park S.-B., Lih E., Park K.-S., Joung Y. K., Han D. K.* Biopolymer-based functional composites for medical applications // Progress in Polymer Science. 2017. V. 68. P. 77-105.

5. *Zheng Y., Monty J., Linhardt R. J.* Polysaccharide-based nanocomposites and their applications // Carbohydrate Research 2015. V. 405. P. 23-32.

6. *Perucca O.C., DeGirolamo L., Perteghella S., Stanco D., Chlapanidas T., Vigan M., Torre M.L.* Alginate beads as a vehicle for mesenchymal stem cells isolated from adipose tissue and tendon tissue: in vitro evaluation of a new approach for the treatment of tendinopathies, // J. Sports Traumatol. 2014. V. 31. P. 23-31.

7. *Rinaudo M.* Biomaterials based on a natural polysaccharide alginate // Revista Especializada en Ciencias Químico-Biológicas, 2014. V. 17(1). P. 92-96,

8. *Zhang L., Tang P., Xu M., Zhang W., Chai W., Wang Y.*, Effects of crystalline phase on the biological properties of collagen-hydroxyapatite composites // Acta Biomater. 2010. V.6 (6). P. 2189-2199.

9. *Mizushima Y., Ikoma T., Tanaka J., Hoshi K., Ishihara T., Ogawa Y., et al.* Injectable porous hydroxyapatite microparticles as a new carrier for protein and lipophilic drugs. // J Control Release 2006. V.110. P.260–265.

10. *Yanovska A.A., Bolshanina S.B., Stanislavov A.S., Kuznetsov V.N., Mospan A.B., Illiashenko V.Yu., Rogulsky Yu.V., Trofimenko Ya.V., Danilchenko S.N.* Synthesis and characterization of Copper-loaded hydroxyapatite-alginate microspheres // Chemistry, Physics and Technology of Surface. 2017. V. 8. N 4. P. 400-409.

11. Zolotov Yu.A. Fundamentals of analytical chemistry. Practical guide, Vysshaya Shkola, Moscow, 2003.

12. *Bolshanina S.B., Yanovskaya A.A., kuznetsov V.N., Rogulskii Yu.V., Stanislavov A.S., Il'yashenko V.Yu., Sony A...K.* Adsorption of zinc ions with capsules of hydroxyapatite in alginate shell. Investigations of kinetics // Chemical Industry of Ukraine. 2016. № 2 (133). P. 3-11.

СОРБЦІЙНІ ВЛАСТИВОСТІ КОМПОЗИТНИХ МАТЕРІАЛІВ НА ОСНОВІ ГІДРОКСИАПАТИТУ В АЛЬГІНАТНІЙ ОБОЛОНЦІ

Г.О. Яновська[1], С.Б. Большаніна[1], В.Д. Івченко[2], Я.Л. Сидоренко[1], Л.М. Пономарьова[1]

[1]Сумський державний університет, вул. Римського-Корсакова 2, 40007, Суми, Україна, e-mail:yanovskaanna@gmail.com
[2] Сумський національний аграрний університет, вул. Герасима Кондратьєва 160, 40021, Суми, Україна.

Резюме. Композитні матеріали на основі гідроксиапатиту широко використовуються для лікування кісткових дефектів завдяки їх біосумісності та остеопровідності. В даній роботі його було вдало поєднано з альгінатом – біополімером з гелеутворюючою здатністю. Порівняні сорбційні властивості отриманих композитних матеріалів до йонів Cu^{2+} та Zn^{2+}. Показано, що сорбція йонів Zn^{2+} є більш ефективною завдяки особливостям даного йону та формуванню нової нерозчинної фази при контакті з поверхнею капсул.
Ключові слова: гідроксиапатит, сорбція, альгінат, композит.